AD-A135661

12

RADC-TR-83-133
Final Technical Report
June 1983

COMMUNICATION SYSTEM STUDIES FOR THE SUBMARINE LASER COMMUNICATIONS SYSTEM

Riverside Research Institute

Sponsored by
Defense Advanced Research Projects Agency (DOD)
ARPA Order No. 4250

APPROVED FOR PUBLIC RELEASE; DISTRIBUTION UNLIMITED

ROME AIR DEVELOPMENT CENTER
Air Force Systems Command
Griffiss Air Force Base, NY 13441

This report has been reviewed by the RADC Public Affairs Office (PA) and is releasable to the National Technical Information Service (NTIS). At NTIS it will be releasable to the general public, including foreign nations.

RADC-TR-83-133 has been reviewed and is approved for publication.

APPROVED: Donald W. Hanson

DONALD W. HANSON
Project Engineer

APPROVED: Frank J. Rehm

FRANK J. REHM
Technical Director
Surveillance Division

FOR THE COMMANDER: John P. Huss

JOHN P. HUSS
Acting Chief, Plans Office

If your address has changed or if you wish to be removed from the RADC mailing list, or if the addressee is no longer employed by your organization, please notify RADC (OCSP) Griffiss AFB NY 13441. This will assist us in maintaining a current mailing list.

Do not return copies of this report unless contractual obligations or notices on a specific document requires that it be returned.

COMMUNICATION SYSTEM STUDIES FOR THE SUBMARINE LASER COMMUNICATIONS SYSTEM

Jerry Nowakowski
Marek Elbaum
John Mac Eachin, Jr.

Contractor: Riverside Research Institute
Contract Number: F30602-81-C-0239
Effective Date of Contract: 1 July 1981
Contract Expiration Date: 31 October 1982
Short Title of Work: Communication System Studies for the Submarine Laser Communications
Program Code Number: 2E20
Period of Work Covered: Jun 81 - Oct 82

Principal Investigator: Dr. Marek Elbaum
Phone: 212 563-4545

Project Engineer: Dr. Donald W. Hanson
Phone: 315 330-4483

Approved for public release; distribution unlimited.

This research was supported by the Defense Advanced Research Projects Agency of the Department of Defense and was monitored by Donald W. Hanson (OCSP), Griffiss AFB NY 13441 under Contract F30602-81-C-0239.

UNCLASSIFIED

SECURITY CLASSIFICATION OF THIS PAGE (When Data Entered)

REPORT DOCUMENTATION PAGE		READ INSTRUCTIONS BEFORE COMPLETING FORM
1. REPORT NUMBER RADC-TR-83-133	2. GOVT ACCESSION NO. AD-A135 [illegible]	3. RECIPIENT'S CATALOG NUMBER
4. TITLE (and Subtitle) COMMUNICATION SYSTEM STUDIES FOR THE SUBMARINE LASER COMMUNICATIONS SYSTEM		5. TYPE OF REPORT & PERIOD COVERED Final Technical Report 26 Jun 81 - 31 Oct 82 6. PERFORMING ORG. REPORT NUMBER T-2/511-3-00
7. AUTHOR(s) Jerry Nowakowski Marek Elbaum John Mac Eachin, Jr.		8. CONTRACT OR GRANT NUMBER(s) F30602-81-C-0239
9. PERFORMING ORGANIZATION NAME AND ADDRESS Riverside Research Institute 330 West 42nd Street New York NY 10036		10. PROGRAM ELEMENT, PROJECT, TASK AREA & WORK UNIT NUMBERS 62301E D2500001
11. CONTROLLING OFFICE NAME AND ADDRESS Defense Advanced Research Projects Agency 1400 Wilson Blvd Arlington VA 22209		12. REPORT DATE June 1983 13. NUMBER OF PAGES 148
14. MONITORING AGENCY NAME & ADDRESS(if different from Controlling Office) Rome Air Development Center (OCSP) Griffiss AFB NY 13441		15. SECURITY CLASS. (of this report) UNCLASSIFIED 15a. DECLASSIFICATION/DOWNGRADING SCHEDULE N/A

16. DISTRIBUTION STATEMENT (of this Report)

Approved for public release; distribution unlimited

17. DISTRIBUTION STATEMENT (of the abstract entered in Block 20, if different from Report)

Same

18. SUPPLEMENTARY NOTES

RADC Project Engineer: Donald W. Hanson (OCSP)

19. KEY WORDS (Continue on reverse side if necessary and identify by block number)

Submarine Laser Communication
Communication Channel
Fading Channel
PPM Modulation
Coding PPM Message
Decoding

20. ABSTRACT (Continue on reverse side if necessary and identify by block number)

Analytical relationships between the parameters of interest to the user and the parameters characterizing the hardware and the propagation channel were established for the Submarine Laser Communications (SLC) system for the first time. These relationships constitute a useful framework to study the effects of a channel on the system performance not only for the ground- or space-based laser transmitter, but for the airborne transmitter as well. In the study, the utility of this analytical framework

DD FORM 1 JAN 73 1473 EDITION OF 1 NOV 65 IS OBSOLETE

UNCLASSIFIED

SECURITY CLASSIFICATION OF THIS PAGE (When Data Entered)

was demonstrated by producing a quantitative characterization of the system performance for different signal processing schemes for fading and nonfading channels. The system optimization for the strategic and tactical applications was discussed explicitly in terms of means for securing minimum scanning time or maximum operational depth, respectively.

TABLE OF CONTENTS

TABLE OF CONTENTS (CONT'D)

TABLE OF CONTENTS (CONT'D)

LIST OF FIGURES

LIST OF FIGURES (CONT'D)

LIST OF FIGURES (CONT'D)

LIST OF TABLES

LIST OF TABLES (CONT'D)

LIST OF TABLES (CONT'D)

1. INTRODUCTION AND SUMMARY

1.1 BACKGROUND

For positive control of the U.S. missile-launching submarine force, command and control messages must be reliably received by the submerged submarines in any part of the ocean in which they may operate. Towards this end, a submarine laser communication (SLC) system is being developed in which messages will be transmitted by blue-green laser light.

The SLC system will be required to deliver messages with acceptable levels of probability of detection and probability of error. Several competing approaches to the design of such a system are being evaluated. As an example, transmitters can be ground- or space-based. In the former case, orbiting mirrors will redirect the light downward over the ocean. The relative merit of each approach will be assessed on the basis of feasibility, cost, and the risks associated with development of the necessary technology.

1.2 OBJECTIVE

This study was intended as a parametric analysis representing a first step towards a quantitative understanding of how the basic SLC system parameters, characterizing hardware performance and channel properties affect the reliability of communications. The study provides a framework allowing designers 1) to redistribute the risk between the ground, space, and receiver segments; 2) to compare the relative merits of the ground-based vs. space-based laser concepts; and 3) to

study the effects not only of signal fading but other major sources of performance degradation such as structured bioluminescence background and pulse stretching due to pulse propagation through clouds. Admittedly, this framework is still tentative, primarily because of the crudeness of the channel model employed in the analysis, but the methodology developed is nonetheless helpful in the assessment of system performance.

It should be made clear that we did not estimate in this study how much uplink-generated fading one can expect or what its effect will be. (The potential sources of the signal fading were identified in the previous RRI report: Interim Technical Report, T-1/511-3-00, "Communication System Studies for the Submarine Laser Communications Uplink Program," 28 February 1982.) Instead, we sought an answer to the questions: 1) is the system sensitive to amplitude fading? 2) what constitutes an adequate statistical model of fading for selected signal processing schemes judged by RRI to be of particular interest in the SLC applications?

This study does not develop a general theory probing systematically into various conceivable alternatives for SLC communications, but instead aims at very specific objectives without the benefit of such a theory.

1.3 ANALYTICAL APPROACH

Up to now, most of the analyses of SLC system performance used idealized models for both the hardware and the channel. These models employed a single parameter, the signal-to-additive noise ratio (SNR) to measure the overall system performance. In such analyses, typically, the relative merit of different technological approaches to the SLC was analyzed in the context of the system's ability to "deliver" some level of SNR required to achieve the desired probability of detection, P_D, to a fixed depth anywhere within an operational region.

This analysis, on the other hand, shows that such an approach is too narrow and may lead to a false perception of available system tradeoffs. Our analysis was driven by the following considerations, which had not been adequately addressed in the past:

a. The SLC performance should not be characterized only in terms of the probability of detection, P_D, but in addition, it must be defined in terms of allowed probability of error, P_E. (We shall show in Section 2.2 that, with certain signal processing techniques of practical interest to the SLC system, $P_E \neq 1 - P_D$.)

b. In some strategic applications it is necessary to deliver the message as fast as possible to any area within the operational region. Therefore, it is useful to know, under fixed transmitter power conditions, the minimum scanning time necessary to deliver, to a specified depth, the required number of information bits with a desired message quality (P_E and P_D). The message format corresponding to the minimum scanning time is also of interest.

In some tactical applications, one is mostly interested in knowing the maximum depth to which a message of desired quality can be delivered within a specified time.

c. The effects of the channel-induced degradations, such as signal fading, pulse stretching, bioluminescence structured background noise, on the overall system performance should be measured in terms of a required signal-power margin and/or additional scanning time necessary to overcome these degradations.

d. The apparent need for system robustness must be reflected in any performance evaluation. The system will operate under a variety of changing conditions, so that the allowed probability of error must be kept below designated levels. Algorithms with this capability are "robust" in our

terminology. An example of a suitable robust algorithm is presented in Section 2.0. There, the message quality is characterized by P_D and $\max\{P_E\}$, where $\max\{P_E\}$ denotes the maximum value of $\{P_E\}$ for any value of SNR.

The parametric analysis establishes relationships between the key performance parameters of interest to the users and the parameters characterizing the hardware performance operating under specific channel-induced constraints. The considered performance parameters of interest are: the message quality $\{\max P_E, P_D\}$ and the scanning time together with operational depth $\{T_{sc}, \ell\}$. The considered parameters characterizing the hardware are: signal-to-noise ratio and the message redundancy r, for different levels of signal fading, {SNR, r}, where r is the ratio of the number of synchronization and parity pulses to the number of information pulses in a message. The analysis format allows system designers to trade the desired message quality with the hardware performance, and the operational environment, i.e.,

$$\{\max P_E, P_D\} \overset{\rightarrow}{\leftarrow} \{SNR, r\} \overset{\rightarrow}{\leftarrow} \{T_{sc}, \ell\}$$

There is a substantial benefit from such an analytical multidimensional parametric framework. To list only a few: 1) one can quantitatively assess the performance margins required to overcome the effects of channel-induced degradations under a fixed message quality constraint; 2) system optimization for tactical or strategic applications can be proposed and quantitatively assessed with regard to the channel; 3) the nonlinear relationship between the user system parameters and the hardware performance parameters can be fully explored and the most suitable processing schemes identified; 4) the effects of the channel on the overall system performance can be bounded.

1.4 SCOPE

The analysis was conducted for pulse position modulated (PPM) messages. A message is constructed of two segments: a synchronization segment consisting of n_s pulses and an information segment composed of Z blocks, each with n_i information and n_p parity check pulses. The synchronization pulses are used to provide a reference for measuring the positions of the pulses in the information segment. The purpose of the parity check pulses is to help achieve desired message quality $\{\max P_E, P_D\}$ despite the channel-induced degradations.

Given SNR and the channel characteristics, the number of synchronization and parity check pulses necessary to achieve a certain message quality depends on the number of information pulses. To study this dependence, we considered two types of messages: the so-called "short" message with two or four information pulses, and the so-called "long" message with two blocks of information pulses and twelve pulses to the block.

Furthermore, the synchronization segment preceding the information segment was varied from two to six pulses for both the short and long messages.

A formal similarity between the synchronization and decoding problems was noted in the computations of probabilities of error and detection for the synchronization and information segments. First, the computations were conducted separately for both segments. For the computation of overall performance, the results were appropriately combined, as shown in Section 2.3. This approach allows: 1) identification of the conditions where the overall performance was limited either by failure in establishing synchronization or in decoding; and 2) tradeoffs between the number of synchronization and parity check pulses associated with a fixed number of information pulses to optimize the overall performance.

The selected patterns for the pulses in the synchronization and information segments are discussed in Section 2.1.5. For better noise rejection, the so-called "maximum distance" patterns and "maximum distance separable" codes were considered for the synchronization and information segments, respectively. (The Reed-Solomon code belongs to the set of "maximum distance separable" codes.)

Two decoding schemes, discussed in Section 2.1.6, were analyzed: "soft" and "hard" decoding. In "soft" decoding, the decision about the positions of the transmitted pulses are made globally by interrogating simultaneously all pulses in a segment. In "hard" decoding, decisions about pulse position are made locally on a frame-by-frame basis and then a suitable algebraic decoding, involving error correction and/or erasure correction, is used.

"Soft" and "hard" decoding can employ different algorithms to detect or estimate the pulse positions. The relative merit of the algorithms considered in our analysis is discussed in Section 2.1.6. The algorithms for pattern detection can be divided in two classes: those that do not use a threshold and those that do. The maximum likelihood techniques giving optimal probability of detection belong to the first class. These algorithms can produce, however, a prohibitively high probability of error P_E, where the weak signal results in small P_D: $P_E = 1 - P_D$. On the other hand, algorithms employing thresholds are suboptimal in P_D but control of P_E is more readily accomplished. The threshold provides an additional condition: when this condition is not satisfied message decoding is not performed. This type of decision is referred to as the failure

mode. For the algorithms investigated in this report

$$P_E = 1 - P_F - P_D, \quad (P_E \neq 1 - P_D)$$

where P_F is the probability that the signal and noise pattern are below some threshold value. The idea here is to reduce tne probability of error to an acceptable level without a substantial reduction of probability of detection.

The effect of the channel-induced signal fading on the system performance was investigated systematically following an approach outlined below:

The system performance for a deterministic signal (non-fading signal) in Gaussian noise was analyzed first to develop a convenient bench mark for assessing the effects of the fading. (The considered Gaussian channel is discussed in Section 2.4.1.) The tradeoffs between the number of synchronization and parity check pulses vs. SNR were performed for short and long messages. (The SNR was defined as the ratio of signal-to-additive noise power per pulse.) The above tradeoffs were conducted separately for the synchronization and message segments. The probabilities of error and detection of the segments were appropriately combined to produce the overall message quality. Both "soft" and "hard" decoding were considered. The tradeoffs were carried out under two different sets of constraints: 1) the desired probability of detection, for the detection algorithms with no thresholds; and 2) the desired probability of detection and maximum allowable probability of error, for the detection algorithms with thresholds. Typical results are shown in Section 3.3.

It was felt that the SLC system will have to operate under the latter set of constraints. For robust signal processing employing thresholds, the tradeoffs between the synchronization and parity pulses vs. SNR were conducted by 1) selecting the

threshold values to bound the probability of error P_E; 2) finding values of SNR to obtain the desired probability of detection P_D for different message structures; and 3) computing corresponding scanning time T_{sc}.

Scanning time was computed from the following expression:

$$T_{sc} = \frac{A_T}{A} t \alpha n \cdot \sqrt{SNR}$$

where A_T = total operational area,

A = area of laser message beam at ocean surface,

t = message duration,

$$SNR = N_s^2/\sigma_o^2 \alpha 1/A^2,$$

where N_s = average number of signal photocounts in a single pulse registered by the receiver during a time slot allocated to a single pulse,

σ_o^2 = average noise power in the time slot in absence of signal,

n = total number of pulses in message.

Based on the above analysis, a "hard" decoder with thresholds emerged as a good signal processing scheme for its robustness and simplicity. This scheme was considered when studying the effects of signal fading.

The signal fading-induced performance degradation was investigated quantitatively for short and long messages. A

very simple, yet adequate, model was used for the fading statistics. The fading distribution is defined in Section 2.4.2. The distribution in its simplest form is characterized by two parameters: the mean and variance. The ratio of the standard deviation to the mean, referred to as the fading contrast C, is proportional to the square root of the probability of "losing" a signal pulse.

Throughout the analysis, we wish to answer the question: "What is the degradation measured in terms of additional SNR and/or redundancy {ΔSNR, Δr} and the corresponding increase in the scanning time ΔT_{sc} and/or the decrease in the operational depth $\Delta \ell$, for a system designed to operate with a given max P_E and P_D, {max P_E, P_D} for different values of contrast C?," i.e.,

$$\{\max P_E, P_D\} \overset{\rightarrow}{\leftarrow} \{SNR + \Delta SNR(C), r + \Delta r(C)\} \overset{\rightarrow}{\leftarrow}$$

$$\{T_{sc} + \Delta T_{sc}(C), \ell - \Delta \ell(C)\}$$

with the understanding that when C = 0, $\Delta SNR = \Delta r = \Delta T_{sc} = \Delta \ell = 0$.

A more detailed discussion of the scope and approach of the analysis is presented in Section 2.0.

1.5 SUMMARY OF RESULTS

This section summarizes the results of the study presented in more detail in Section 4.0 of this report.

1.5.1 Channel: Negligible fading, additive Gaussian noise

The following results were based on the analysis of tradeoffs between the number of synchronization and parity pulses and SNR, under constraint of message quality.

1.5.1.1 Detection algorithms with no thresholds

For the detection algorithms with no thresholds, the "soft" decoders are optimal in probability of detection and

perform appreciably better than the "hard" decoders for both the short and long messages; the difference in performance increases with the probability of detection. As an example, for the same number of parity checks, the "soft" decoder can achieve $P_D = 0.9999$ for the long and short messages with SNR lower by 2 or 3 dB than that required by the "hard" decoder.

We rejected the algorithms with no thresholds as the candidates for the SLC applications despite their optimality in P_D; the algorithms are not robust and, therefore, they can yield prohibitively high probability of error for weak signals. We focused our attention on the algorithms with thresholds for which $P_E \neq 1 - P_D$.

1.5.1.2 Detection algorithms with thresholds

In our analysis the thresholds were selected to control the probability of error under different channel conditions, thereby achieving a necessary amount of robustness. The resulting signal processing scheme is suboptimal in probability of detection. The "price" in P_D or SNR that one has to pay to secure system robustness is relatively low (one needs SNRs higher by 0.5 to 2 dB for the considered message formats, maximum probability of error, and given level P_D). Comparing, under the same conditions, the "soft" and "hard" decoders with thresholds, one concludes, based on the discussion in Section 4.1, that the "soft" decoder performs better for both the short and long messages: typically, SNRs required by the "soft" decoder are lower by 1 to 3 dB than the corresponding values for the "hard" decoder.

It is instructive to notice that, for a fixed message quality and equal number of parity pulses, the required SNRs are higher by 1 to 2 dB for the long messages than those for the short messages.

1.5.1.3 Numerical Examples: "Soft" vs. "hard" decoding for strategic applications

For a message quality of {max $P_E = 10^{-8}$, $P_D = 0.9999$} and both the long and short messages with two blocks of information pulses, twelve pulses to a block and four information pulses, respectively, we wished to know the SNR and the corresponding scanning time, T_{sc}, which is of interest in the strategic applications. Sample results are shown below.

Minimum Scanning Time, Min$\{T_{sc}\}$

		"Soft"	"Hard"	
Short Message $n_i = 4$ $Z = 1$	Min$\{T_{sc}\}$	1.00	1.05	
	SNR	17.6	20.4	dB
Long Message $n_i = 12$ $Z = 2$	Min$\{T_{sc}\}$	1.00	1.17	
	SNR	13.9	16	dB

The above results are typical for the considered message formats.

In this study the tradeoffs were performed for the minimum scanning time necessary to deliver a message to a specified depth. The results of the tradeoffs can be readily used to obtain numerical values of the maximum depth to which one can transmit messages in a specified time and with a specified quality.

1.5.2 Channel: Fading signal in Gaussian additive noise

The analysis of a fading signal was carried out for the "hard" decoder with thresholds. This signal processing scheme was identified as suitable for the SLC applications. because of its robustness and relative simplicity.

Our approach was to quantify the fading-induced degradation on the system employing signal processing designed and optimized under an assumption that fading was negligible.

The results of Section 4.2 indicate that the signal processing schemes designed for a nonfading signal are often not adequate for a fading signal. The performance degradation is more substantial for short rather than long messages: as an example, if one uses the redundancy which produces the minimum scanning time for nonfading signal, then such a system will fail in presence of even moderate fading. One needs to use up to five synchronization and parity pulses to compensate for the considered fading that results in an increase of the scanning time of up to 40%.

For those message formats where the considered signal processing allows communications with required message quality, the SNR margin necessary to compensate for the fading is not larger than 1 dB and the associated increase in the scanning time is 10% for the short messages. Corresponding margins for the long message are negligible.

As expected, for both the short and long messages, an increase in redundancy rather than in SNR proves to be a better way to combat fading.

1.6 SUGGESTION FOR FUTURE WORK

Analytical relationships between the parameters of interest to the user and the parameters characterizing the hardware and the propagation channel were established for SLC system for the first time. These relationships constitute a useful framework to study the effects of a channel on the system performance not only for the SLC-SAT systems with the ground- or space-based laser transmitter, but for SLC-AIR as well. In the study, the utility of this analytical framework was

demonstrated by producing a quantitative characterization of the system performance for different signal processing schemes for fading and nonfading channels. The system optimization for the strategic and tactical applications was discussed explicitly in terms of means for securing minimum scanning time or maximum operational depth, respectively.

Usefulness of this framework to the SLC community can be substantially increased by considering a more complete set of parameters characterizing the hardware performance and the channel. A more complete analysis should relate the parameters of interest to the user, i.e., the message quality associated with the required number of information bits, I_{inf}, {max P_E, P_D; I_{inf}} and scanning time T_{sc}, and the operational depth, {T_{sc}, ℓ} with the hardware and channel parameters which include, in addition to the already discussed SNR, redundancy r, and fading contrast C, the following ones: PRF of the transmitting laser, time slot, t_s, assigned to a pulse in a PPM frame, number of time slots in a frame, q, channel-induced pulse dispersion, Δw, and random pulse position modulation, Δk. Such a framework will allow the following tradeoffs:

$$\{\max P_E,\ P_D;\ I_{inf}\} \overset{\rightarrow}{\leftarrow} \{SNR,\ r,\ C,\ \Delta w,\ \Delta k,\ PRF,\ q\} \overset{\rightarrow}{\leftarrow} \{T_{sc},\ \ell\}$$

where

$$\max P_E \{I_{inf} = n_i \log q\},$$

and

$$P_D(n_i,\ n_s,\ q,\ SNR,\ C,\ \Delta w,\ \Delta k,\ PRF).$$

It follows that the suggested analysis will identify methods of combating the channel-induced performance degradations which can include as an example, the laser PRF and choice of t_s and q, in addition to the signal processing schemes.

Lastly, analytic framework chosen from the variety discussed above should become a valuable model for the SLC systems of interest. An experimental validation of such a model can be used as a criterion for defining the success of the SLC-AIR experiment.

2. PROBLEM DEFINITION

2.1 GENERAL

2.1.1 Modulation

The message in the SLC system is transmitted by pulse interval modulation (PIM). Two implementations of this modulation are of interest: pulse position modulation (PPM) and differential pulse interval modulation (DPIM). PPM conveys information by assigning the absolute position of pulse within one time interval, and, therefore, requires a sequence of synchronizing pulses. On the other hand, DPIM conveys information by the time differences between pulses; here synchronization is not necessary (asynchronous PPM). Following Ref. 1, this study considers only PPM. (DPIM or other implementations of PIM may have some merit, especially for "short" messages.)

2.1.2 Message Format

A message is defined by two segments: a synchronization segment and an information segment. First, the information is encoded onto a message segment by assigning a pulse's position to one of the q time slots within the time interval t_F. Each time slot is of duration t_s. The time interval t_F is referred to as a "frame", there is only one pulse in the frame, the pulse position in the frame defines a symbol. Since a pulse can be in one of the q positions in a frame, the PPM frame carries $\log_2 q$ information bits. Following this PPM frame encoding, the information is further encoded into "words", each word being a sequence

of the symbols (PPM frames). A word consisting of n_F symbols corresponds to a block $n_F \log_2 q$ bits long. Finally, the information segment is generated by forming Z blocks each of which contains n_i information pulses and n_p parity check pulses. The synchronization segment is defined by a known pattern consisting of n_s synchronization pulses. The total number of pulses is given by:

$$n = n_s + Z\ (n_i + n_p) = n_s + Zn_F \tag{2.1}$$

where n_F is the number of frames in an information block.

The detection of synchronization pattern, and message decoding, are analyzed in the following sections.

2.1.3 Synchronization

The problem of synchronization is one of estimating the position, in time, of a known pattern of synchronization pulses. The following simplifying assumptions will be useful in evaluating different synchronization schemes.

As shown in Fig. 2.1, the synchronization pulses (n_s pulses in a known pattern) are sent during observation time T. The width of each pulse is t_s. We divide the total observation time T into Q slots of width t_s.

$$T = Q \cdot t_s \tag{2.2}$$

For the model shown in Fig. 2.1 the problem of the pattern position estimation is equivalent to the problem of detection of a known pattern, when its position is unknown. It is also assumed that the signal pulses have widths comparable with the time slots.

The number of possible pattern positions is Q - d, where d is the separation (in units of t_s) between the first and last synchronization pulses. ($Q-d \approx Q$, since $Q \gg d$, shall be assumed.)

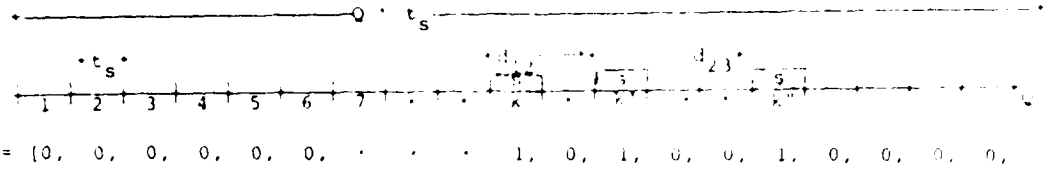

$\underline{m}_k$ = [0, 0, 0, 0, 0, 0, · · · 1, 0, 1, 0, 0, 1, 0, 0, 0, 0,

s = signal

T = $Q \cdot t_s$ = total observation interval

t_s = time slot duration

Q = number of time slots; $Q >> 1$

k = "position" of the signal pattern; $k = 1, 2, \ldots, Q$

d_{ij} = separation between ith and jth signal pulses (pattern shape)

k' = $k + d_{12}$, $k'' = k' + d_{23}$

$\{\underline{m}_k\}$ = set of all possible vectors $\underline{m}_k$

Figure 2.1 Synchronization Pattern

It should be remembered that in more realistic schemes the pattern position is described by a continuous parameter. The modification required in such a case, as well as the possibility of variable pulse shapes, should be considered separately. The model considered here, however, gives a reasonable approximation to the problem at hand whenever the pulse width is narrower than the slot width.

The set of all possible pattern positions can be described by a set of vectors $\underline{m}_k$, $k = 1, \ldots, Q - d \approx Q$. Vector $\underline{m}_k$ has Q components, all of them zero except n_s components which are each equal to one. The relative location of the non-zero components depends on the pattern shape of synchronization pulses. The pattern position is defined here by the location of first non-zero component of a vector $\underline{m}_k$, (See Fig. 2.1) so that the first non-zero component is at kth position, the second at $(k + d_{12})$th, etc.

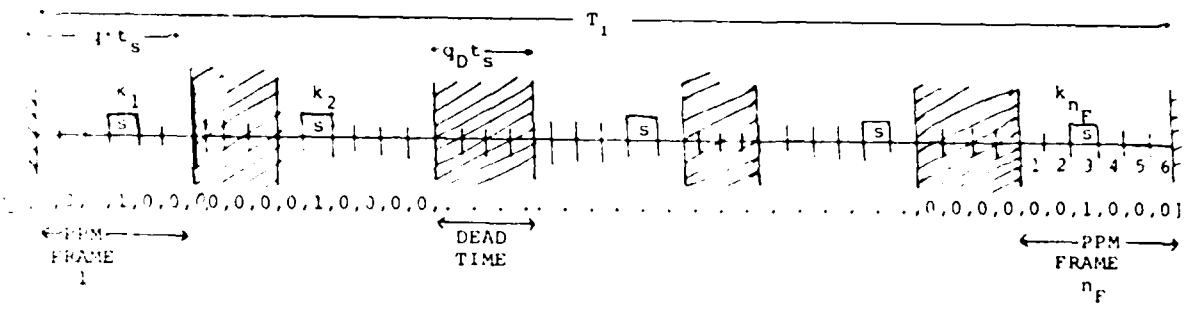

s = signal

$T_i = t_s(n_F q + (n_F - 1)q_D)$ = total duration of information segment

t_s = time slot duration

q = number of slots in PPM frame

n_F = number of frames in information segment

q_D = number of slots in "dead" time

k_i = "position" of signal pulse in i-th frame $k_i = 1, \ldots, q$

$[\alpha]$ = multiindex describing pulses position (pattern shape) $= (k_1, k_2, \ldots, k_{n_F})$

$\{\underline{m}_\alpha\}$ = set of all possible vectors $\underline{m}_\alpha$

Figure 2.2 Information Segment Pattern (One Block)

The synchronization problem is to find the pattern position k in the presence of noise. In this case k can take one of Q values, and pattern shape (i.e., d_{12}, d_{23}, ...) is known "a priori".

2.1.4 Decoding

The decoding problem is formally similar to that of synchronization. Data is encoded into words, each word is considered as a sequence of PPM frames. The resulting pattern is shown schematically in Fig. 2.2. Such a pattern can be described by a vector $\underline{m}_{\alpha}$ with non-zero components corresponding to the positions of pulses in the frames.

The decoding problem is to find a pattern shape $(\alpha) = (k_1, k_2, \ldots, k_{n_F})$ in the presence of noise. (α) can take one of q^{n_i} values for separable codes considered in this report. Thus, decoding is similar to the synchronization problem, except that the pattern position is described by a multi-index (α) rather than by a single number (k on Fig. 2.1).

Throughout this report we use the following notions interchangably: "pattern position estimation" with "pattern detection" for processing the synchronization segment, and "pattern shape estimation" with "decoding" for processing of the information segment.

2.1.5 Classification of Synchronization and Information Patterns (Coding)

For synchronization patterns and coding schemes it is useful to introduce the concept of "distance" between two patterns or codewords.

For instance, for the synchronization patterns the "distance" $d(k,\ell)$ between patterns $\underline{m}_k$ and $\underline{m}_\ell$ can be defined as:

$$d(k, \ell) = n_s - I(k,\ell), \tag{2.3}$$

where

$$I(k,\ell) = \underline{m}_k \cdot \underline{m}_\ell \tag{2.4}$$

is the number of overlaps between the signal slots in patterns $\underline{m}_k$ and $\underline{m}_\ell$. The possible range of values of I is between 0 and n_s. These definitions are analogous to those used in coding. Distance between patterns $\underline{m}_\alpha$ and $\underline{m}_{\alpha'}$ (Hamming distance) is defined as:

$$d(\alpha,\alpha') = n_F - I(\alpha,\alpha') \tag{2.5}$$

where

$$I(\alpha,\alpha') = \underline{m}_\alpha \cdot \underline{m}_{\alpha'} \tag{2.6}$$

is the number of overlaps between the signal slots in patterns $\underline{m}_\alpha$ and $\underline{m}_{\alpha'}$. The range of possible values of I is between 0 and n_F. A preferable set of patterns is characterized by values of d which are as large as possible for better noise rejection.

Another useful concept is the "distance enumerator" A(d) which gives the number of patterns separated by d from a fixed pattern.

A special class of useful synchronization patterns is referred here as "maximum distance" patterns. For these patterns $d(k,\ell)$ may take only two values, n_s and $n_s - 1$, for $k \neq \ell$. A less useful class of synchronization patterns consists of equally separated pulses. For these patterns $d(k,\ell)$ may take all values between n_s and 1 for $k \neq \ell$. The following two examples serve as an illustration of these two classes of patterns:

2.1.5.1 For "maximum distance" patterns

($d_{min} = n_s - 1$ for $k \neq \ell$),

$A(1) = \ldots = A(n_s - 2) = 0$, $A(n_s - 1) = n_s(n_s-1)$, $A(n_s) = Q$

As an example, for three synchronization pulses ($n_s = 3$) separated by non equal intervals ($d_{12} \neq d_{23}$) and distributed among Q time slots, one finds that:

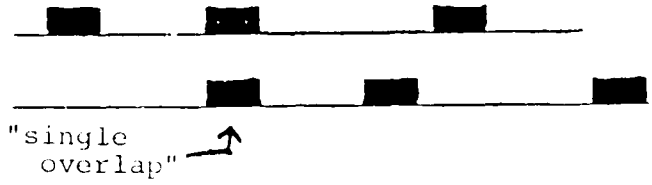

There is only one pattern (mask) which will overlap with the fixed signal pattern completely (in all three signal slots), ($I = 3$; $d = 0$; $A(0) = 1$).

There is no pattern (mask) which will overlap with the fixed signal pattern across two signal slots. ($I = 2$; $d = 1$; $A(1) = 0$).

There are six patterns (masks) which will overlap with the fixed signal pattern across one signal slot. ($I = 1$; $d = 2$; $A(2) = 6$).

There are approximately Q patterns (masks) which will not overlap with the fixed signal pattern across any of the signal slots, when $Q >> 1$. ($I = 0$; $d = 3$; $A(3) = Q$).

2.1.5.2 For equal intervals between pulses

$A(1) = A(2) = \ldots = A(n_s - 1) = 2;\ A(n_s) \simeq Q$

E.g., $n_s = 3$, $d_{12} = d_{23}$

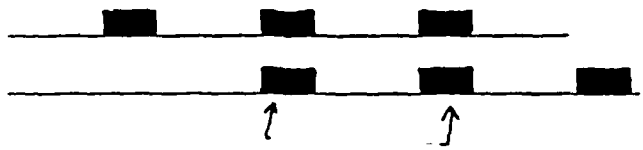

"double overlap"

I = 3, or 2, or 1, or 0

A(0) = 1

A(1) = 2

A(2) = 2

$A(3) \simeq Q$

2.1.5.3 For "maximum distance separable" (MDS)

In this study we considered MDS codes where

$$d_{min} = n_F - n_i + 1 = n_p + 1 \qquad (\alpha \neq \alpha') \tag{2.7}$$

$$A(d) = \binom{n_F}{d} \frac{(q-1)}{(q)^{d_{min}}} \sum_{i=0}^{d-d_{min}} (-1)^i \binom{d-1}{i} q^{d-i} \tag{2.8}$$

Examples of such codes are the Reed-Solomon codes for $n_F \leq q - 1$ where q is a prime number or a power of a prime number. (The Reed-Solomon codes are a family of linear q-nary codes with $d = n_p + 1$ and number of symbols $n = q - 1$. They have a check matrix of the form $H = (\alpha^{ij})$, where α is a primitive root of GF(q), $i = 0, 1, \ldots, n_p - 1$ and $j = 0, 1, \ldots, q - 2$. An MDS code with $n_F \leq n$ can be constructed from the $n_p \times (q - 1)$ check matrix of a Reed-Solomon code by selecting any subset of n_F columns out of a set of n columns).[2,3]

2.1.6 Algorithms

The choice of the detection algorithm for the synchronization pattern and decoding algorithm depends on signal and background statistics as well as on performance requirements. The condition that signal processing be performed within given time limits can restrict even further the class of applicable algorithms. Listed below are several algorithms selected either because they are optimal under certain conditions (additive, gaussian noise) or have a simple, "natural" form. We considered (Table 2.1) the following algorithms for estimating synchronization pattern position. The same algorithms are used for decoding with the replacement $k \rightarrow \alpha$. Here, vector $\underline{n}$ describes a received pattern. Algorithm A gives the maximum probability of detection for a deterministic signal in additive Gaussian background noise (most likely pattern position). It is a complete detection algorithm, i.e., it will always select some pattern position (even when no signal pattern was actually sent).

Algorithms B, C, D are incomplete detection algorithms; they have a failure mode, i.e., in certain situations, a pattern position will not be selected even if a pattern is actually sent. Such a "failure" mode, in spite of its negative connotations, can be a desirable mode if it offers robustness and/or leads to a reduction of probability of error.

TABLE 2.1 SELECTED ALGORITHMS FOR PATTERN POSITION ESTIMATION

Pattern is in kth position

ALGORITHM	COMMENTS
A*. $\underline{n} \cdot \underline{m}_k > \underline{n} \cdot \underline{m}_{k'}$	Most likely position (soft decoder Optimal for Gaussian statistics Not robust
B*. $\underline{n} \cdot \underline{m}_k > \underline{n} \cdot \underline{m}_{k'} + \alpha$ α = threshold	Failure mode
C*. $\underline{n} \cdot \underline{m}_k > \underline{n} \cdot \underline{m}_{k'}$, and $\underline{n} \cdot \underline{m}_k > \beta$; β = threshold	Failure mode Robust
D. $\underline{n} \cdot \underline{m}_k > \gamma$ for first value of k	Failure mode Poor performance

*For all k'; $k \neq k'$

Algorithm B selects the most likely pattern position and tests whether the next most likely position is separated by a sufficient energy gap ("distance"). If the result of this test is negative, suggesting some ambiguity, it declares a detection failure. This type of algorithm is attractive for systems operating with fixed and known SNR and leads to the optimal probability of detection while keeping probability of error at a desired level.

Algorithm C selects the most likely pattern position and tests whether the energy output exceeds the desired level. The proper selection of threshold will bound the probability of error for all SNR and at the same time maintain the probability of detection at a reasonable level.

Algorithm D can be used to detect pulse position within the frame and is clearly suboptimal. In detection of the position of the synchronization pattern it exhibits pathological behavior; for sufficiently large signal values it will commit an error with the probability approaching unity.

Algorithms A, B, and C make decisions based on some "global" considerations such as "largest" total energy output, etc. We will refer to the decoding schemes employing algorithms A, B, or C as "soft" decoding (with different types of thresholds). An algorithm which makes decisions based on "local" considerations and for which a more detailed discussion is important, is called a "hard" decoder.

In the "hard" decoder, pulse position estimation in a particular frame is determined independent of a decision made in any other frame. For pulse detection in a frame one of the algorithms listed above (A to D) can be used with replacement $\underline{m}_k \rightarrow \underline{m}_A$ where $\underline{m}_A$ is a vector indicating pulse position in frame A as shown in Fig. 2.3.

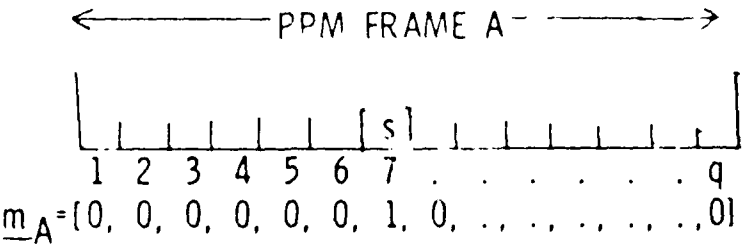

Figure 2.3 Frame Pattern

In general, there are three possible outcomes of pulse position estimation in each frame.

- Pulse position could be determined correctly with probability a_d
- Pulse position could be determined incorrectly with probability a_E
- There would be detection failure (erasure) with probability a_e (algorithms B, C and D).

All these probabilities are related:

$$a_d + a_E + a_e = 1 \tag{2.9}$$

After detection of pulse position in all frames, an appropriate algebraic decoding (error detecting, error and/or erasure correcting) scheme is applied. It is not difficult to show that a minimum distance of at least $t_E + t_d + t_e + 1$ is necessary and sufficient for correcting all combinations of t_E errors, t_e erasures and simultaneously detecting errors of magnitude $t_d \geq t_E$. (See Ref. 2.)

Other types of algorithms could also be attractive; in particular, algorithms making decisions on the basis of combination of local and global considerations. Examples of such algorithms will be given in other sections of this report.

2.2 PERFORMANCE CHARACTERIZATION

Assuming simple models of signal and background statistics (section 2.4), we shall discuss the merit of several detection and decoding algorithms described in section 2.1.6. The goal is to establish the relationship between the different quantities listed below, necessary to characterize the performance

evaluation. First, we shall give a description of these important parameters.

The signal-to-noise ratio (SNR) per pulse shall be defined as follows:

$$SNR = \frac{(\bar{N}_s)^2}{\sigma_0^2} \tag{2.10}$$

where $\bar{N}_s$ is an average value of the signal photocounts in a time slot containing a pulse and σ_0^2 is the variance of the number of photocounts registered in a slot with no signal.

The probability of decoding (P_D) is the probability that the received pattern will be decoded as the transmitted codeword.

The probability of error (P_E) is the probability that the received pattern will be decoded as the wrong codeword (other than the one transmitted).

The probability of failure (P_F) is the probability that the received pattern will not be decoded as any of the possible transmitted message words.

Note that these probabilities are related:

$$P_D + P_E + P_F = 1 \tag{2.11}$$

A decoding failure is preferable to a decoding error, but correct decoding is preferable to either of these events. Therefore, depending on performance requirements one can make tradeoffs between P_D, P_E and P_F by modifying the signal processing. An example of an algorithm which decodes any received pattern into one of the possible transmitted codewords is given by algorithm A in Section 2.1.6 (applied both for location of synchronization pulses and decoding). It is a complete decoding algorithm for which the probability of decoding failure is zero. If the cost of committing a decoding error is high, one may prefer an in-

complete decoding algorithm which will not decode any sufficiently ambiguous received pattern.

In general, the probability of detection and probability of error depend on SNR values. In the SLC system SNR will vary over considerable range for a variety of reasons (weather and water conditions, receiver depth, etc.). The demand that the SLC system should operate with P_D attaining some required value under all such conditions may not be reasonable. It is sensible, however, to require that the probability of error, P_E, should never exceed certain levels. Therefore, we have chosen the maximum allowable error probability over the entire range of SNR values to be one of the parameters defining system performance. In this sense the considered signal processing is "robust".

There are other parameters which can be useful in performance characterization. For instance, the minimum energy necessary to deliver a message, with the required probability P_D, is given by

$$E_{min} \sim \sqrt{(SNR)^*} \cdot n \tag{2.12}$$

where we assumed that $E \sim \bar{N}_s$ so that $E \sim \sqrt{SNR}$, $(SNR)^*$ - is the minimum signal-to-noise ratio required to deliver a message with the required P_D (for a given max P_E), and n denotes the total number of pulses in the message.

Since $(SNR)^*$ is an implicit function of redundancy (n_s, n_p) we can establish what message formats lead to the smallest value of E_{min}. Another example of a useful parameter (under similar conditions; given P_D and max P_E per message, etc.) is given by the total minimum energy which has to be delivered to a scanned area. Let A_T denote total scanned area (step stare mode) and A the laser message beam size. Then the number of steps required

(neglecting the possible need for overlaps) is (A_T/A). However, $\bar{N}_s \sim \sqrt{SNR} \sim (1/A)$ and therefore

$$E_{min}^{sc} \sim \frac{A_T}{A} \cdot \sqrt{(SNR)^*} \cdot n \sim (SNR)^* \cdot n \qquad (2.13)$$

Again, one can establish the tradeoffs between redundancy and E_{min}^{sc}.

The most appropriate additional parameter for performance characterization of the SLC system is, in our opinion, the minimum scanning time T_{sc}. If we denote the message duration by t we obtain

$$T_{sc} \sim (A_T/A) \cdot t \sim \sqrt{(SNR)^*}\, t$$

$$\sim \sqrt{(SNR)^*}\, [Z(n_i + n_p)(q + q_D) + n_s q_D + \Delta]t_s \qquad (2.14)$$

Here t_s denotes time slot duration and Δ denotes some small factor ($\Delta << q_D$) taking into account that synchronization pulses will not be sent at the maximum rate (for "maximum distance" synchronization patterns). We have also assumed that the laser beam moves from one spot to the next in a time no longer than $q_D t_s$.

Another formula for the minimum scanning time may be obtained under the constraint of a fixed value of PRF. If the value of $(q + q_D)t_s$ equals the inverse of the maximum allowable PRF, then the expression for minimum scanning time is of the form:

$$T_{sc} \sim \sqrt{(SNR)^*} \cdot \left[Z(n_i + n_p) + n_s\right] (q + q_D)t_s =$$

$$= \sqrt{(SNR)^*} \cdot n \cdot (q + q_D)t_s \qquad (2.15)$$

This is similar to the minimum energy necessary to deliver a message under required performance conditions.

To summarize, the selected set of parameters for performance characterization consists of max P_E, a desirable value of P_D, a required minimum SNR/pulse and scanning time as well as redundancy. Note that a complete performance characterization will require more knowledge of the background and signal statistics. The tradeoff space may be also enlarged by varying slot size as well as the number of slots per frame. One should also consider the merits of variable message formats.

It should be noted that there are different definitions of the signal-to-noise ratio depending on application as well as on signal processing. For example, another standard definition frequently used[4] is:

$$\widetilde{SNR} \approx \frac{(N_s)^2}{\text{var } n_k} \tag{2.16}$$

where n_k is the number of photocounts registered in the time slot containing the signal.

Our definition of SNR allows us to write equations used in this section in a simple form. It will be useful in a later discussion since it is independent of fading. However, neither of the definitions allows one to evaluate the performance of the system in terms of a single parameter in the case of a fluctuating signal.

2.3 APPROACH TO TRADEOFF ANALYSIS

In the diagram shown in Fig. 2.4, we present schematically the approach followed in this study leading to tradeoffs between the parameters which are of interest in the SLC system.

After selecting a message format consisting of a synchronization and an information segment, we discuss the performance of two components of a signal processing algorithm: an algorithm which detects the position of the synchronization pattern and a decoding algorithm.

Assuming additive white Gaussian background noise and a deterministic signal, we shall first discuss the performance of algorithms without thresholding. Algorithm A of Section 2.1.6 gives the maximum probability of detection of the position of synchronization pulses and, when applied to decoding ("soft" decoder), the maximum probability of correct decoding. We can, therefore, bound the value of SNR necessary to perform those tasks at the required confidence level. On the other hand, the "hard" decoder is clearly suboptimal (with the exception of zero parity checks when "soft" and "hard" decoding coincides). The choice of different decoding schemes illustrates the tradeoffs between the probabilities of error and detection.

Since algorithm A has the undesirable property that the error probability approaches unity when SNR approaches zero, some type of threshold must be applied to bound the probability of error. Threshold values were determined from the condition that maximum probability of error (for all SNR values) does not exceed some predetermined value. Note that, for the "hard" decoder, thresholding is either necessary for a given amount of redundancy, or desirable. After selection of threshold values (and proper decoding schemes for the "hard" decoder) the synchronization and decoding algorithms were combined. The relationship between different performance parameters was then discussed.

Next, we employed a simple fading signal model, and discussed fading-induced degradations of the signal processing schemes designed to meet the performance requirements for nonfading signals.

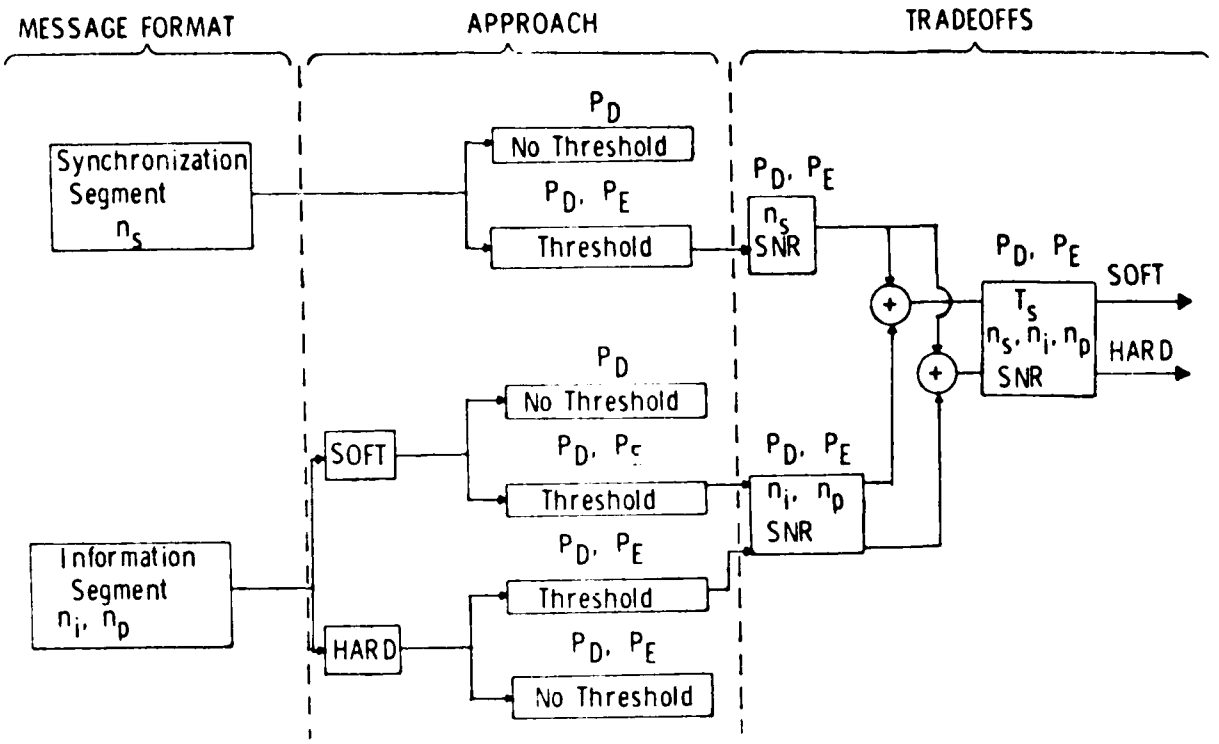

n_s = number of synchronization pulses
n_i = number of information pulses
n_p = number of parity checks
P_D = probability of detection
P_E = probability of error
T_s = scanning time
SNR = signal-to-noise ratio per pulse

Fig. 2.4 Schematic Representation of Approach Leading to Tradeoffs Between Redundancy, SNR, and Scanning Time

Let us point out certain simplifications made in the performance evaluation. Assuming appropriate algorithms for detection of the synchronization pattern and for message decoding, the evaluation of overall performance may be described by the diagram in Fig. 2.5.

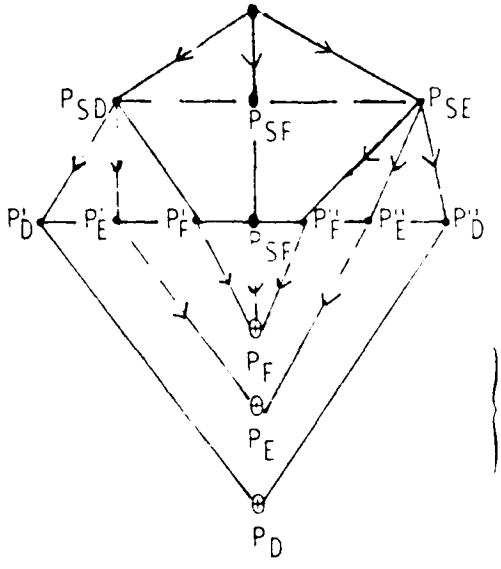

- Detection of Synchronization Pulses

  $P_{SD} + P_{SF} + P_{SE} = 1$

- Decoding

  $P'_D + P'_F + P'_E = 1$; correct synchronization

  $P''_D + P''_F + P''_E = 1$; error in synchronization

- Performance Measures

  $(P_D + P_F + P_E = 1)$

$$P_D = P_{SD}P'_D + P_{SE}P''_D$$
$$P_F = P_{SF} + P_{SD}P'_F + P_{SE}P''_F$$
$$P_E = P_{SD}P'_E + P_{SE}P''_E$$

Fig. 2.5 Schematic Representation of Performance Evaluation

In general there are three possible outputs of the algorithm for detection of synchronization pulses: probability of correct synchronization (P_{SD}), probability of synchronization error (P_{SE}) and probability of synchronization failure (P_{SF}). If detection of the synchronization pattern is correct there are three possible decoding algorithm outputs: P'_D, P'_E, and P'_F corresponding to the performance of the decoder for correct synchronization. If

detection of the synchronization pattern is erroneous, the possible outputs of the decoding algorithm are denoted by P''_D, P''_E, and P''_F. P''_D for most coding and decoding algorithms can be set at zero. Values of P''_E and P''_F depend on the type of synchronization error and the choice of decoding algorithm.

Two inequalities can easily be established:

$$1 - P_D \leq (1 - P_{SD}) + (1 - P'_D)$$

$$P_E \leq P'_E + P_{SE} \qquad (2.17)$$

The first of these gives a rather tight approximation of $(1 - P_D)$. The tightness of the second inequality depends on the choice of the decoding algorithm. If synchronization error leads to the decoding error, then this inequality is also rather tight.

The performance was bounded by evaluating $(1 - P_{SD}) + (1 - P'_D)$ and $(P'_E + P_{SE})$. Since this approach may result, for some decoding algorithms, in overestimation of the probability of error, a more extensive analysis based on an exact expression for P_E could be useful. However, such an analysis would be incomplete unless the degree to which the presence of the pulse information segment affects the errors in synchronization is also included. This depends on the relative configuration of the synchronization pulses with respect to the pulses in an information segment, the separation between frames (at present taken as equal to "dead" time), etc.

2.4 BACKGROUND AND SIGNAL STATISTICS

In the study, to bound the SLC system performance we considered two models for the channel. In the first model, discussed in Section 2.4.1, the channel does not degrade the

signal but it does introduce an additive Gaussian noise which is statistically mutually independent in all time slots during the observation time. Each time slot contains the same amount of noise power σ_0^2. Thus, the statistics of the energy registered by the receiver detector is Gaussian with the mean given by the total power in the signal and variance σ_0^2 (Eq. 2.18). In the second model, discussed in Section 2.4.2, the channel modulates the signal randomly and adds Gaussian noise with the same statistical properties as in the first model. The signal is not deterministic and the registered energy is not governed by Gaussian statistics. The performance and tradeoffs performed for the first model provide a useful limit or reference for measuring the effects of the degradations generated by the fading channel.

2.4.1 Deterministic Signal

Without any loss of generality, we assume that at the receiver, the output of a detector recording photoelectrons in different time slots is measured relative to the mean background photoelectron level. Therefore, the probability of receiving pattern $\underline{n} = (n_1, n_2, \ldots, n_Q)$ where n_ℓ is the number of photocounts in the ℓth slot, conditioned on sending the synchronization pattern characterized by $\underline{m}_k$, can be written in the compact form:

$$P(\underline{n}|\underline{m}_k) = (\sqrt{2\pi}\,\sigma_0)^{-Q} \exp[-(\underline{n} - N_s\underline{m}_k) \cdot (\underline{n} - N_s\underline{m}_k)/2\sigma_0^2] \qquad (2.18)$$

The analogous probability distribution for the information block, relevant to the decoding problem at hand, is of a similar form, with the following replacements: $Q \to n_F q + (n_F - 1)q_D$ and $\underline{m}_k \to \underline{m}_\alpha$.

2.4.2 Fading Signal

If the signal is not deterministic, it is useful to introduce the vectors $\underline{M}_k(\underline{N}_s)$ and $\underline{M}_\alpha(\underline{N}_s)$ related to the vectors

$\underline{m}_k$ and $\underline{m}_\alpha$, respectively. Vector $\underline{M}_k(\underline{N}_s)$ can be obtained from vector $\underline{m}_k$ by replacing its non-zero components (equal to one) at positions k, $k + d_{12}$, ..., $k + d_1 n_s$ by N_{s1}, N_{s2}, ..., N_{sns}. Similar relations hold between $\underline{M}_\alpha(\underline{N}_s)$ and $\underline{m}_\alpha$. With this notation we can write

$$P(\underline{n}|\underline{m}_k, \underline{N}_s) = P(\underline{n}|\underline{M}_k(\underline{N}_s)) =$$

$$= (\sqrt{2\pi}\,\sigma_0)^{-Q} \exp[-(\underline{n} - \underline{M}_k(\underline{N}_s)) \cdot (\underline{n} - \underline{M}_k(\underline{N}_s))/2\sigma_0^2] \qquad (2.19)$$

and

$$P^F(\underline{n}|\underline{m}_k) = \int_0^\infty \cdots \int P(\underline{n}|\underline{M}_k(\underline{N}_s)) p(\underline{N}_s) d^{n_s} N_s \qquad (2.20)$$

Here, $P^F(\underline{n}|\underline{m}_k)$ is the probability of receiving pattern $\underline{n}$ conditioned on sending a synchronization pattern characterized by $\underline{m}_k$ for fading signals: $P(\underline{n}|\underline{M}_k(\underline{N}_s))$ is the probability of receiving pattern $\underline{n}$ conditioned on sending a synchronization pattern characterized by $\underline{M}_k(\underline{N}_s)$: and $p(\underline{N}_s)$ is the probability distribution describing the fading of the signal.

In this study we assume that pulses are uncorrelated; therefore,

$$p(\underline{N}_s) = \prod_{i=1}^{n_s} p(N_{si}) \qquad (2.21)$$

The probability distribution for the information block has a similar form (with obvious replacements).

At present, there exists no satisfactory model of pulse fading for the problem at hand. Therefore, we decided to use a much simpler fading model which allows us to probe

into fading-induced performance degradation. A natural generalization of this model can lead to the establishment of bounds on the performance degradation, as well as a better understanding of how accurately the fading law has to be known in order to allow a sufficiently tight performance evaluation. Our approach is discussed below.

Let the signal fading be governed by some probability distribution which looks like the one shown on Fig. 2.6.

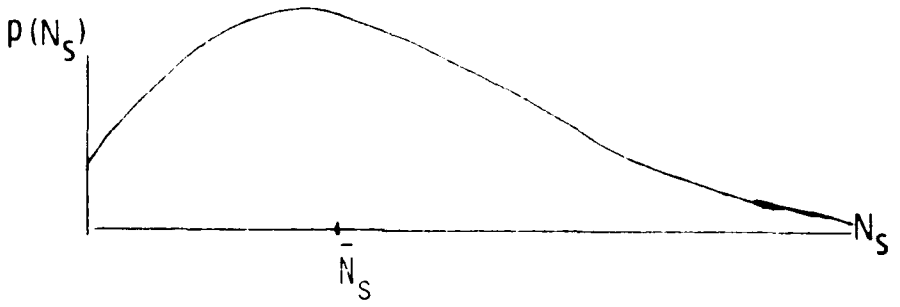

Figure 2.6 Hypothetical Probability Distribution of Fading Signal
$\bar{N}_s$ = mean value

To bound the performance of the signal processing schemes of interest we can replace the distribution in Fig. 2.6 by a much simpler distribution shown in Fig. 2.7.

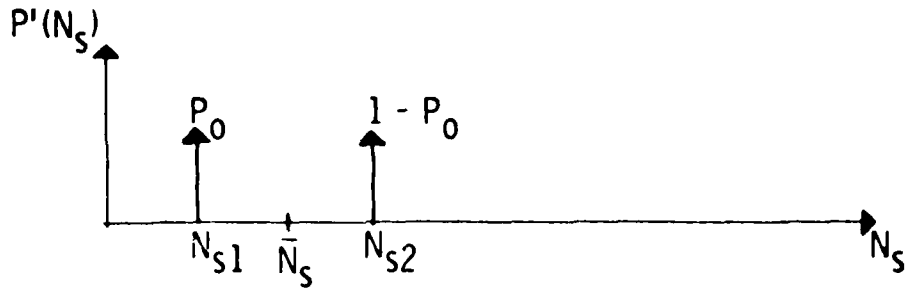

Figure 2.7 Simple Model of Fading Signal
P_o = Probability of N_s taking on value N_{s1}

This distribution is given by a combination of two Dirac delta functions

$$P'(N_s) = P_o \delta(N_s - N_{s1}) + (1 - P_o) \delta(N_s - N_{s2}); \tag{2.22}$$

The following simple relations hold:

$$\bar{N}_s = P_o N_{s1} + (1 - P_o) N_{s2},$$

$$\overline{(N_s - \bar{N}_s)^2} = \text{Var}(N_s) = P_o(1 - P_o) [N_{s1} - N_{s2}]^2 = (N_{s2} - \bar{N}_s)(\bar{N}_s - N_{s1}),$$

$$\overline{(N_s - \bar{N}_s)^3} = (2\bar{N}_s - N_{s1} - N_{s2})(\bar{N}_s - N_{s1})(\bar{N}_s - N_{s2}), \tag{2.23}$$

where the bar denotes averaging in the ensemble sense.

The term "contrast", C, is defined as

$$C = \frac{[\mathrm{Var}\{N_s\}]^{1/2}}{\bar{N}_s} \tag{2.24}$$

These expressions could be used, to relate P_o, N_{s1}, and N_{s2} to the first three moments of distribution $p(N_s)$. On the other hand, one can determine the two lowest moments and vary the remaining parameter to produce different types of fluctuating signal behavior.

Of special interest is a distribution in which N_{s1} is equal to zero. Then P_o can be interpreted as the probability of "losing" a pulse (actually, for some algorithms with a threshold, a pulse will be "lost" when N_{s1} falls below the threshold value).

In this case,

$$C = \left[\frac{P_o}{1 - P_o}\right]^{1/2} ,$$

$$\bar{N}_s = N_{s2}(1 - P_o) , \tag{2.25}$$

and for small values of P_o

$$C \approx P_o^{1/2} ,$$

$$\bar{N}_s \approx N_{s2} . \tag{2.26}$$

The natural generalization of the fading model, mentioned previously, consists of taking a combination of more than two Dirac delta functions, i.e.,

$$p^{(k)}(N_s) = \sum_{\ell=0}^{k-1} P_\ell \; \delta(N_s - N_{s\ell}),$$

where

$$\sum_{\ell=0}^{k-1} P_\ell = 1 \, , \tag{2.27}$$

and k is a small integer. Some of the parameters of this distribution can be determined from the moments of the distribution $p(N_s)$; other parameters can be estimated from global considerations; and some could be allowed to vary, reflecting the lack of precise knowledge of the fading law.

Let us also point out that with the choice of $N_{so} = 0$ and P_ℓ interpreted as a probability of a signal falling into an interval $(N_{s\ell}, N_{s\ell} + 1)$, the probability distribution $p^{(k)}(N_s)$ can be used to bound the performance degradation of a larger class of detection algorithms.

Note that the SNR defined in Section 2.4 is given by:

$$\text{SNR} = \frac{(\bar{N}_s)^2}{\sigma_0^2} \tag{2.28}$$

Thus, its numerical value does not depend on the fading. In comparison, the other definition, given in Section 2.2, has the form:

$$\widetilde{\text{SNR}} = \frac{\text{SNR}}{1 + C^2 \, \text{SNR}} \, , \tag{2.29}$$

when fading is present.

In the limit of large signal values and for fixed contrasts

$$\widetilde{\text{SNR}} \underset{\bar{N}_s \to \infty}{\approx} 1/C^2 \, . \tag{2.30}$$

(Eq. 2.29 is valid only when the signal-generated shot noise is negligible.)

2.5 SPECIFIC VALUES OF SELECTED PARAMETERS

Two types of messages are considered in this work; a "short" message (2 or 4 information pulses) and a "long" message (24 information pulses). Following reference (1), for short messages Z (number of information blocks) is taken to be unity and for long messages Z is set at two. There are some differences between the "long" message formats discussed and those suggested in Ref. (1). Those differences will not substantially alter the conclusions of the analysis.

The number of parity checks and synchronization pulses vary over a range encompassing the values suggested in Ref. (1). The number of synchronization pulses was varied from two to six and the number of parity checks per block was varied from zero to five. In the detailed analysis to follow, all numerical values for the number of time slots q in a frame, the number of time slots q_D in the "dead" time, time slot duration t_s, and observation time T, were taken from Ref. (1). Following Ref. (1), we assumed that messages are sent every T minutes for both the "short" and the "long" messages. (Selection of different values of T for the "short" and "long" messages may be more practical.)

The values of the thresholds of different algorithms were selected to give maximum error probabilities (per synchronization segment or information block) equal to 10^{-4}, 10^{-8} and 10^{-12}. Assuming a continuous mode of operation of the SLC (messages sent every T minutes), the higher value of Max P_E (10^{-4}) will give the number of incorrectly decoded messages as being smaller than (52.5/T) (1 + Z) per year, approximately.

Several figures and tradeoffs will be presented for probabilities of correct decoding taking on values .99, .999 or .9999 per message.

3. PERFORMANCE COMPUTATIONS

3.1 UNION BOUND

An exact performance evaluation of the several algorithms listed in Section 2.1.6 may require a rather tedious numerical analysis. Consider for instance algorithm A: the pattern is in position k if:

$$S_k = \underline{n} \cdot \underline{m}_k > S_\ell = \underline{n} \cdot \underline{m}_\ell \qquad (3.1)$$

for $\ell = 1, \ldots, Q, \ell \neq k$.

If k denotes the true pattern position of the synchronization pulses, then the probabilities of correct synchronization P_{SD} and erroneous synchronization P_{SE} are given by:

$$P_{SD} = \int dn_1 \ldots \int dn_Q \, p(\underline{n}|\underline{m}_k) \, \theta(S_k;S_\ell) \qquad (3.2)$$

$$P_{SE} = 1 - P_{SD}$$

where

$$\theta(S_k;S_\ell) = \begin{cases} 1 \text{ if } S_k > S_\ell \\ 0 \text{ otherwise} \end{cases} \qquad \text{for } \ell = 1, \ldots, Q, \ \ell \neq k$$

and $\underline{n}$ are continuous random variables (therefore, the probability that different S_k's are equal is negligible).

If a signal pattern consists of a single pulse, the exact calculations (for Gaussian probability distribution) are straightforward, and one can obtain compact expressions for P_{SD} or P_{SE}.

For patterns consisting of many pulses, calculations can be quite tedious and, in practice, one computes approximate values or bounds on these probabilities. One of the bounds allowing a simple interpretation is the so called "union" bound.

The following diagram illustrates the possible outcomes of pattern detection.

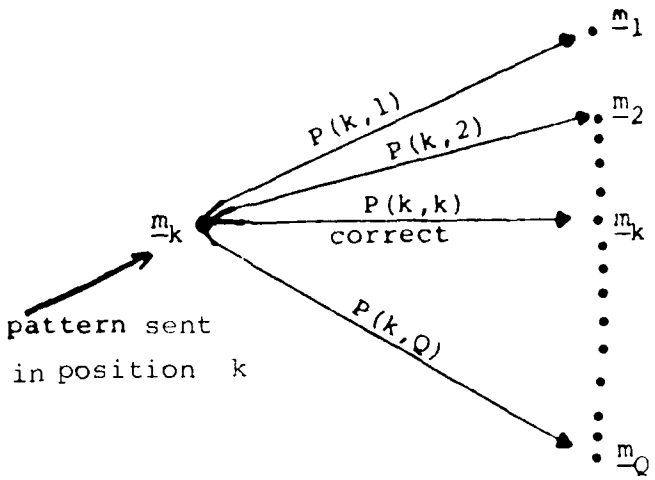

Figure 3.1 Possible Outcomes of Pattern Position Detection (Complete Detection Algorithm)

Here, the pattern was sent at position k; P(k, k) is the probability of correct detection and P(k, ℓ), ($\ell \neq k$), is the probability of detecting the pattern at an erroneous position ℓ.

The probability of erroneous synchronization and correct synchronization are given by:

$$P_{SE} = \sum_{\substack{\ell=1 \\ \ell \neq k}}^{Q} P(k,\ell);$$

$$P_{SD} = 1 - P_{SE}. \qquad (3.3)$$

Calculations of $P(k, \ell)$ are of the same level of difficulty as those for P_{SD}. These calculations are simplified by the introduction of the union bound obtained when the probabilities $P(k, \ell)$ are replaced by $\tilde{P}(k, \ell)$, where $\tilde{P}(k, \ell)$ denotes the pairwise error probability when pattern $\underline{m}_k$ was sent and pattern $\underline{m}_\ell$ was the only alternative as shown on the diagram below (Fig. 3.2).

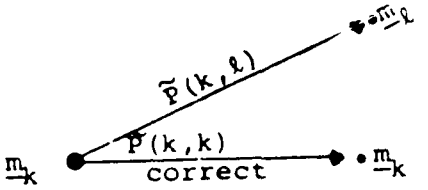

Figure 3.2 Pairwise Error Probability $\tilde{P}(k, \ell)$

Since $\tilde{P}(k, \ell) > P(k, \ell)$ we obtain the "union" bound

$$1 - P_{SD} = P_{SE} = \sum_{\substack{\ell=1 \\ \ell \neq k}}^{Q} P(k,\ell) \leq \sum_{\substack{\ell=1 \\ \ell \neq k}}^{Q} \tilde{P}(k,\ell) \quad . \tag{3.4}$$

A tighter upper bound on error probability is given by the Gallager bound.[5] Further simplification can be obtained by using a bound on $\tilde{P}(k, \ell)$. Either the Chernoff bound or its special case, the Bhattacharryya bound may be used for this purpose.[5] It is not difficult to devise a variety of other bounds which are useful in calculations of error probability.

Note that a possible outcome of the detection algorithm may include a failure component as shown in Fig. 3.3.

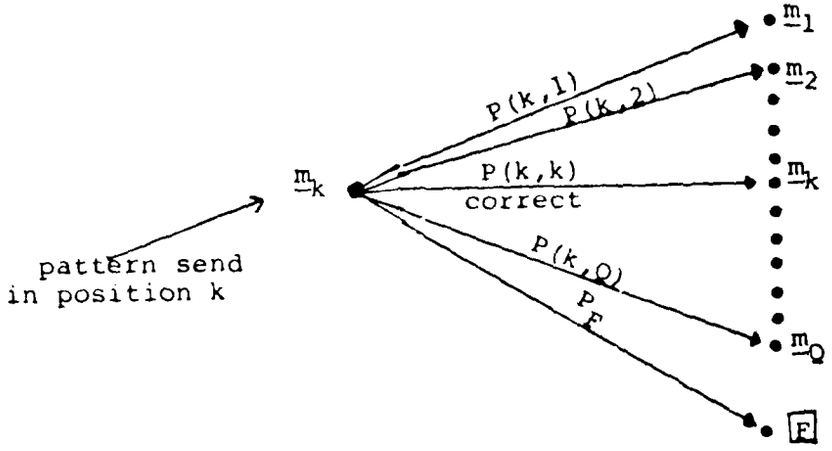

Figure 3.3 Possible Outcomes of Incomplete Detection Algorithm

This is the case when incomplete detection algorithms B or C (see Table 2.1) are used to establish the pattern position.

In this case probabilities of error and detection are given by:

$$P_{SE} = \sum_{\substack{\ell=1 \\ \ell \neq k}}^{Q} P(k,\ell) \ ,$$

$$P_{SD} = 1 - P_{SE} - P_{SF} \ , \qquad (3.5)$$

and a properly modified "union" bound may be used to bound probabilities of error and detection.

Note that the algorithms B and C (Table 2.1) can be implemented in two steps. For instance, algorithm C can be implemented by first applying algorithm A, to select the most likely pattern position k and then test if the sum of the outputs from the signal slots exceeds the threshold value. This is illustrated with Fig. 3.4. These two steps may be performed in reverse order as well. The discussed approach applies to the decoding problem and the problem of detection of the pulse position within a single frame.

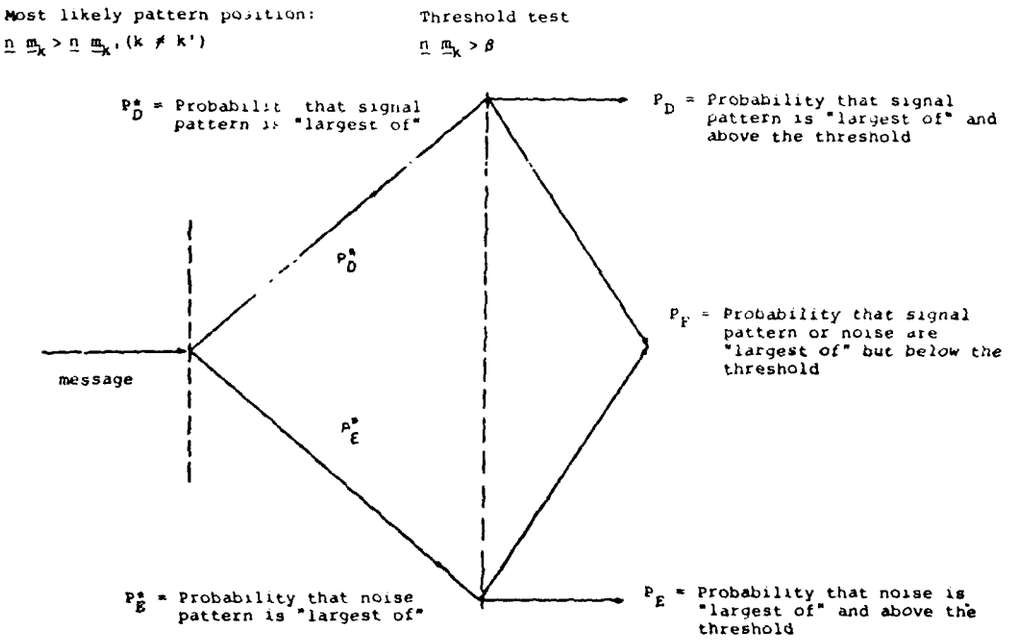

Figure 3.4 Two-step implementation of algorithm C

3.2 PERFORMANCE EVALUATION FORMULAS

In this section, we present the expressions for the probabilities of error and detection used in our performance evaluation. The derivations are based on the union bound with appropriate modifications when necessary. If we assume a deterministic signal and additive Gaussian background noise, we obtain the following formulas.

3.2.1 Algorithm A (Most likely pattern position)

$$k: \{\underline{n} \cdot \underline{m}_k > n \cdot \underline{m}_{k'} \text{ for all } k' \neq k\}$$

$$1 - P_{SD} = P_{SE} \lesssim \sum_{d=1}^{n_s} A(d)\, \tilde{P}[d \cdot SNR], \tag{3.6}$$

where

$$\tilde{P}(x) = 1/2 \text{ erfc } (\sqrt{x}/2) \ .$$

This algorithm can also be applied in decoding ("soft" decoder) with replacements $(k, k') \to (\alpha, \alpha')$, $n_s \to n_F$, etc., as well as for computation of frame errors a_E. (In this case $d = 1$ and $A(1) = q - 1$.)

3.2.2 "Hard" Decoder In Absence of Erasures

For the "hard" decoder we have considered three error correcting and error detecting schemes.

3.2.2.1 Error detection , $n_p \geq 0$

$$P_D = a_d^{n_F}$$

$$P_E = \frac{1}{(q-1)^{n_p}} \sum_{k=n_p+1}^{n_F} \binom{n_F}{k} a_E^k\, a_d^{n_F-k} \tag{3.7}$$

3.2.2.2 Single error correction, $n_p \geq 2$

$$P_D = a_d^{n_F} + \binom{n_F}{1} a_E \, a_d^{n_F-1}$$

$$P_E \simeq \frac{1}{(q-1)^{n_p-1}} \left\{ (n_F - n_p) \binom{n_F}{n_p} a_E^{n_p} a_d^{n_F-n_p} + n_F \sum_{k=n_p+1}^{n_F} \binom{n_F}{k} a_E^{k} a_d^{n_F-k} \right\} \qquad (3.8)$$

3.2.2.3 Double error correction, $n_p \geq 4$

$$P_D = (a_d)^{n_F} + \binom{n_F}{1} a_E \, a_d^{(n_F-1)} + \binom{n_F}{2} a_E^2 \, a_d^{(n_F-2)}$$

$$P_E \simeq \frac{1}{(q-1)^{n_p-2}} \left\{ \frac{(n_F - n_p)(n_F - n_p+1)}{2} \binom{n_F}{n_p-1} a_E^{(n_p-1)} a_d^{(n_F-n_p+1)} \right.$$

$$\left. + \frac{(n_F - n_p)(n_F+n_p-1)}{2} \binom{n_F}{n_p} a_E^{n_p} a_d^{(n_F-n_p)} + \frac{n_F(n_F-1)}{2} \sum_{k=n_p+1}^{n_F} \binom{n_F}{k} a_E^{k} a_d^{(n_F-k)} \right\} \qquad (3.9)$$

Note that although $a_E + a_d = 1$, $P_E \neq 1 - P_D$.

3.2.3 Algorithms B and C (Thresholds)

Algorithm B

$$k: \{\underline{n} \cdot \underline{m}_k > \underline{n} \cdot \underline{m}_{k'} + \alpha; \text{ for all } k' \neq k\} \qquad (3.10)$$

and α: {max P_{SE} = selected value}

$$P_{SE} \leq \sum_{d=1}^{n_s} A(d)\ (1/2)\ \mathrm{erfc}\ \{Z(d)\}$$

$$1 - P_{SD} \leq \sum_{d=1}^{n_s} A(d)\ (1/2)\ \mathrm{erfc}\ \{Y(d)\}\ , \qquad (3.11)$$

where

$$Z(d) = \frac{1}{2\sqrt{d}} \left\{ \sqrt{a_{TH}} + d\sqrt{SNR} \right\},$$

$$Y(d) = \frac{1}{2\sqrt{d}} \left\{ -\sqrt{a_{TH}} + d\sqrt{SNR} \right\},$$

and

$$a_{TH} = \left(\frac{\alpha}{\sigma_0}\right)^2 .$$

In the derivation of $1 - P_{SD}$ in Eq. 3.11, we have assumed that if the synchronization pattern position was detected correctly using algorithm A, it still must exceed all other possible outputs of the algorithm by a required margin. A failure to pass any of such comparisons results in a detection failure. The expression for the bound on $1 - P_{SD}$ is tight when the probability of a single failure in any of $Q - 1$ comparisons is sufficiently small.

Algorithm C

$$k: \left\{ \underline{n} \cdot \underline{m}_k > \underline{n} \cdot \underline{m}_{k'} \text{ and } \underline{n} \cdot \underline{m}_k > \beta \text{ for all } k' \neq k \right\} \quad \text{and} \quad \underline{\beta}: \left\{ \max P_{SE} = \text{selected value} \right\} \tag{3.12}$$

$$P_{SE} \leq \sum_{d=1}^{n_s} A(d)\, P(n_s, SNR, d)$$

$$1 - P_{SD} \leq 1/2 \sum_{d=1}^{n_s} A(d)\, \operatorname{erfc}\left(\sqrt{\frac{d\, SNR}{2}} \right) + 1/2\, \operatorname{erfc}\left\{ \sqrt{\frac{n_s\, SNR}{2}} - \frac{\beta/\sigma_0}{\sqrt{2\, n_s}} \right\} \tag{3.13}$$

$$b_{TH} = (\beta/\sigma_0)^2$$

where

$$P(n_s, SNR, d) = \frac{1}{2\sqrt{2\pi n_s}} \int_{\beta/\sigma_0}^{\infty} e^{-\frac{(z - (n_s - d)\sqrt{SNR})^2}{2n_s}} \operatorname{erfc}(L)\, dz$$

$$L = \frac{1}{\sqrt{2n_s - d}} \left\{ \frac{(2n_s - d)\sqrt{SNR} - z}{\sqrt{2}} \right\}$$

The second term in expression (3.13) for $(1-P_{SD})$, gives the probability that the synchronization pattern, when detected correctly, will not exceed the required threshold.

Algorithms B and C can also be applied in decoding ("soft" decoder with threshold) with replacements $(k, k') \rightarrow (\alpha, \alpha')$, $n_s \rightarrow n_F$, etc., as well as for computation of probabilities of error, erasure and detection of pulse within the frame. Note, however, that the computation of a threshold value in case of the "hard" decoder depends on the choice of a particular error and/or erasure correction, error detection mode.

3.2.4 "Hard" Decoding in Presence of Erasures

The number of possible algebraic decoding modes increases considerably when one of the possible outputs of a pulse detection algorithm within a frame is an erasure.

To describe different decoding modes it is useful to introduce the following notation:

$t_E(m)$ = number of errors corrected in presence of m erasures

$t_e(m')$ = number of erasures corrected in presence of m' errors

e.g.: $5_E(2)$ = five errors corrected in presence of two erasures.

Then different decoding modes can be described by a set of numbers.

$$\{t\} = \{t_E(0), \ldots, t_E(k); t_e(0), \ldots, t_e(k')\}$$

The decoding modes listed in Section 2.1.6, in this notation, are given by

error and erasure detecting mode, $n_p \geq 0$,

$$\{O_E(m) = O_E; O_e(m') = O_e)\}$$

$$\{t\} = \{O_E; O_e\} \quad ,$$

single error correcting, erasure detecting mode, $n_p \geq 2$,

$$\{t\} = \{1_E(0);\ 0_e\},$$

double error correcting, erasure detecting mode, $n_p \geq 4$,

$$\{t\} = \{2_E(0);\ 0_e\}\ .$$

One example of the decoding modes we have considered is described by

$$\{t\} = \{2_E(0),\ 1_E(2);\ 2_e(1),\ t_e(0)\}, n_p \geq 4,\ 2 \leq t \leq n_p$$

In this mode all double errors are corrected in the absence of erasures, all single errors are corrected in the presence of double and single erasures, (also single and double erasures are corrected in the presence of a single error), and t_e erasures are corrected in absence of errors.

We have listed below some of the formulas used to evaluate the probability of correct decoding and the probability of error:

- $\underline{\{0_E,\ 0_e\}}$

$$P'_D(0_E,\ 0_e) = a_d^{(n_F)}$$

$$P'_E(0_E,\ 0_e) = (q-1)^{-n_p} \sum_{k=n_p+1}^{n_F} \binom{n_F}{k} a_E^{(k)}\ a_d^{(n_F-k)} \qquad (3.14)$$

- $\underline{\{0_E,\ t_e(0)\}}$

$$P'_D(0_E,\ t_e(0)) = P'_D(0_E,\ 0_e) + \sum_{k=1}^{t} \binom{n_F}{k} a_e^{(k)}\ a_d^{(n_F-k)} \qquad (3.15)$$

$$P'_E(0_E,\ t_e(0)) = P'_E(0_E,\ 0_e) + \sum_{i=1}^{t} \frac{a_e^{i}}{(q-1)^{n_p-i}} \sum_{k=n_p+1}^{n_F} \binom{n_F}{k}\binom{k}{i} a_E^{(k-i)}\ a_d^{(n_F-k)}$$

- $\{1_E(0),\ 0_e\}$

$$P'_D(1_E(0),\ 0_e) = P'_D(0_E,\ 0_e) + \binom{n_F}{1} a_E\, a_d^{(n_F-1)} \tag{3.16}$$

$$P'_E(1_E(0),\ 0_e) \simeq (q-1)^{-n_p+1} \left\{ (n_F - n_p) \binom{n_F}{n_p} a_E^{(n_p)}\, a_d^{(n_F-n_p)} + n_F \sum_{k=n_p+1}^{n_F} \binom{n_F}{k} a_E^{(k)}\, a_d^{(n_F-k)} \right\}$$

- $\{1_E(0),\ t_e(0)\}$

$$P'_D(1_E(0),\ t_e(0)) = P'_D(1_E(0),\ 0_e) + \sum_{k=1}^{t} \binom{n_F}{k} a_e^{(k)}\, a_d^{(n_F-k)} \tag{3.17}$$

$$P'_E(1_E(0),\ t_e(0)) \simeq P_E(1_E(0),\ 0_e) + \sum_{\ell=1}^{t} \frac{a_e^{(\ell)}}{(q-1)^{n_p-\ell}} \sum_{k=n_p+1}^{n_F} \binom{n_F}{k}\binom{k}{\ell} a_E^{(k-\ell)}\, a_d^{(n_F-k)}$$

- $\{1_E(1);\ 1_e(1),\ t_e(0)\}$

$$P'_D(1_E(1);\ 1_e(1),\ t_e(0)) = P'_D(1_E(0),\ t_e(0)) + \binom{2}{1}\binom{n_F}{2} a_e\, a_E\, a_d^{(n_F-2)} \tag{3.18}$$

$$P'_E(1_E(1),\ 1_e(1),\ t_e(0)) \simeq P'_E(1_E(0),\ t_e(0)) +$$

$$+ (q-1)^{-n_p+2} \left[(n_F-n_p) \binom{n_F}{n_p}\binom{n_p}{1} a_e\, a_E^{(n_p-1)}\, a_d^{(n_F-n_p)} + (n_F-1) a_e \sum_{k=n_p+1}^{n_F} \binom{n_F}{k}\binom{k}{1} a_E^{(k-1)} a_d^{(n_F-k)} \right]$$

- $\{2_E(0),\ 0_e\}$

$$P'_D(2_E(0),\ 0_e) = P'_D(1_E(0),\ 0_e) + \binom{n_F}{2} a_E^2\, a_d^{(n_F-2)} \tag{3.19}$$

$$P'_E(2_E(0),\ 0_e) \simeq (q-1)^{-n_p+2} \left[\frac{(n_F-n_p)(n_F-n_p+1)}{2} \binom{n_F}{n_p-1} a_E^{(n_p-1)}\, a_d^{(n_F-n_p+1)} \right.$$

$$\left. + \frac{(n_F-n_p)(n_F+n_p-1)}{2} \binom{n_F}{n_p} a_E^{(n_p)}\, a_d^{(n_F-n_p)} + \frac{n_F(n_F-1)}{2} \sum_{k=n_p+1}^{n_F} \binom{n_F}{k} a_E^{(k)}\, a_d^{(n_F-k)} \right]$$

- $\{2_E(0),\ t_e(0)\}$

$$P'_D(2_E(0),\ t_e(0)) = P'_D(2_E(0),\ 0_e) + \sum_{k=1}^{t} \binom{n_F}{k} a_e^{(k)} a_d^{(n_F-k)} \tag{3.20}$$

$$P'_E(2_E(0),\ t_e(0)) \simeq P'_E(2_E(0),\ 0_e) + \sum_{\ell=1}^{t} \frac{a_e^{\ell}}{(q-1)^{n_p-\ell}} \sum_{k=n_p+1}^{n_F} \binom{n_F}{k}\binom{k}{\ell} a_E^{(k-\ell)} a_d^{(n_F-k)}$$

- $\{2_E(0),\ 1_E(1);\ 1_e(1),\ t_e(0)\}$

$$P'_D(2_E(0),\ 1_E(1);\ 1_e(1),\ t_e(0)) = P'_D(2_E(0),\ t_e(0)) + \binom{n_F}{2}\binom{2}{1} a_e a_E a_d^{(n_F-2)} \tag{3.21}$$

$$P'_E(2_E(0),\ 1_E(1);\ 1_e(1),\ t_e(0)) \simeq P'_E(2_E(0),\ t_e(0)) + (q-1)^{-n_p+2}$$

$$\left[(n_F-n_p) \binom{n_F}{n_p}\binom{n_p}{1} a_e a_E^{(n_p-1)} a_d^{(n_F-n_p)} + (n_F-1)\ a_e \sum_{k=n_p+1}^{n_F} \binom{n_F}{k}\binom{k}{1} a_E^{(k-1)} a_d^{(n_F-k)} \right]$$

- $\{2_E(0),\ 1_E(2);\ 2_e(1),\ t_e(0)\}$

$$P'_D(2_E(0),\ 1_E(2);\ 2_e(1),\ t_e(0)) = P'_D(2_E(0),\ 1_E(1);\ 1_e(1),\ t_e(0)) + \tag{3.22}$$

$$+ \binom{n_F}{3}\binom{3}{2} a_e^2 a_E a_d^{(n_F-3)}$$

$$P'_E(2_E(0),\ 1_E(2);\ 2_e(1),\ t_e(0)) \simeq P'_E(2_E(0),\ 1_E(1);\ 1_e(1),\ t_e(0)) +$$

$$+ (q-1)^{-n_p+3} \left[(n_F-n_p) \binom{n_F}{n_p}\binom{n_p}{1} a_e^2 a_E^{(n_p-2)} a_d^{(n_F-n_p)} + (n_F-2)\ a_e^2 \sum_{k=n_p+1}^{n_F} \binom{n_F}{k}\binom{k}{2} a_E^{(k-2)} a_d^{(n_F-k)} \right]$$

3.2.5 Performance Formulas in the Presence of Fading

Let $p(\underline{N}_S)$ be a probability distribution describing the fading of the signal. We assume that pulses are uncorrelated, therefore,

$$p(\underline{N}_S) = \prod_{i=1}^{n_S} p(N_{Si}) \tag{3.23}$$

Denoting the average of the function $f(\cdot)$ by $\langle f(\underline{N}_s) \rangle_{\underline{N}_s}$

where

$$\langle f(\underline{N}_s) \rangle_{\underline{N}_s} = \int_0^\infty dN_{s1} \cdots \int_0^\infty dN_{sn_s} \; f(\underline{N}_s) p(\underline{N}_s) \tag{3.24}$$

we can write a generalization of the expressions in sections 3.2.1 and 3.2.2 in the following form

3.2.5.1 Algorithm A

$$1 - P_{SD} \lesssim \sum_{d=1}^{n_s} A(d) \; \tilde{P}^*(d),$$

where (3.25)

$$\tilde{P}^*(d) = \frac{1}{2} \left\langle \operatorname{erfc} \frac{N_{s1} + N_{s2} + \ldots N_{sd}}{2\sqrt{d}} \right\rangle_{\underline{N}_s} .$$

3.2.5.2 Algorithm B

$$P_{SE} \lesssim \sum_{d=1}^{n_s} A(d) \, 1/2 \left\langle \operatorname{erfc} Z^*(d) \right\rangle_{\underline{N}_s} ,$$

$$1 - P_{DE} \lesssim \sum_{d=1}^{n_s} A(d) \, 1/2 \left\langle \operatorname{erfc} Y^*(d) \right\rangle_{\underline{N}_s} , \tag{3.26}$$

where

$$Z^*(d) = \frac{1}{2\sqrt{d}} \left\{ \sqrt{a_{th}} + \frac{N_{s1} + N_{s2} + \ldots + N_{sd}}{} \right\} ,$$

and

$$Y^*(d) = \frac{1}{2\sqrt{d}} \left\{ -\sqrt{a_{th}} + \frac{N_{s1} + N_{s2} + \ldots + N_{sd}}{} \right\} .$$

3.2.5.3 Algorithm C

$$P_{SE} \leq \sum_{d=1}^{n_s} A(d)\ P^*(n_s,\ d),$$

$$1 - P_{SD} \leq 1/2 \sum_{d=1}^{n_s} A(d)\ \left\langle \operatorname{erfc}\left(\frac{N_{s1} + N_{s2} + \ldots + N_{sd}}{2(\sqrt{d})\ \sigma_0}\right)\right\rangle_{N_s}$$

$$+ 1/2\ \left\langle \operatorname{erfc}\left(\frac{N_{s1} + N_{s2} + \ldots + N_{sn_s} - \beta}{\sqrt{2n_s}\ \sigma_0}\right)\right\rangle_{N_s},$$

(3.27)

where

$$P^*(n_s,\ d) = \frac{1}{2\sqrt{\pi}} \left\langle \int_b^{\infty} e^{-y^2} \operatorname{erfc}\left(\frac{a - y(1 - \rho)}{1 - \rho^2}\right) dy \right\rangle_{N_s}$$

and

$$a = \frac{N_{s1} + N_{s2} + \ldots + N_{sd}}{\sqrt{2n_s}\ \sigma_0},$$

$$b = \frac{\beta - (N_{sd} + \ldots + N_{sn_s})}{\sqrt{2n_s}\ \sigma_0},$$

$$\rho = 1 - \frac{d}{n_s}.$$

where

$$\tilde{P}_D(m) = Q/2 \text{ erfc } \left\{ \frac{(n_s - m)\sqrt{SNR}}{2\sqrt{n_s(1 - P_o)}} \right\}$$

$$+ (n_s - 1)(n_s - m)\ 1/2 \text{ erfc } \left\{ \frac{(n_s - m - 1)\sqrt{SNR}}{2\sqrt{n_s - 1}\ (1 - P_o)} \right\}$$

$$+ 1/2 \text{ erfc } \left\{ \frac{-\sqrt{b_{TH}} + (n_s - m)\sqrt{SNR/(1 - P_o)}}{\sqrt{2n_s}} \right\},$$

$$\tilde{P}_E(m) = \frac{Q}{2\sqrt{\pi}} \int_{b_o}^{\infty} dy\ e^{-y^2}\ \text{erfc}[a_o(m) - y]$$

$$+ (n_s - 1)(n_s - m)\ \frac{1}{2\sqrt{\pi}} \int_{b_1(m)} dy\ e^{-y^2}\ \text{erfc}\left[\frac{a_1(m) - y(1-\rho)}{\sqrt{1-\rho^2}} \right],$$

$$b_o = \sqrt{\frac{b_{TH}}{2n_s}}\ ,\quad a_o(m) = \frac{(n_s - m)\sqrt{SNR}}{\sqrt{2n_s}\ (1 - P_o)}\ ,$$

$$b_{TH} = (s/J_o)^2\ ,\quad b_1(m) = \frac{\sqrt{b_{TH}} - \sqrt{SNR/(1 - P_o)}}{\sqrt{2n_s}}\ ,$$

$$\rho = 1/n_s\ ,\quad a_1(m) = \frac{(n_s - m - 1)\sqrt{SNR}}{\sqrt{2n_s}\ (1 - P_o)}\ .$$

Again, values of $\tilde{P}_E(m)$ and $\tilde{P}_D(m)$ should not exceed unity.

The above formulas, bounding probabilities of error and detection, are valid for the decoding problem as well as the pulse detection within a single frame. For certain models of fluctuating signals the bounds may not be sufficiently tight. One should also remember that in evaluating terms of the form

$$\langle A(d)\ f(d, \underline{N}) \rangle_{\underline{N}_s}$$

the value of $\langle A(d)\ f(d, \underline{N}) \rangle$ can not exceed unity.

In addition, one can easily obtain better approximations for certain fading models. For instance, when the model of a fluctuating signal in which a pulse is "lost" with probability P_o was used (see Section 2.4), we bounded the performance of algorithm C for the detection of "maximum" distance synchronization patterns using the following formulas:

$$1 - P_{SD} \lesssim P_o^{n_s} + n_s P_o^{n_s-1} (1 - P_o) + \sum_{m=0}^{n_s-2} P_o^m (1 - P_o)^{n_s-m} \binom{n_s}{m} \tilde{P}_D(m) , \tag{3.28}$$

$$P_{SE} \lesssim \sum_{m=0}^{n_s-1} P_o^m (1 - P_o)^{n_s-m} \binom{n_s}{m} \tilde{P}_E(m) + P_o^{n_s} \cdot \frac{2}{2\sqrt{\pi}} \int_{b_o}^{\infty} dy\ e^{-y^2}\ \mathrm{erfc}(-y)$$

3.3 SELECTED NUMERICAL RESULTS AND DISCUSSION

In this section the performance of different signal processing schemes will be evaluated for the selected parameters discussed in Section 2.5. The numerical results are based on the formulas presented in Section 3.2.

3.3.1 Algorithm A (Synchronization, "soft" decoder, frame errors)

In Fig. 3.5 we have plotted the union bound as applied to the probabilities of synchronization (on a logarithmic scale) vs. SNR for a number of synchronization pulses and two classes of synchronization patterns defined in Section 2.1.5: "maximum distance" synchronization patterns (patterns a) and patterns of equally separated pulses (patterns b). The value for Q was taken from Ref. (1). When the bounds on the probability of error approach unity (which is a region of little interest to us), the bounds are not very tight. Indeed, the probability of error never attains unity even for SNR = 0 (then it is equal to $1 - 1/Q$).

The probability of synchronization error decreases rather rapidly as we increase the number of pulses for patterns a. Note that for a relatively low SNR, the term proportional to $Q \cdot P(n_s SNR)$ dominates the error probability. In this case the error patterns are distributed (with similar probabilities) among all $Q - 1 \simeq Q$ possible pattern positions. In this region of SNR the probability of error for patterns a and b are approximately the same.

As SNR increases, the subclass of possible error patterns which overlap with the true pattern position begins to dominate the error probability. In particular, for patterns a, for sufficiently high SNR, $P_{SE} \simeq n_s(n_s - 1)\,\tilde{P}((n_s - 1)SNR)$. For patterns b, $P_{SE} \simeq 2\,\tilde{P}(SNR)$ and is independent of n_s (for $n_s \geq 2$). This type of behavior is displayed in Fig. 3.5. As SNR increases,

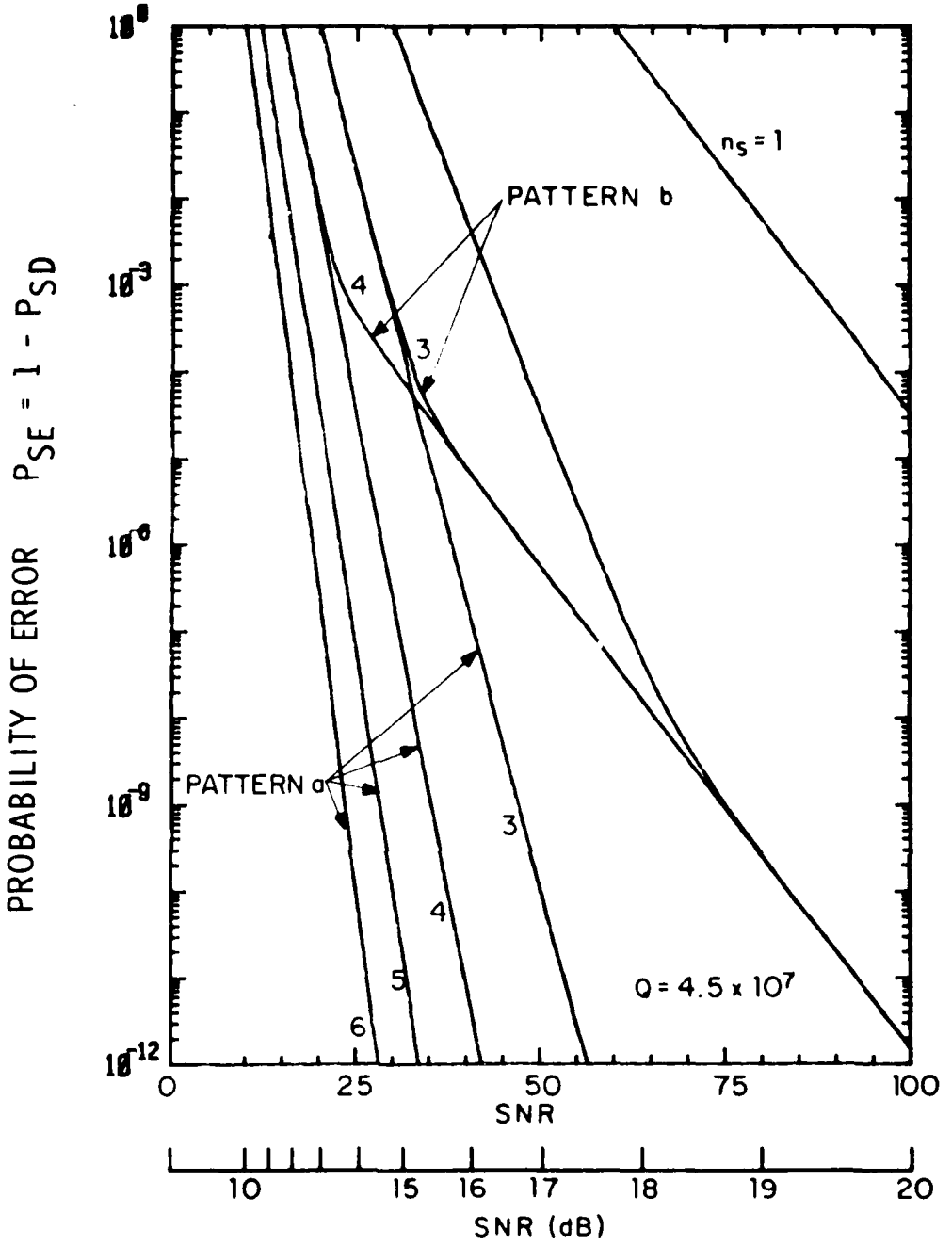

Fig. 3.5 Performance of synchronization algorithm A
Probability of synchronization error vs SNR/pulse for different numbers of synchronization pulses n_s

Pattern a is maximum distance pattern
Pattern b is pattern of equally separated pulses
Q = number of possible pattern position during observation time

the probability of error for patterns b (for three and four synchronization pulses) decreases at a slower rate than for patterns a. At some value of SNR, the probabilities of error for patterns b with three and four synchronization pulses are practically equal and at larger values of SNR the probability of error for these patterns approaches the probability of error for the pattern of two pulses. Note also that the probability of error can be well approximated by segments of straight lines in different regions of SNR values. It is obvious that the "maximum distance" synchronization patterns are far better than the patterns of equally separated pulses. Therefore, this is the type of pattern which was selected by us for the trade-off analysis.

In the detection of synchronization patterns, the formulas for probability of error do not take into account the effect of the presence of information pulses. It is clear, however, that we should add at least $n \cdot Z \cdot n_F$ terms, each term equal to $\tilde{P}((n_s-1)SNR)$ which corresponds to the synchronization error patterns having a single overlap with the information pulses. In addition, there might be terms corresponding to two or more overlaps (they are message-dependent). As noted before, in order to have a complete expression one needs to know the relative configuration of synchronization pulses vs. the pulses in the information segment, the separation between the frames, etc. The degradation due to these effects can be controlled to some extent but it deserves further attention.

The probability of error vs. SNR for a "soft" decoder (single block) is illustrated in Fig. 3.6 for three values of the number of information pulses. The graphs show how the probability of error changes with the increase of the number of parity checks. There is a change in slope of the

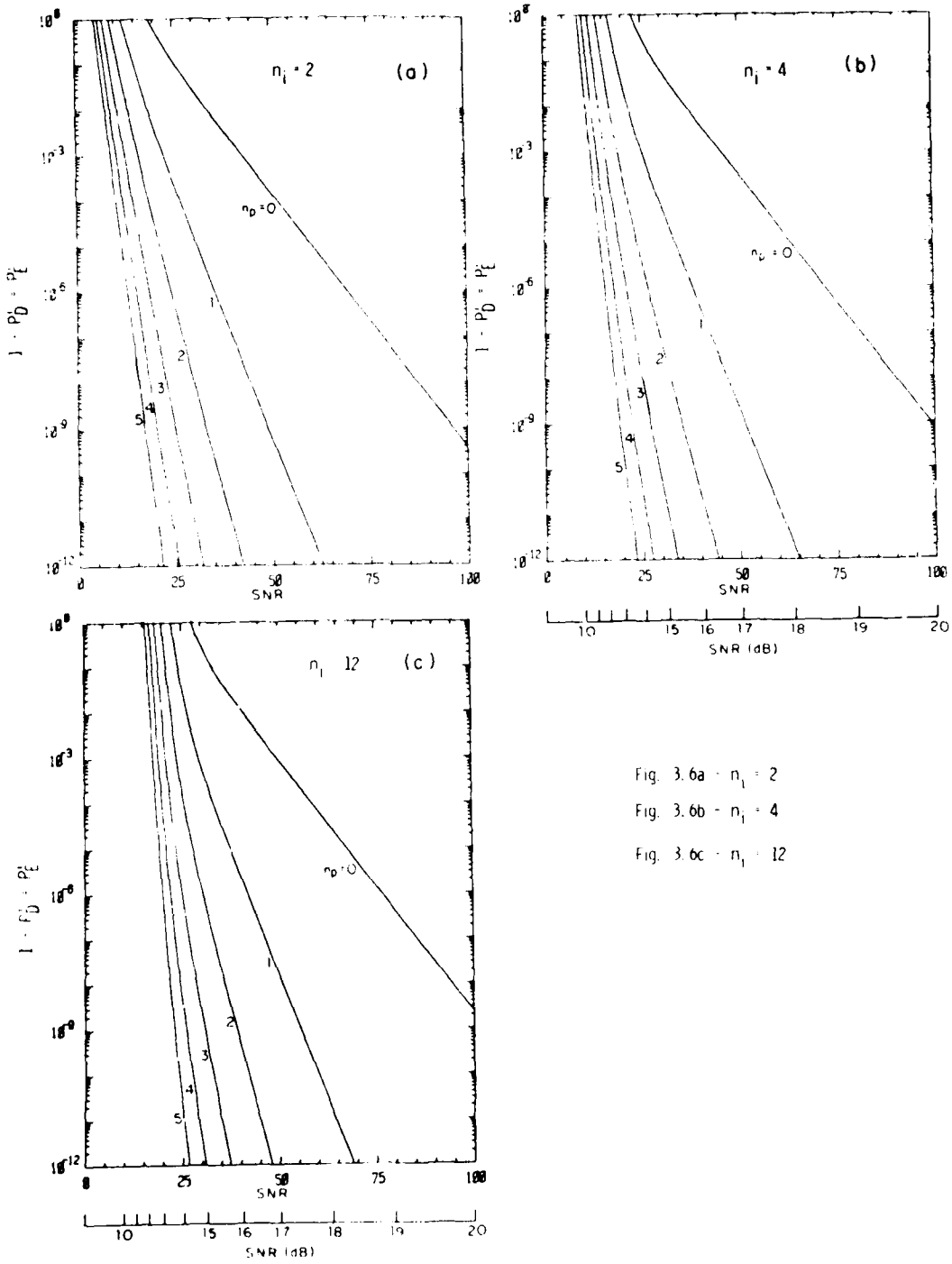

Fig. 3.6a - $n_i = 2$

Fig. 3.6b - $n_i = 4$

Fig. 3.6c - $n_i = 12$

Fig. 3.6 Performance of "soft" decoder, algorithm A. Probability of decoding error vs SNR/pulse for different number of information pulses n_i and parity check pulses n_p

curves as the number of parity checks varies, and as the value of SNR increases. The latter change is more noticeable for the lowest numbers of parity checks. In addition there is a shift toward lower SNR values as the number of parity checks increases. When SNR approaches zero, the probability of error approaches unity; in the region where probability of error is high the graphs are not very accurate (an undesirable property of the "union" bound).

In general, the comparison of the three graphs in Fig. 3.6 is indicative of a general tendency, i.e.: probability of error increases with the number of information pulses. It is clear, however, that for a fixed number of parity checks a small relative change in the number of information pulses will cause only a small change in the probability of error.

Fig. 3.7 shows the probability of frame error vs. SNR. Since the computations were based on the "union" bound, at very low SNR values (probability of error approaching one) the graph does not give a tight approximation of the error probability. It is worth noting, however, that numerical calculations of the error probability can be carried out using the exact expression for the frame error probability:

$$a_E = 1 - \frac{1}{\sqrt{\pi}} \int_{-\infty}^{\infty} \exp\left\{-\left(x - \sqrt{\frac{SNR}{2}}\right)^2\right\} \left(1 - \frac{1}{2}\,\mathrm{erfc}\,x\right)^{q-1} dx \qquad (3.29)$$

3.3.2 "Hard" Decoder In Absence of Erasures

In Fig. 3.8 - 3.10 we have plotted the probability of decoding and the probability of error for a different number of information pulses and parity checks in three detection modes

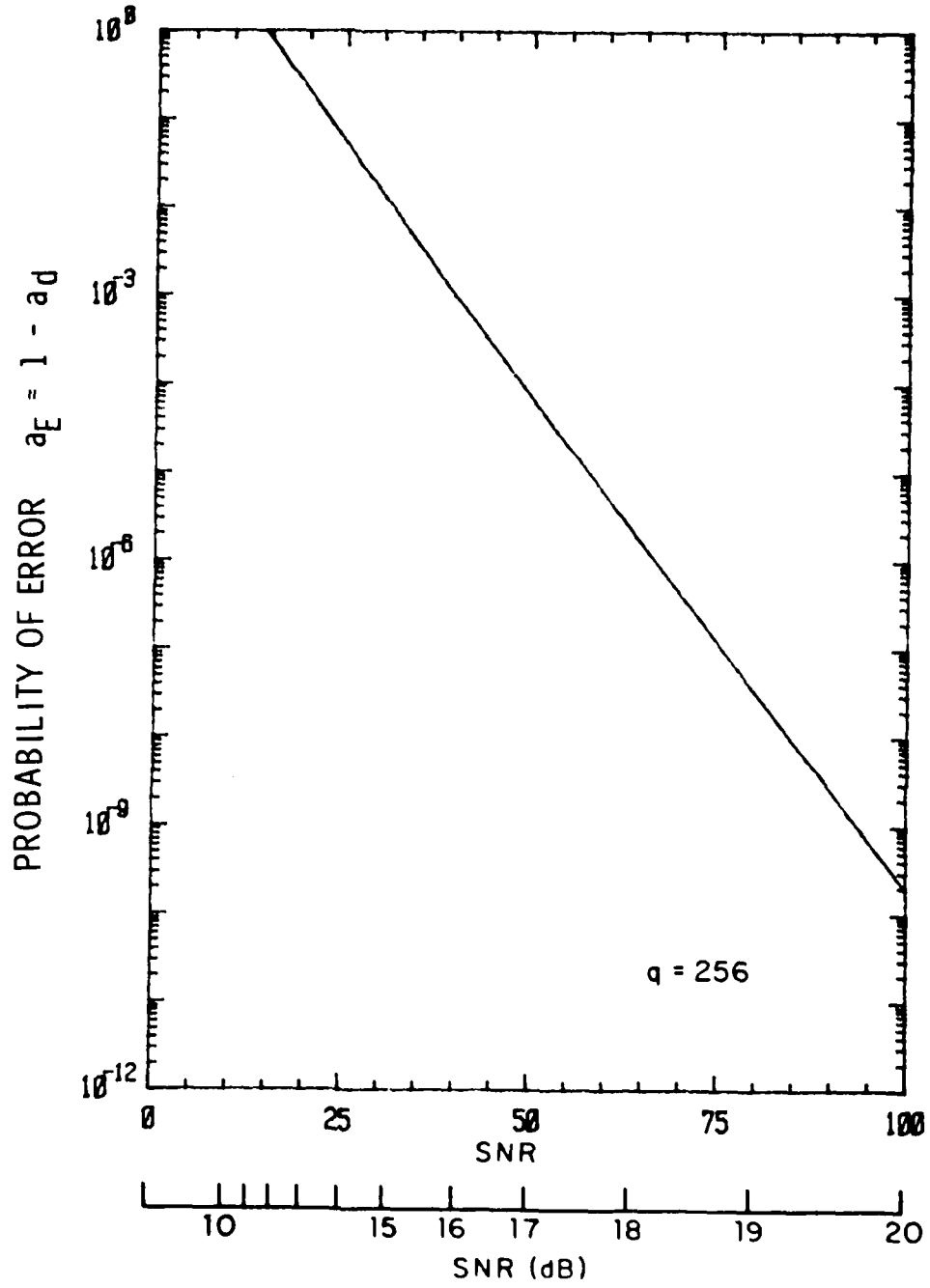

Fig. 3.7 Probability of frame error vs SNR/pulse for algorithm A (q is the number of time slots in a frame)

based on the probability of the frame error shown in Fig. 3.7. Figures 3.8a, 3.9a and 3.10a show this dependence in the error detection mode.

The probability of detection decreases slightly when the number of parity checks increases, and the change is smallest for twelve information pulses (because this produces a smaller relative change in total number of pulses in the block).

The probability of error decreases rapidly with an increase in the number of parity checks. Note the abrupt change of the probability of error at low SNR values is artificial. In the region where the "union" bound fails to give a tight approximation to the probability of frame error, we bounded the error probability by $\leq 1/q^{n_p}$. A better numerical approximation for the probability of frame error will give a smoother transition. When the probabilities of decoding and decoding error are considered in the single error correction mode ($n_p \geq 2$), (Figs. 3.8b, 3.9b and 3.10b) we note that the probability of detection improves in comparison with the error detection mode, but at the cost of a higher probability of error. At low SNR/pulse values the probability of error is bounded by $\leq n_p/q^{n_p-1}$.

Other relationships such as the dependence of the probabilities of error and detection on the number of information pulses and parity checks are similar to those described for Figs. 3.8a, etc. A continuation of the tradeoffs between the probabilities of decoding and decoding error is illustrated in Figs. 3.8c, 3.9c and 3.10c for $n_p \geq 4$. Here the decoder is operating in the double error correction mode. The probability of error at low SNR values is bounded by $n_F(n_F-1)/2q^{n_p-2}$. Note that, in contrast to the soft decoder (without threshold), the

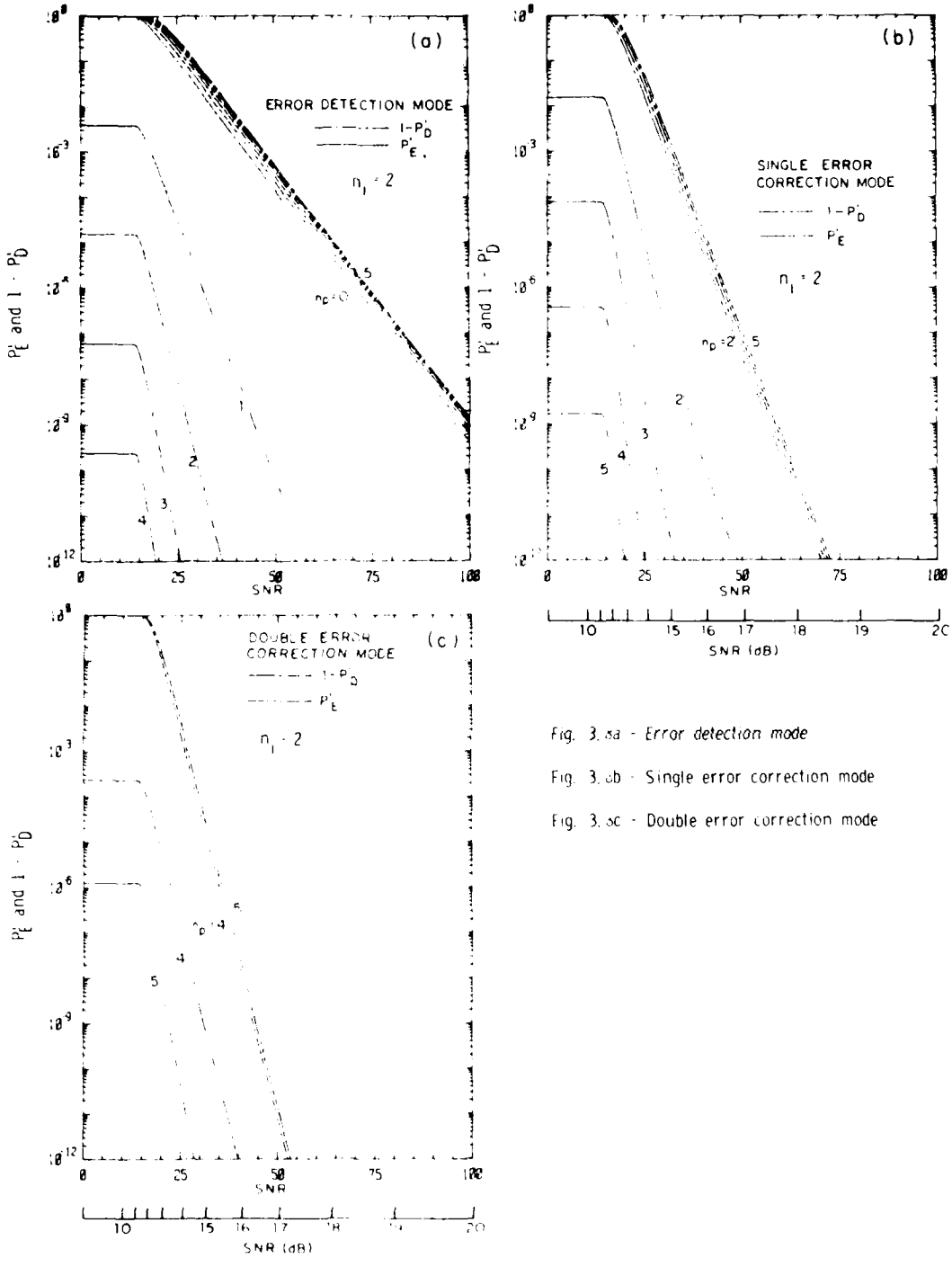

Fig. 3.5a - *Error detection mode*

Fig. 3.5b - Single error correction mode

Fig. 3.5c - Double error correction mode

Fig. 3.5 Performance of "hard" decoder. Probability of correct decoding and decoding error vs SNR pulse for two information pulses n_I, different number of parity checks n_p, and selected decoding modes.

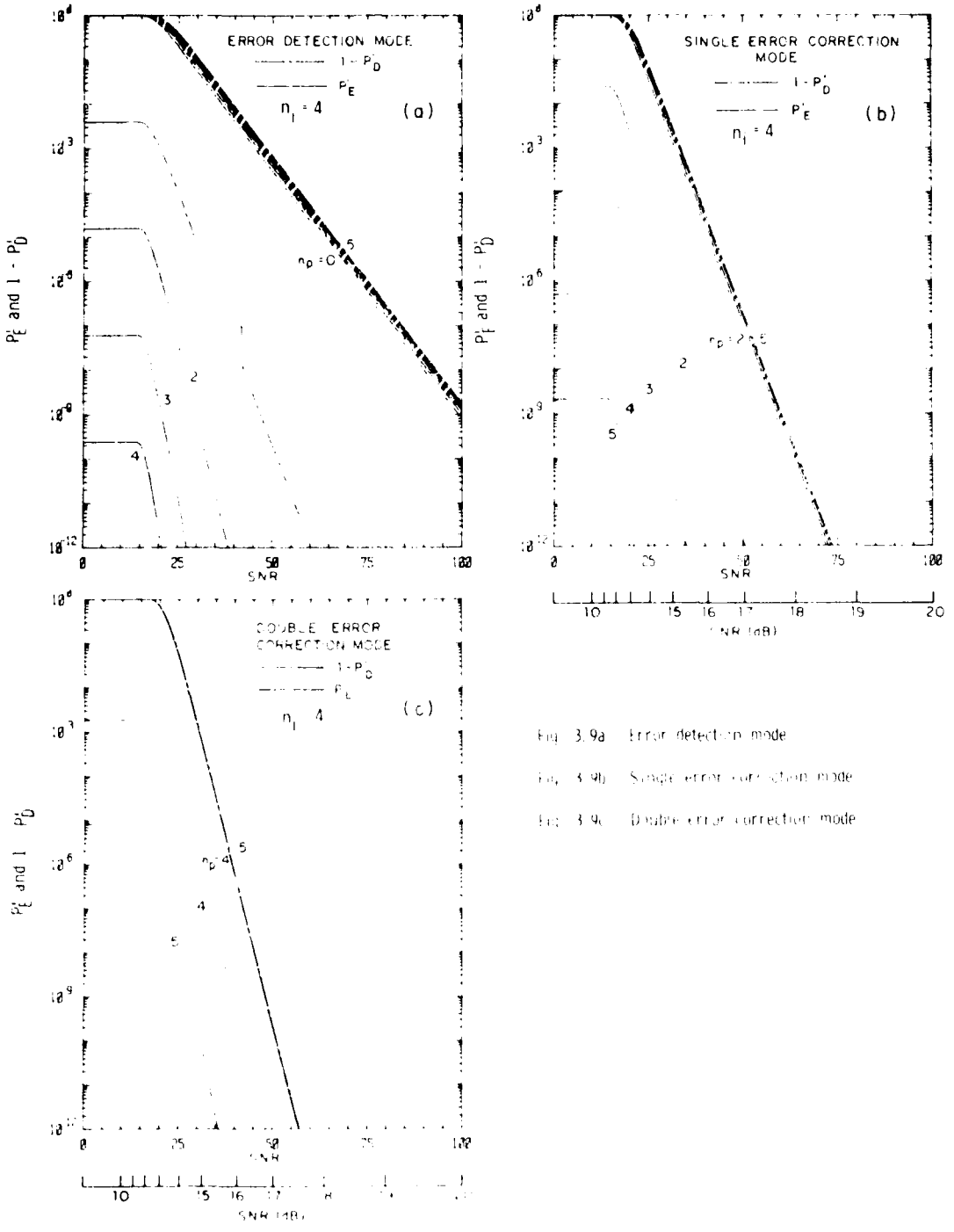

Fig. 3.9a Error detection mode

Fig. 3.9b Single error correction mode

Fig. 3.9c Double error correction mode

Fig. 3.9 Performance of hard decoder. Probability of correct decoding and decoding error vs. SNR/pulse for four information pulses n_I, different number of parity checks n_p, and selected decoding modes.

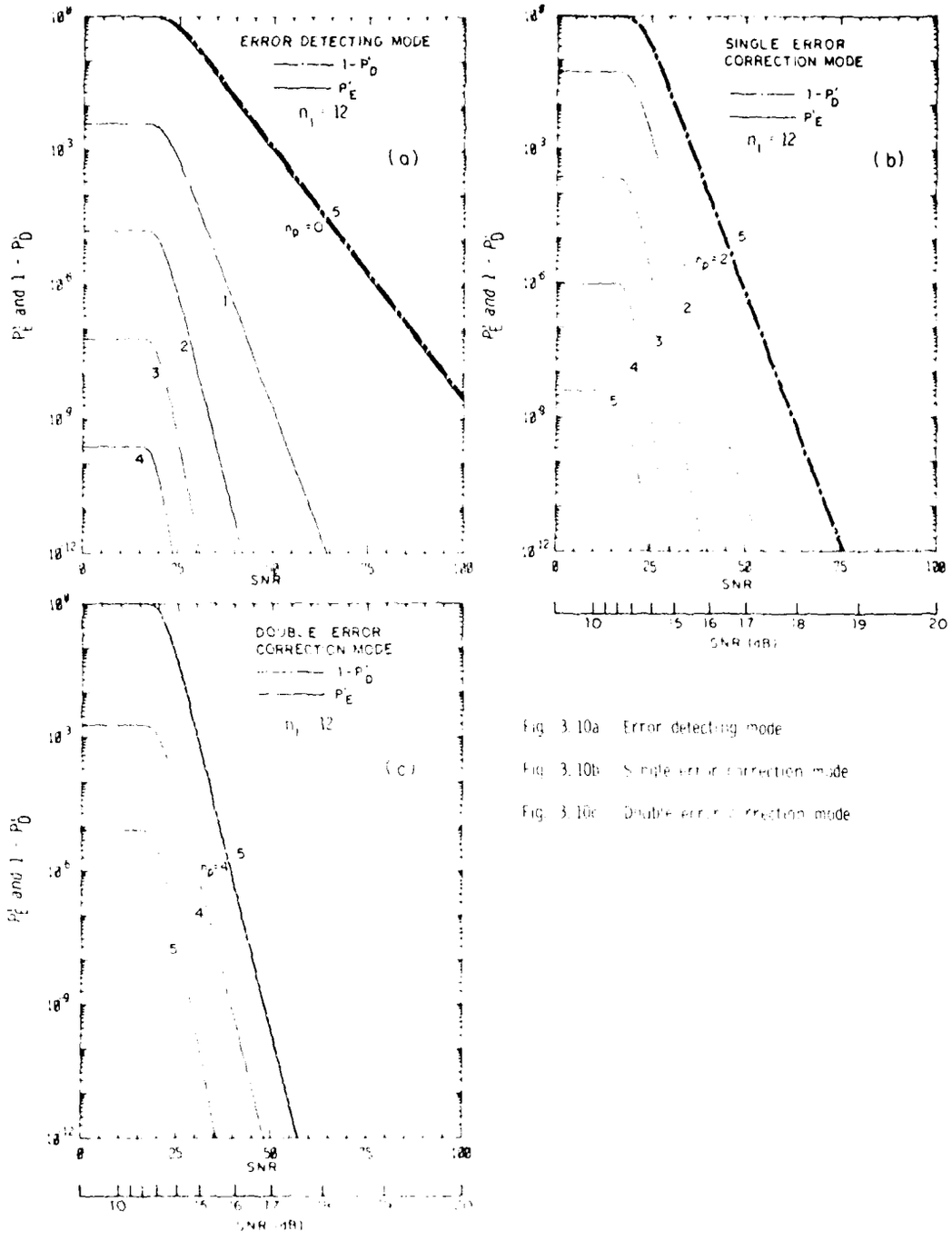

Fig. 3.10a Error detecting mode

Fig. 3.10b Single error correction mode

Fig. 3.10c Double error correction mode

Fig. 3.10 Performance of 'hard' decoder. Probability of correct decoding and decoding errors vs SNR pulse for twelve information pulses n_1, different number of parity checks n_D and selected decoding modes

probability of error does not approach unity (for $n_p \neq 0$) when SNR approaches zero. For any given number of parity checks and SNR values, the "soft" decoder gives a better probability of detection, as should be expected. A "hard" decoder might give a lower error probability. However, to compare the performance of the "soft" and "hard" decoders when the probability of error is one of the performance parameters (in addition to the probability of correct decoding), one should modify the decoding algorithms appropriately, by introducing a failure mode, which can be implemented in a form of thresholding. Thresholding may also be beneficial when introduced at the level of pulse detection within a single frame.

3.3.3 Algorithms B and C

Figures 3.11, a through c, show the probabilities of detection of the synchronization pattern for three different values of maximum probability of error, max P_E, when algorithm B was used in detection. The values of the thresholds, $\sqrt{a_{TH}}$, for different numbers of synchronization pulses are tabulated below.

n_s \ max P_E	10^{-4}	10^{-8}	10^{-12}
2	13.84	16.24	18.35
3	16.95	19.89	22.47
4	19.57	22.98	25.94
5	21.88	25.69	29.01
6	23.96	28.14	31.78

It is evident that the probability of detection calculated with algorithm B deteriorates rather rapidly with increases in max P_E and also with decreases in the number of synchronization pulses.

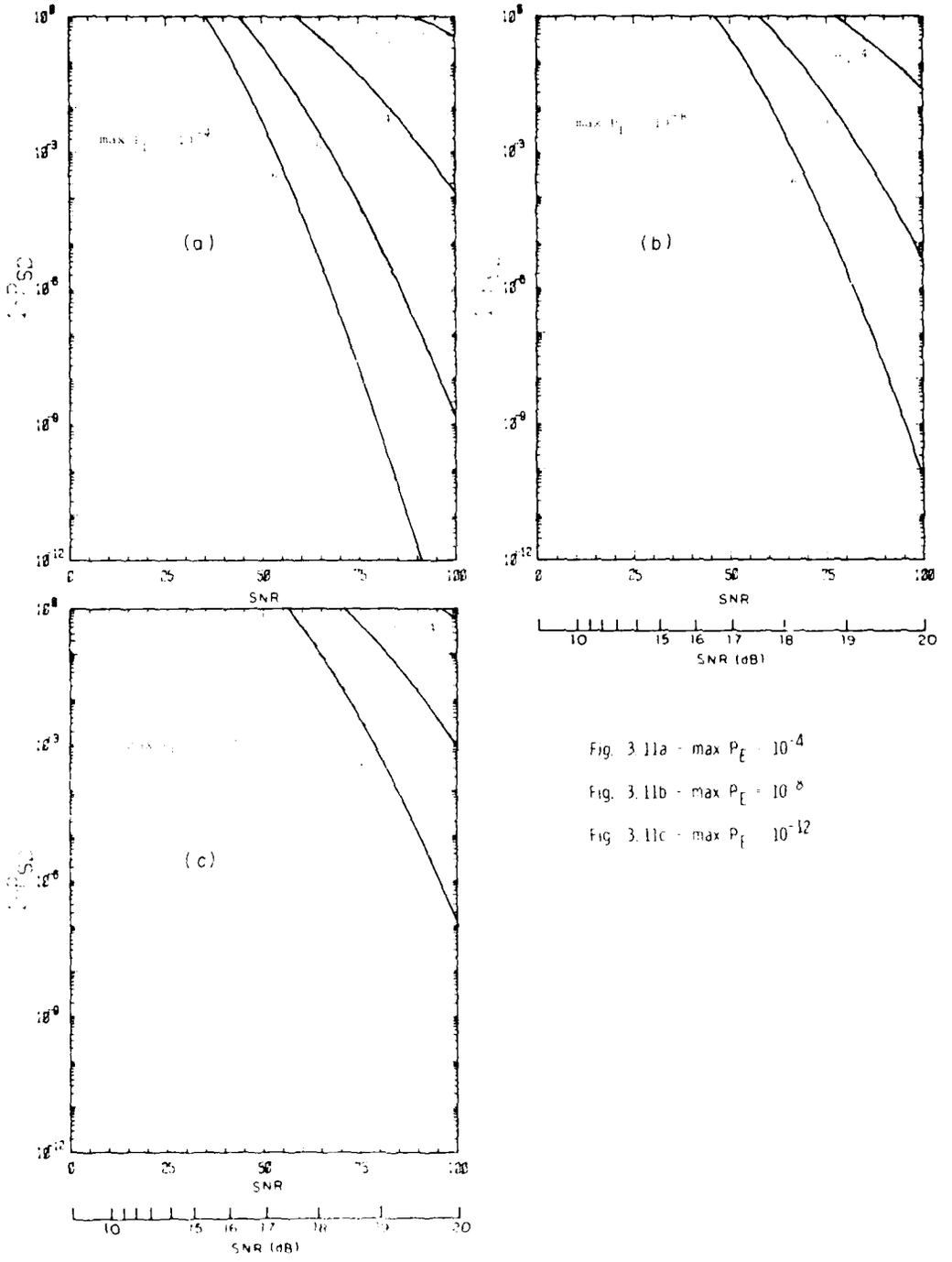

Fig. 3.11a - max $P_E = 10^{-4}$

Fig. 3.11b - max $P_E = 10^{-8}$

Fig. 3.11c - max $P_E = 10^{-12}$

Fig. 3.11 Performance of synchronization, algorithm B. Probability of detection vs SNR pulse for different number of synchronization pulses n_s and different allowable maximum probability of error max P_E.

Analogous graphs for algorithm C are shown in Fig. 3.12. The values of the thresholds, $\sqrt{b_{TH}}$, for different numbers of synchronization pulses are tabulated below.

n_s \ max P_E	10^{-4}	10^{-8}	10^{-12}
2	9.78	13.40	16.90
3	11.98	14.16	17.32
4	13.83	16.24	18.61
5	15.46	18.16	20.52
6	16.94	19.89	27.4[illegible]

The performance of algorithm C is clearly superior to that of algorithm B. The same is true for the decoding algorithm, and also for pulse detection within the single frame. Therefore, in the following investigations we consider only algorithm C.

Let us note, however, that a combination of algorithms B and C may offer some advantages deserving future attention. Such an algorithm would have the general form:

The pattern is in k-th position if

$$\underline{m}_k \cdot \underline{n} > \underline{m}'_k \cdot \underline{n} + \alpha \qquad \text{for all } k' \neq k$$
$$\text{and} \qquad (3.30)$$
$$\underline{m}_k \cdot \underline{n} > \beta ,$$

with thresholds chosen in such a way that max P_{SE} does not exceed some preselected value. The additional freedom that we have in selection of the threshold values could be used to minimize the value of SNR/pulse for which the probability of detection attains a satisfactory value.

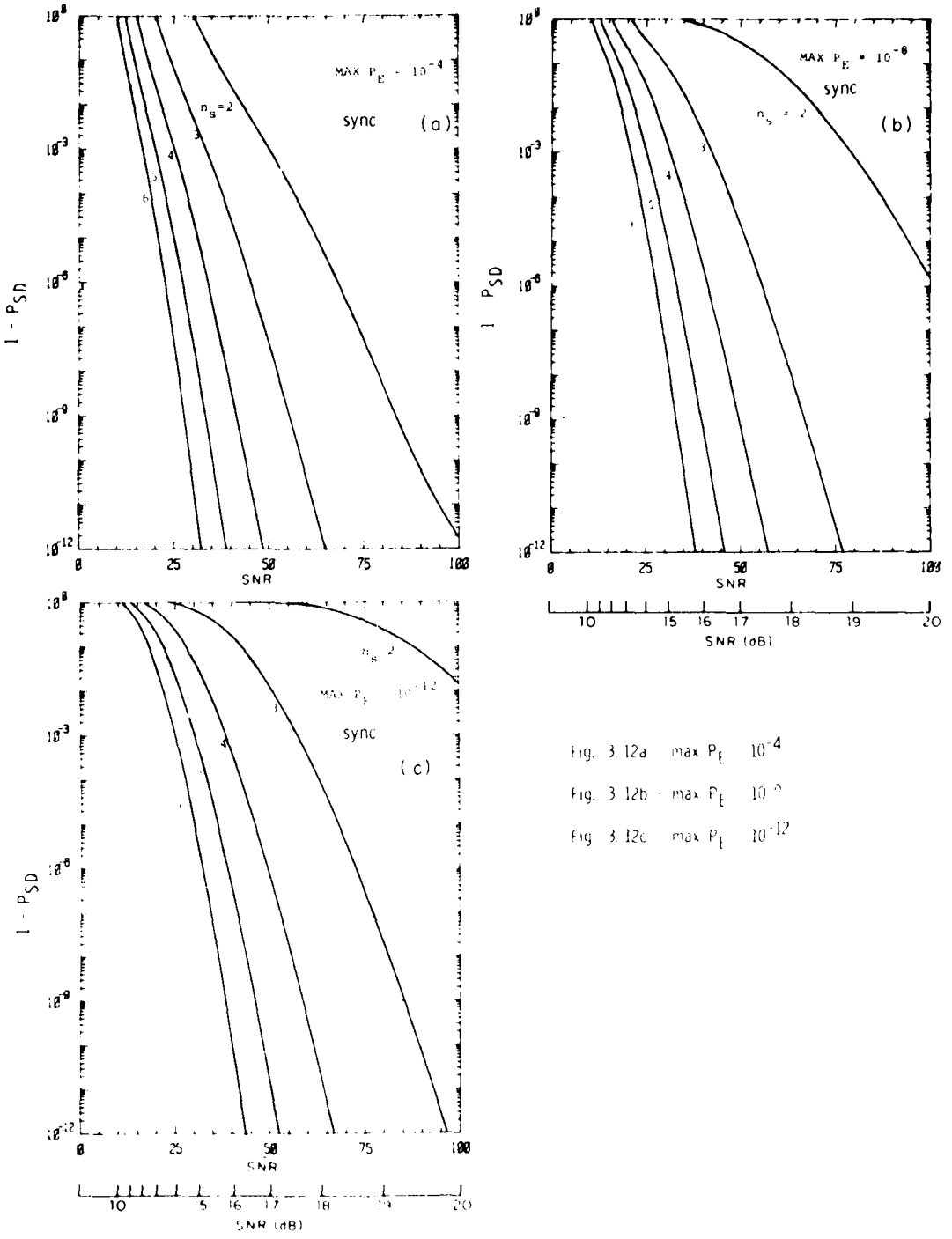

Fig. 3.12a max P_E 10^{-4}

Fig. 3.12b max P_E 10^{-8}

Fig. 3.12c max P_E 10^{-12}

Fig. 3.12 Performance of synchronization algorithm (c). Probability of detection vs SNR pulse for different number of synchronization pulses n_s and different allowable maximum probability of error max P_E.

The probability of decoding vs. SNR/pulse is shown in Figs. 3.13, 3.14 and 3.15 for two, four and twelve information pulses per block, respectively. In all of these we have considered three different values of max P_E. The values of the thresholds, $\sqrt{b_{TH}}$, for different numbers of information pulses and parity checks are tabulated below for algorithm C.

n_i	max P_E / n_p	10^{-4}	10^{-8}	10^{-12}
2	0	11.75	15.59	18.71
	1	12.02	15.80	18.86
	2	12.90	16.82	20.01
	3	13.90	17.98	21.34
	4	14.95	19.14	22.70
	5	15.99	20.30	24.02
4	0	26.13	34.27	40.89
	1	22.81	29.54	35.07
	2	22.30	28.44	33.64
	3	22.63	28.41	33.46
	4	23.30	28.83	33.79
	5	24.13	29.47	34.40
12	0	86.32	110.92	131.24
	1	68.90	86.39	101.23
	2	63.16	76.92	89.42
	3	60.92	72.18	83.23
	4	60.03	69.62	79.61
	5	59.76	68.27	77.41

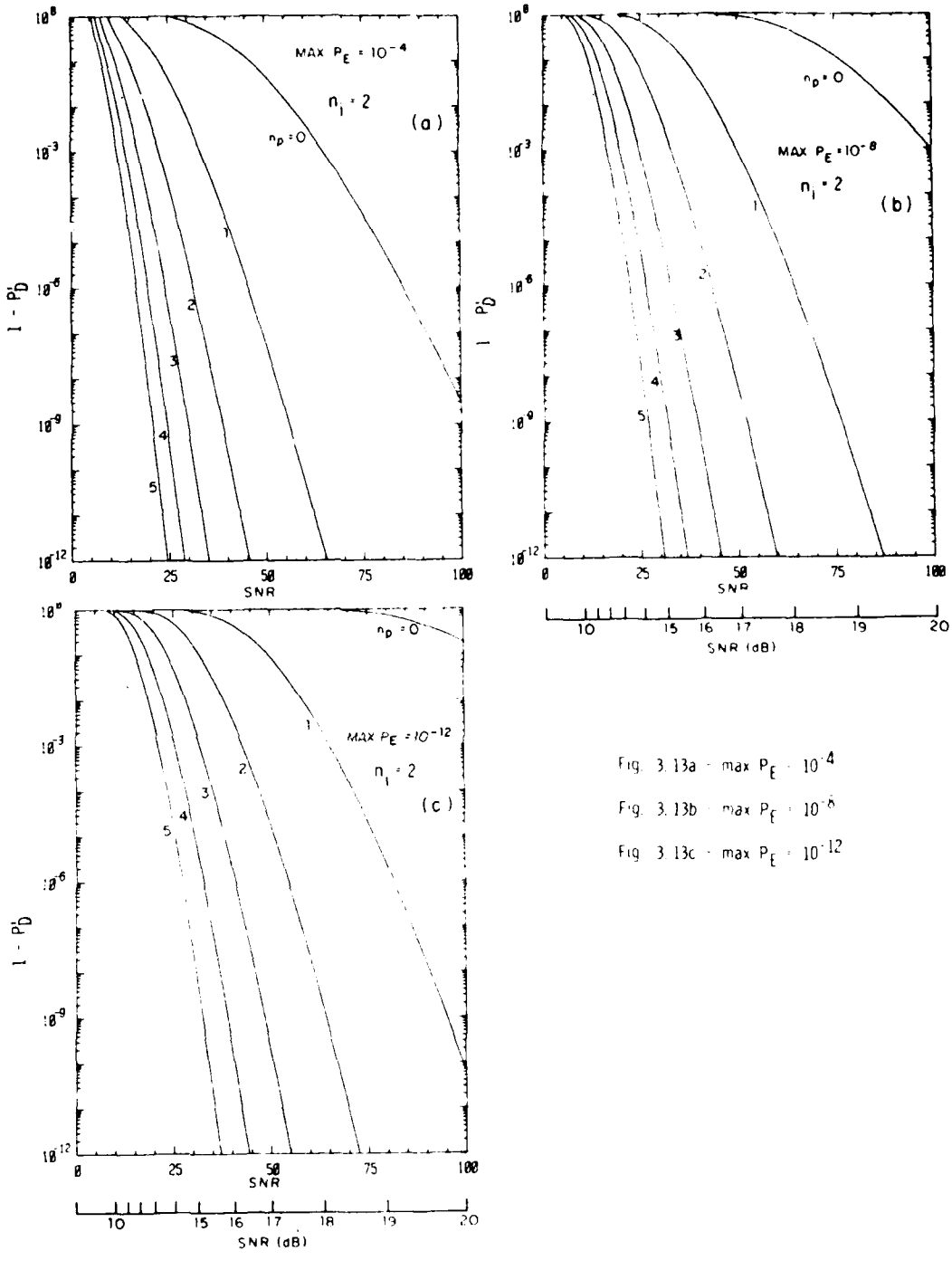

Fig. 3.13a - max $P_E = 10^{-4}$

Fig. 3.13b - max $P_E = 10^{-8}$

Fig. 3.13c - max $P_E = 10^{-12}$

Fig. 3.13 Performance of "soft" decoder, algorithm C. Probability of decoding vs SNR/pulse for two information pulses n_1, different number of parity checks n_p and different maximum allowable probability of error max P_E

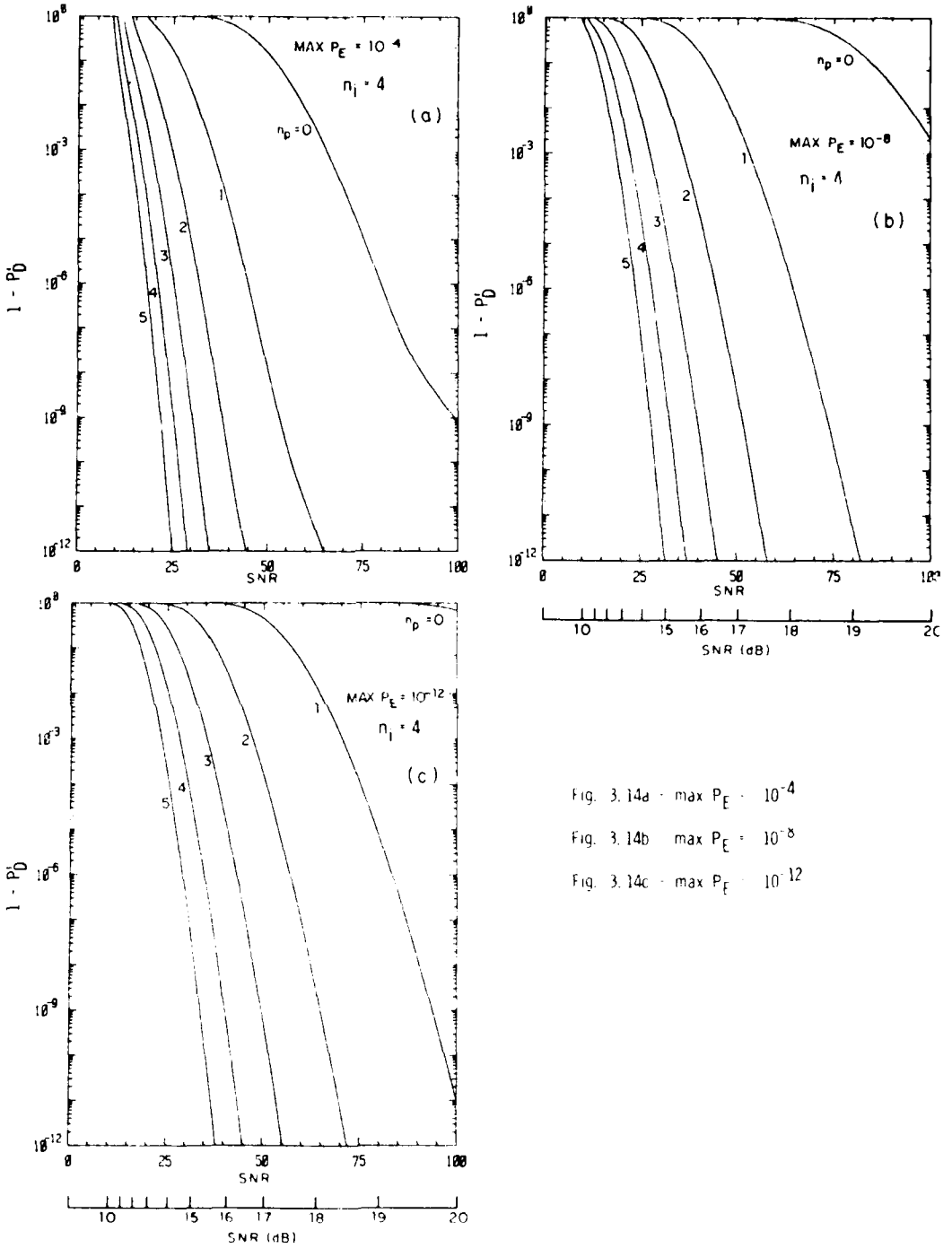

Fig. 3.14a - max P_E = 10^{-4}

Fig. 3.14b - max P_E = 10^{-8}

Fig. 3.14c - max P_E = 10^{-12}

Fig. 3.14 Performance of "soft" decoder, algorithm C. Probability of decoding vs SNR/pulse for four information pulses n_i, different number of parity checks n_p and different maximum allowable probability of error max P_f

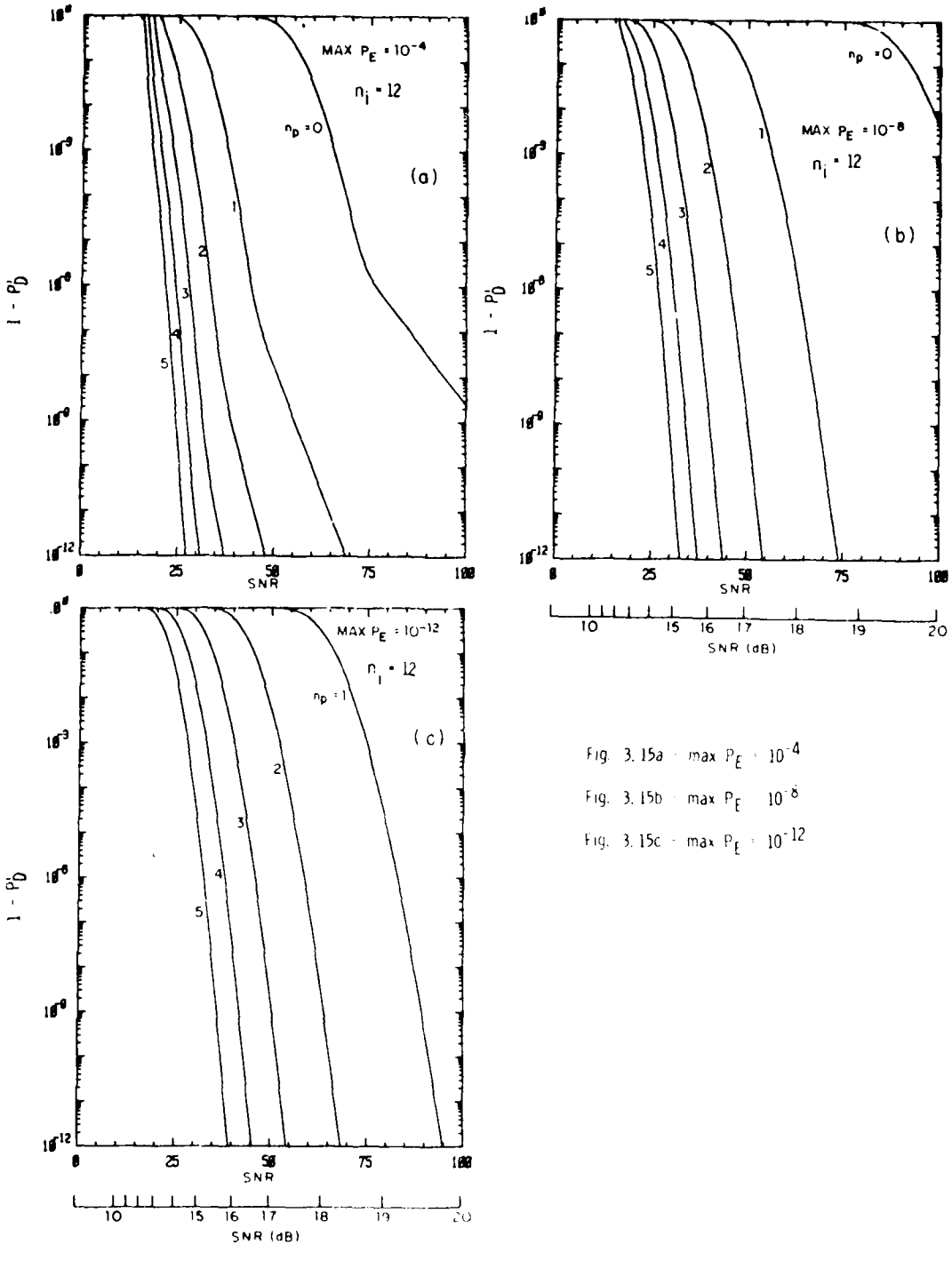

Fig. 3.15a - max $P_E = 10^{-4}$

Fig. 3.15b - max $P_E = 10^{-8}$

Fig. 3.15c - max $P_E = 10^{-12}$

Fig. 3.15 Performance of "soft" decoder, algorithm C. Probability of decoding vs SNR pulse for twelve information pulses n_i, different number of parity checks n_p and different maximum allowable probability of error max P_E

Together with Fig. 3.6 where max P_E = 1 ("soft" decoder without thresholds) these graphs show the dependence of the probability of decoding on max P_E. The figures also show the range of decoding improvement obtained with an increase in the number of parity checks. Note that the peak of the error probability (not shown) is not at SNR = 0.

3.3.4 "Hard" Decoder in Presence of Erasures

Finally, we have applied algorithm C for pulse detection in a frame; the results are then used to compute the overall performance of the "hard" decoder. Since there are many decoding modes, we selected those which gave the minimum value of SNR when the required probability of detection was of the order of 0.9999 for a given value of max P_E. The selected decoding modes are presented below in tabular form.

n_1	n_p \ max P_E	10^{-4}	10^{-8}	10^{-12}
2	0	$\{0_E, 0_e\}$	$\{0_E, 0_e\}$	$\{0_E, 0_e\}$
	1	$\{0_E, 0_e\}$	$\{0_E, 0_e\}$	$\{0_E, 0_e\}$
	2	$\{1_E(0), 1_e(0)\}$	$\{1_E(0), 1_e(0)\}$	$\{1_E(0), 1_e(0)\}$
	3	$\{1_E(0), 1_e(1), 2_e(0)\}$	$\{1_E(0), 1_e(0)\}$	$\{1_E(0), 1_e(0)\}$
	4	$\{2_E(0), 1_E(2), 2_e(1), 3_e(0)\}$	$\{2_E(0), 1_E(1), 1_e(1), 2_e(0)\}$	$\{1_E(0), 1_e(0)\}$
	5	$\{2_E(0), 1_E(2), 2_e(1), 4_e(0)\}$	$\{2_E(0), 1_E(2), 2_e(1), 3_e(0)\}$	$\{2_E(0), 1_E(1), 1_e(1), 2_e(0)\}$
4	0	$\{0_E, 0_e\}$	$\{0_E, 0_e\}$	$\{0_E, 0_e\}$
	1	$\{0_E, 0_e\}$	$\{0_E, 0_e\}$	$\{0_E, 0_e\}$
	2	$\{1_E(0), 1_e(0)\}$	$\{0_E, 1_e(0)\}$	$\{1_E(0), 1_e(0)\}$
	3	$\{1_E(1), 1_e(1), 2_e(0)\}$	$\{1_E(0), 1_e(0)\}$	$\{1_E(0), 1_e(0)\}$
	4	$\{2_E(0), 1_E(2), 2_e(1), 3_e(0)\}$	$\{2_E(0), 1_E'1), 1_e(1), 2_e(0)\}$	$\{1_E(0), 1_e(0)\}$
	5	$\{2_E(0), 1_E(2), 2_e(1), 4_e(0)\}$	$\{2_E(0), 1_E(2), 2_e(1), 3_e(0)\}$	$\{2_E(0), 1_E(1), 1_e(1), 2_e(0)\}$
12	0	$\{0_E, 0_e\}$	$\{0_E, 0_e\}$	$\{0_E, 0_e\}$
	1	$\{0_E, 0_e\}$	$\{0_E, 0_e\}$	$\{0_E, 0_e\}$
	2	$\{1_E(0), 1_e(0)\}$	$\{0_E, 1_e(0)\}$	$\{0_E, 1_e(0)\}$
	3	$\{1_E(1), 1_e(1), 2_e(0)\}$	$\{1_E(0), 1_e(0)\}$	$\{1_E(0), 1_e(0)\}$
	4	$\{2_E(0), 1_E(2), 2_e(1), 3_e(0)\}$	$\{1_E(1), 1_e(1), 2_e(0)\}$	$\{1_E(0), 1_e(0)\}$
	5	$\{2_E(0), 1_E(2), 2_e(1), 4_e(0)\}$	$\{2_E(0), 1_E(1), 1_e(1), 2_e(0)\}$	$\{1_E(1), 1_e(1), 2_e(0)\}$

The values of the thresholds, $\sqrt{b_{TH}}$, corresponding to the selected decoding modes for different numbers of information pulses and parity checks, are tabulated below.

n_i	n_p \ max P_E	10^{-4}	10^{-8}	10^{-12}
2	0	4.86	6.39	7.68
	1	3.10	4.28	5.21
	2	3.22	4.39	5.33
	3	3.27	3.34	4.16
	4	3.33	3.46	3.46
	5	3.14	3.46	3.45
4	0	4.86	6.39	7.68
	1	2.87	4.28	5.21
	2	3.11	4.39	5.33
	3	3.22	3.34	4.16
	4	3.34	3.46	3.34
	5	3.13	3.46	3.46
12	0	4.86	6.38	7.68
	1	2.87	4.28	5.21
	2	3.34	4.39	5.33
	3	3.45	3.46	4.28
	4	3.46	3.57	3.46
	5	3.15	2.75	3.57

The resulting probability of decoding is shown in Figs. 3.16, 3.17 and 3.18 for two, four and twelve information pulses per block, respectively, and selected decoding modes. As for the "soft" decoder, we have considered three different values

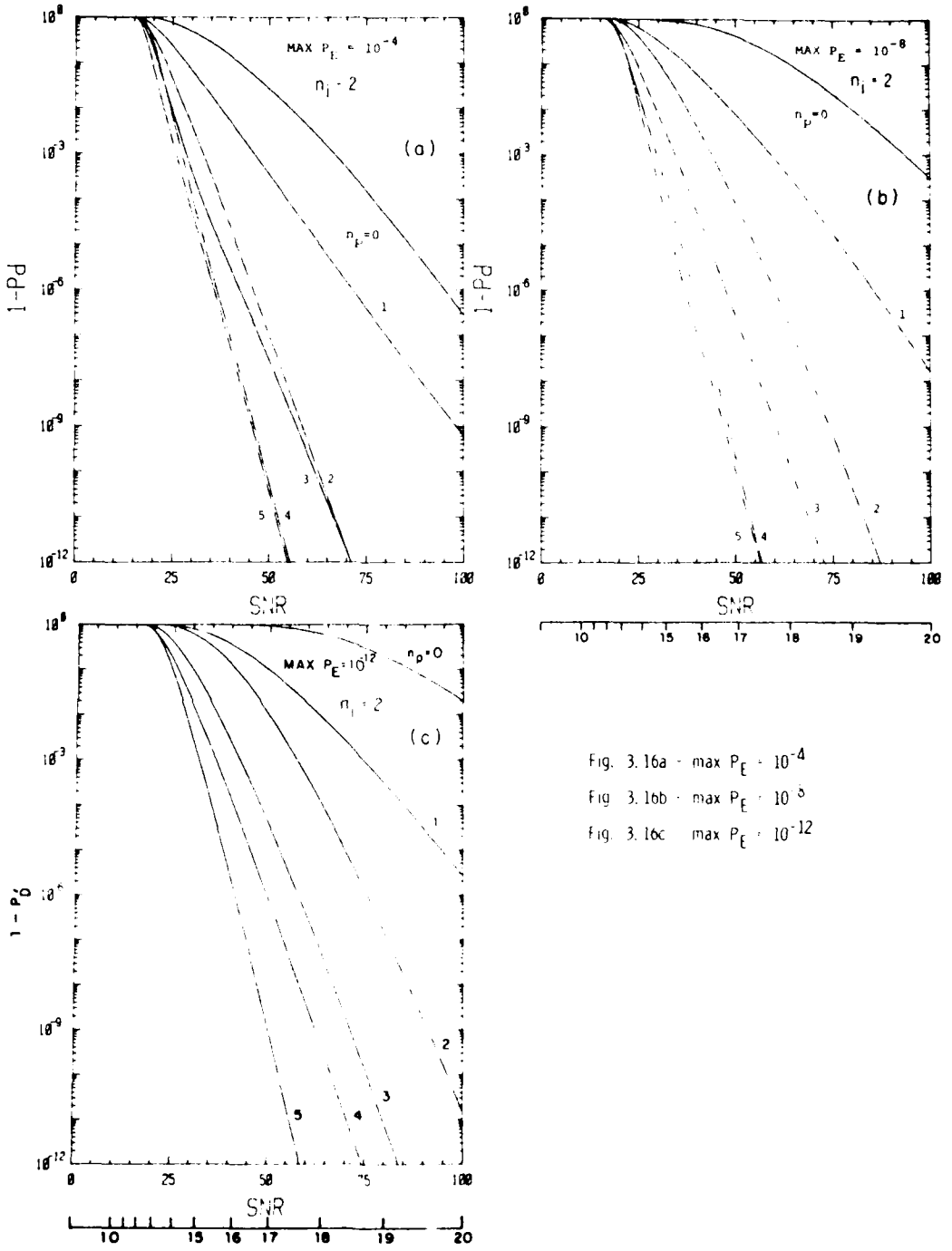

Fig. 3.16a - max $P_E = 10^{-4}$

Fig. 3.16b - max $P_E = 10^{-8}$

Fig. 3.16c - max $P_E = 10^{-12}$

Fig. 3.16 Performance of "hard" decoder, algorithm C for pulse detection, selected decoding modes. Probability of decoding vs SNR pulse for two information pulses n_I, different number of parity checks n_p and different allowable probability of decoding error max P_E

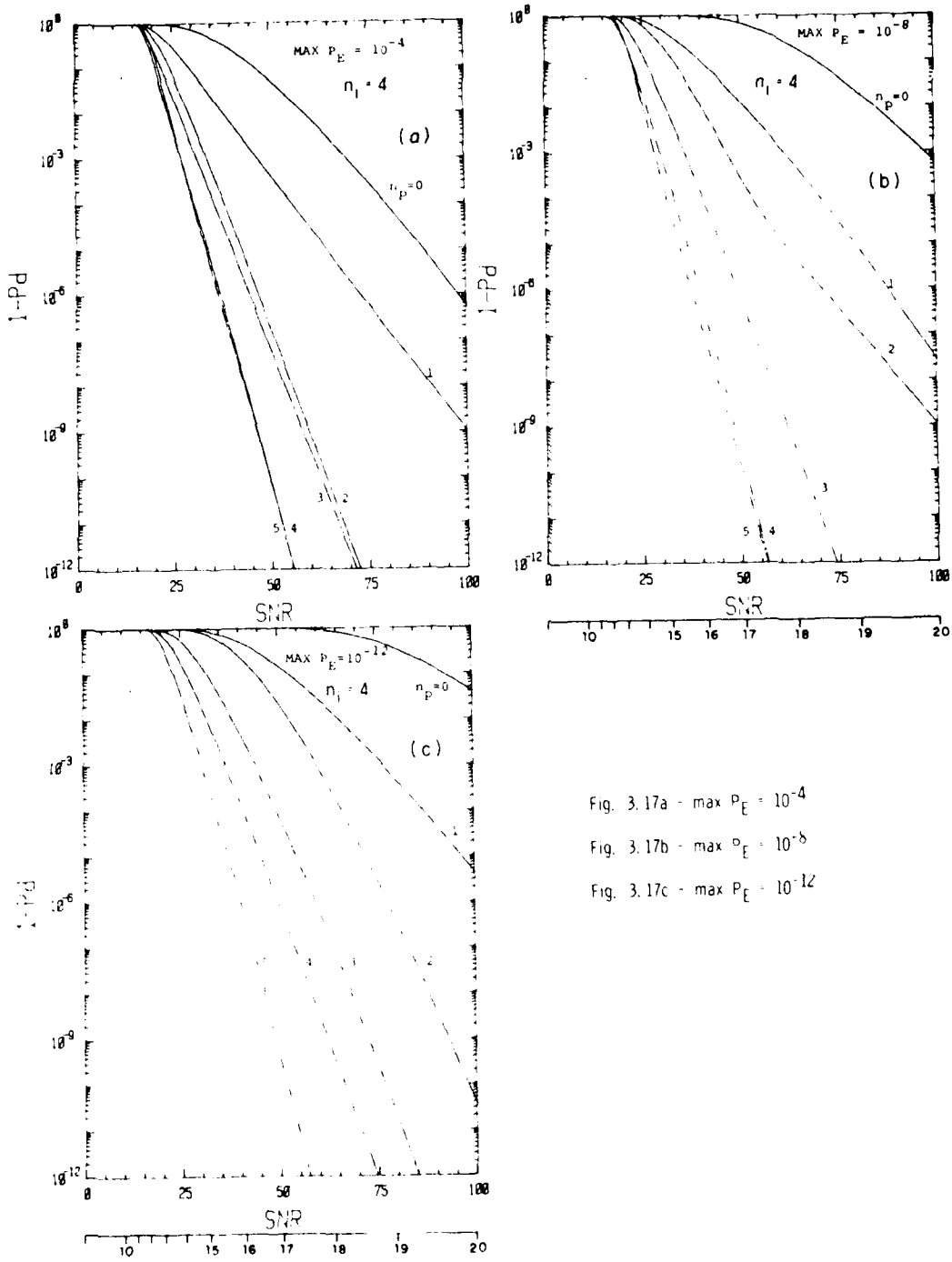

Fig. 3.17a - max $P_E = 10^{-4}$

Fig. 3.17b - max $P_E = 10^{-8}$

Fig. 3.17c - max $P_E = 10^{-12}$

Fig. 3.17 Performance of "hard" decoder, algorithm C for pulse detection, selected decoding modes. Probability of decoding vs SNR/pulse for four information pulses n_I, different number of parity checks n_p and different allowable probability of decoding error max P_E.

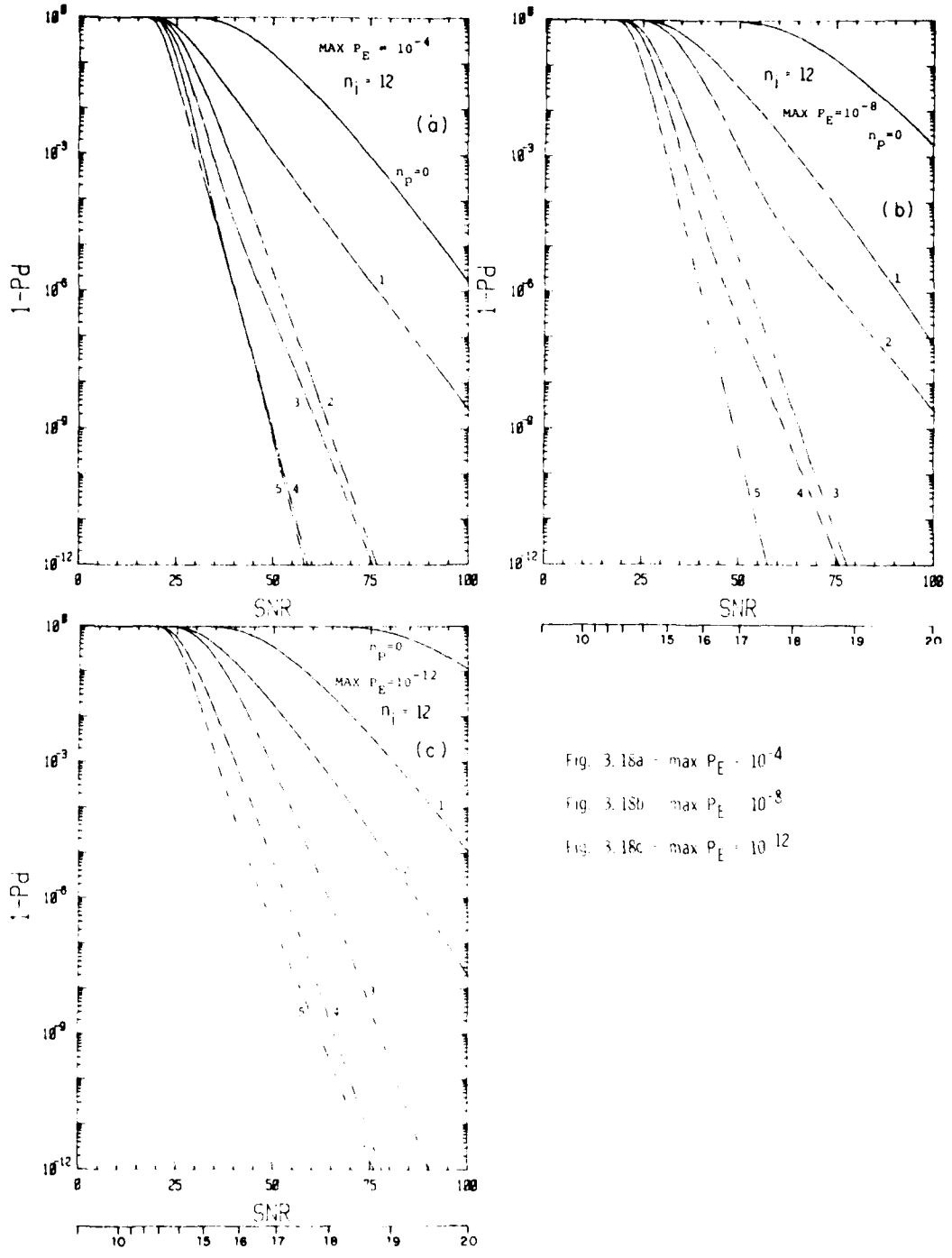

Fig. 3.18a - max $P_E = 10^{-4}$

Fig. 3.18b - max $P_E = 10^{-8}$

Fig. 3.18c - max $P_E = 10^{-12}$

Fig. 3.18 Performance of 'hard' decoder, algorithm C for pulse detection, selected decoding modes. Probability of decoding vs SNR pulse for twelve information pulses n_i, different number of parity checks n_p and different allowable probability of decoding error max P_E

of max P_E and different numbers of parity checks. In the case of a higher number of parity checks and lower error probabilities, thresholding was not required but could lead to some improvement (usually rather small). This happens, for instance, when there is clustering of the curves, e.g., for 5 and 4, or 3 and 2 parity checks and max $P_E = 10^{-4}$. Note that the choice of decoding modes depends also on the selection of the required level of the probability of detection. Other decoding modes often resulted in performance comparable to those selected.

Our computations were based on the "union" bound. When the probability of detection of a pulse was equal to zero, the bound was set to zero for lower values of SNR/pulse. This procedure led to an exaggerated importance of erasures. More precise threshold values and better selection of decoding modes can be made when frame errors are computed numerically from the exact expressions.

It is useful to note that for a larger number of parity checks, the degradation of the decoding probability with an increased requirement on max P_E is small or absent when compared with the performance of the "hard" decoder without erasures, described in Section 3.3.2.

3.3.5 Performance Formulas in Presence of Fading

After selecting the signal processing schemes designed to meet the performance requirements for the non-fading signal, we assessed their performance degradation due to fading. The simplified model of signal fading, which allowed us to probe into possible effects of fading on algorithm performance, was described in Section 2.4. A special case of this fading model in which a pulse is "lost" with probability P_o may lead to an especially serious degradation.

Figures 3.19 through 3.23 illustrate the dependence of the probability of detection of synchronization pulses on SNR

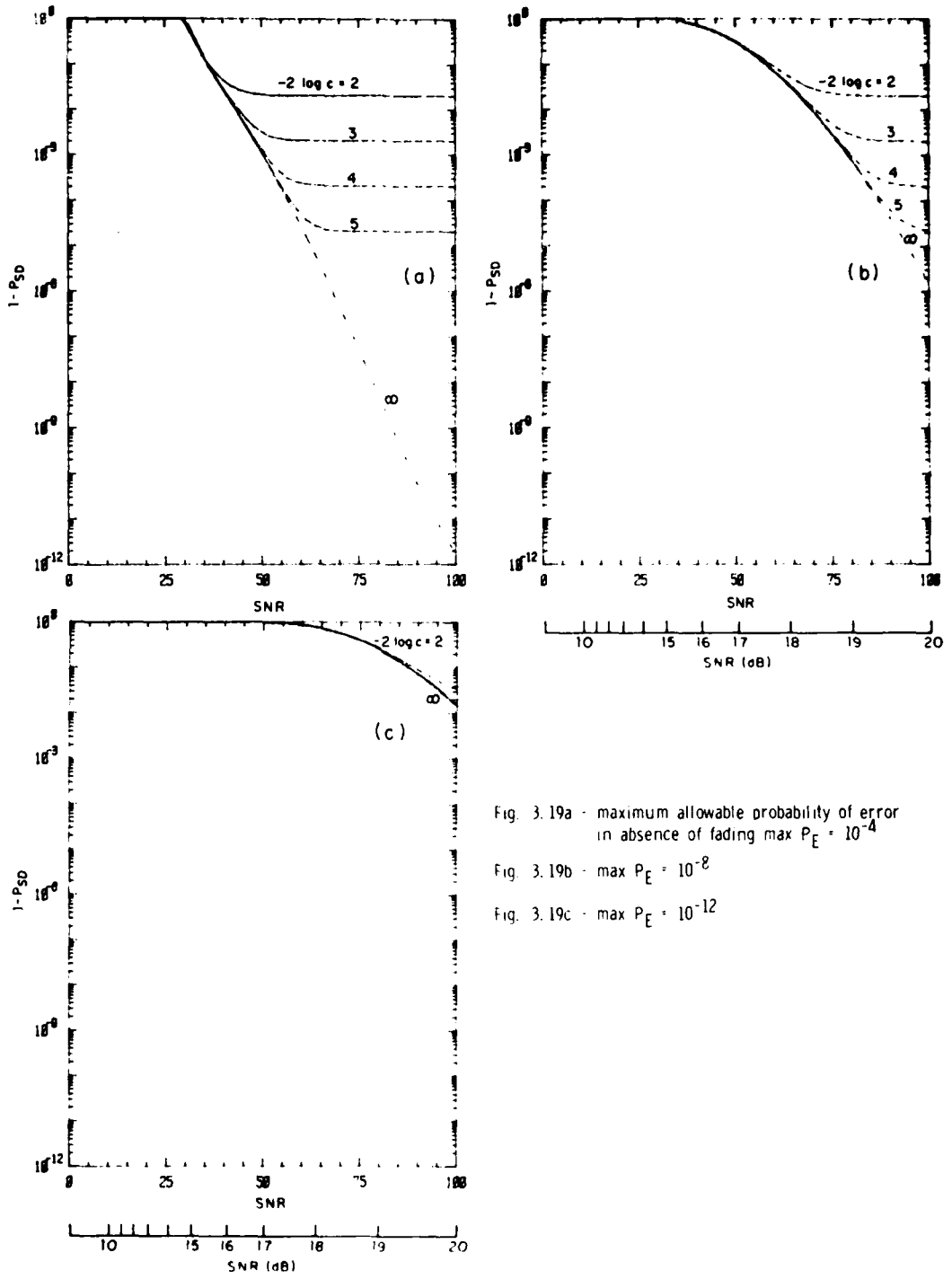

Fig. 3.19a - maximum allowable probability of error in absence of fading max $P_E = 10^{-4}$

Fig. 3.19b - max $P_E = 10^{-8}$

Fig. 3.19c - max $P_E = 10^{-12}$

Fig. 3.19 Performance of synchronization algorithms in presence of fading. Probability of detection vs SNR/pulse for two synchronization pulses and different level of fading contrast c.

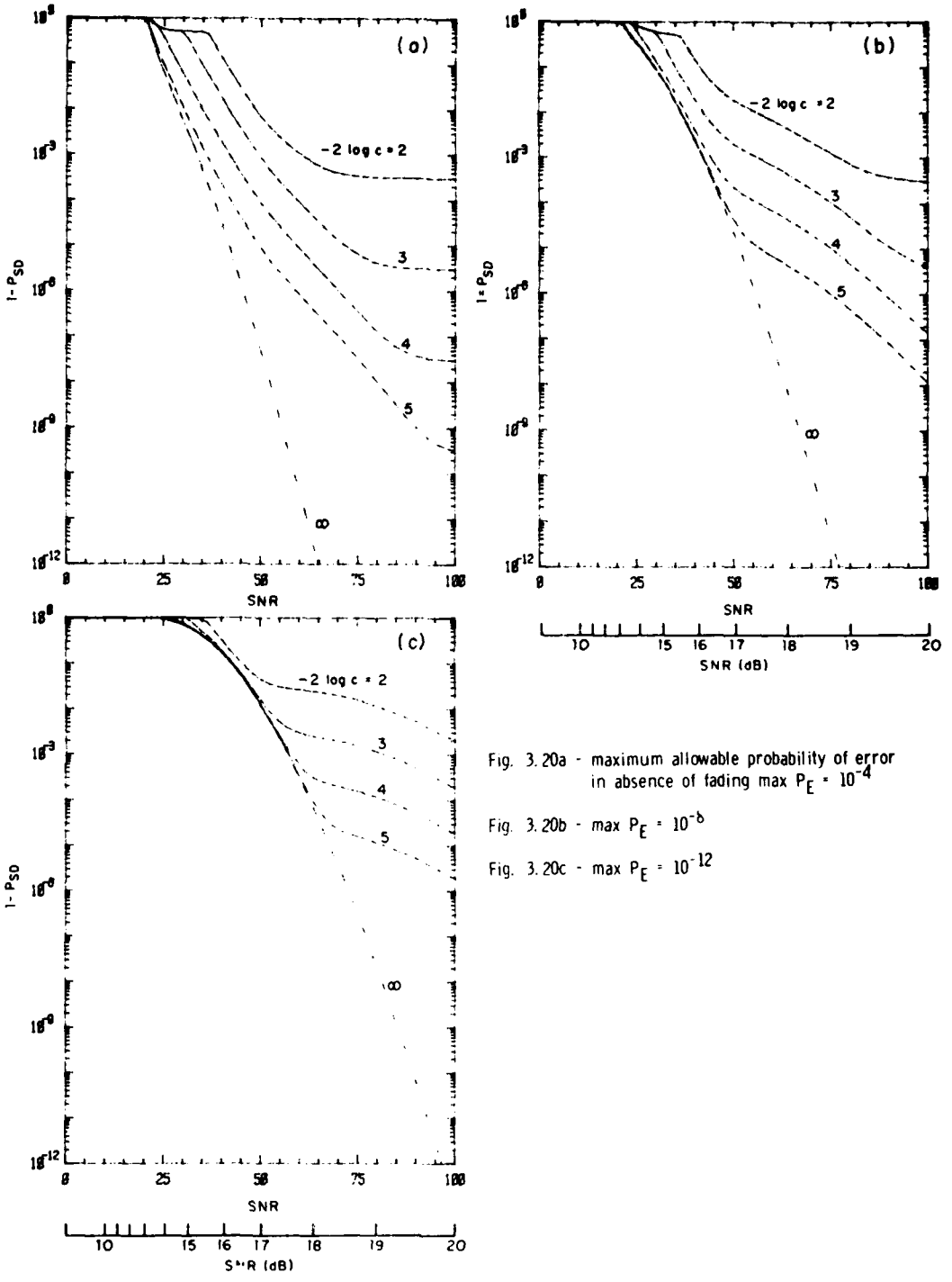

Fig. 3.20a - maximum allowable probability of error in absence of fading max $P_E = 10^{-4}$

Fig. 3.20b - max $P_E = 10^{-6}$

Fig. 3.20c - max $P_E = 10^{-12}$

Fig. 3.20 Performance of synchronization algorithms in presence of fading. Probability of detection vs SNR/pulse for three synchronization pulses and different levels of fading contrast c.

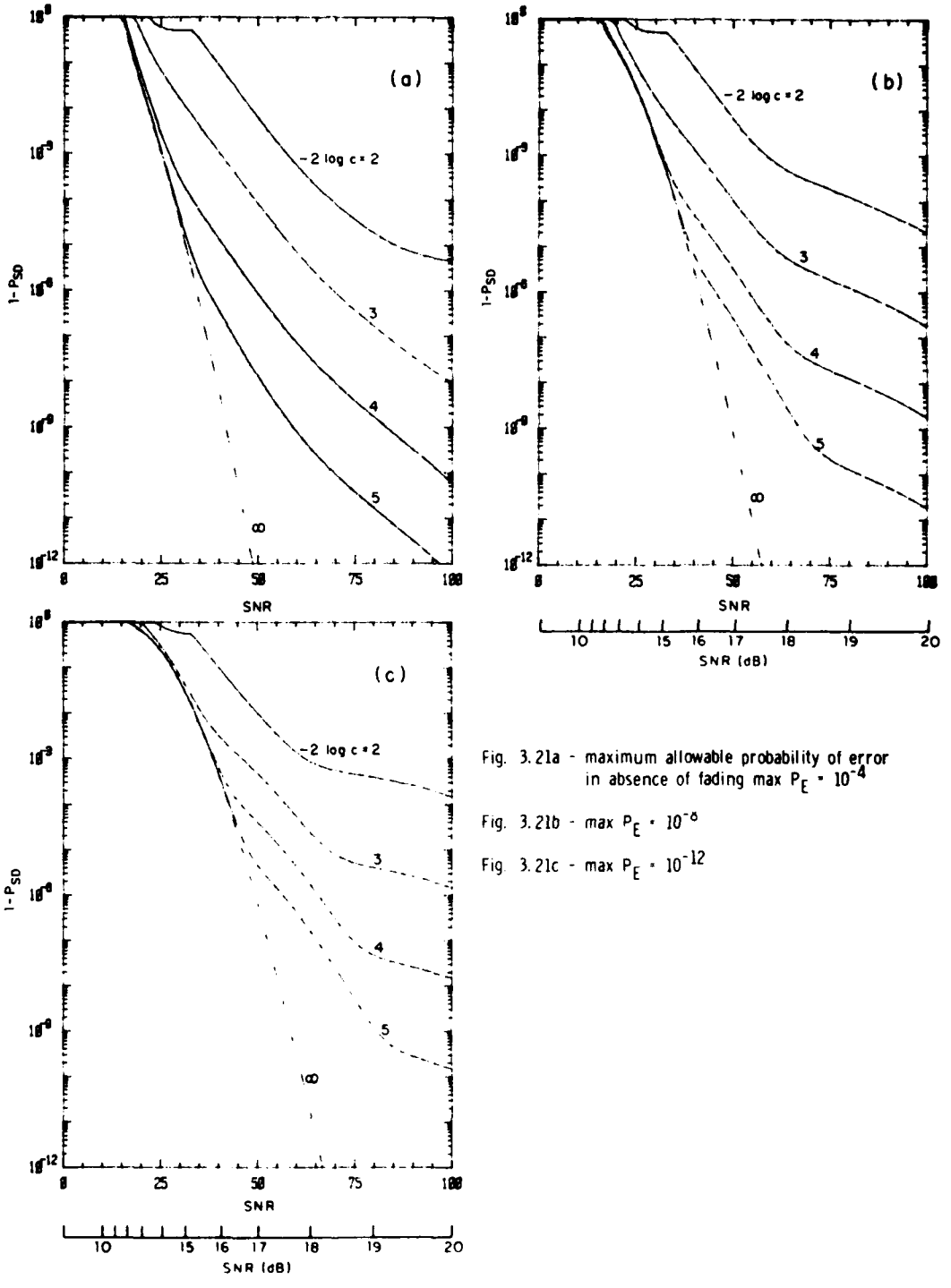

Fig. 3.21a - maximum allowable probability of error in absence of fading max $P_E = 10^{-4}$

Fig. 3.21b - max $P_E = 10^{-6}$

Fig. 3.21c - max $P_E = 10^{-12}$

Fig. 3.21 Performance of synchronization algorithms in presence of fading. Probability of detection vs SNR/pulse for four synchronization pulses and different levels of fading contrast c.

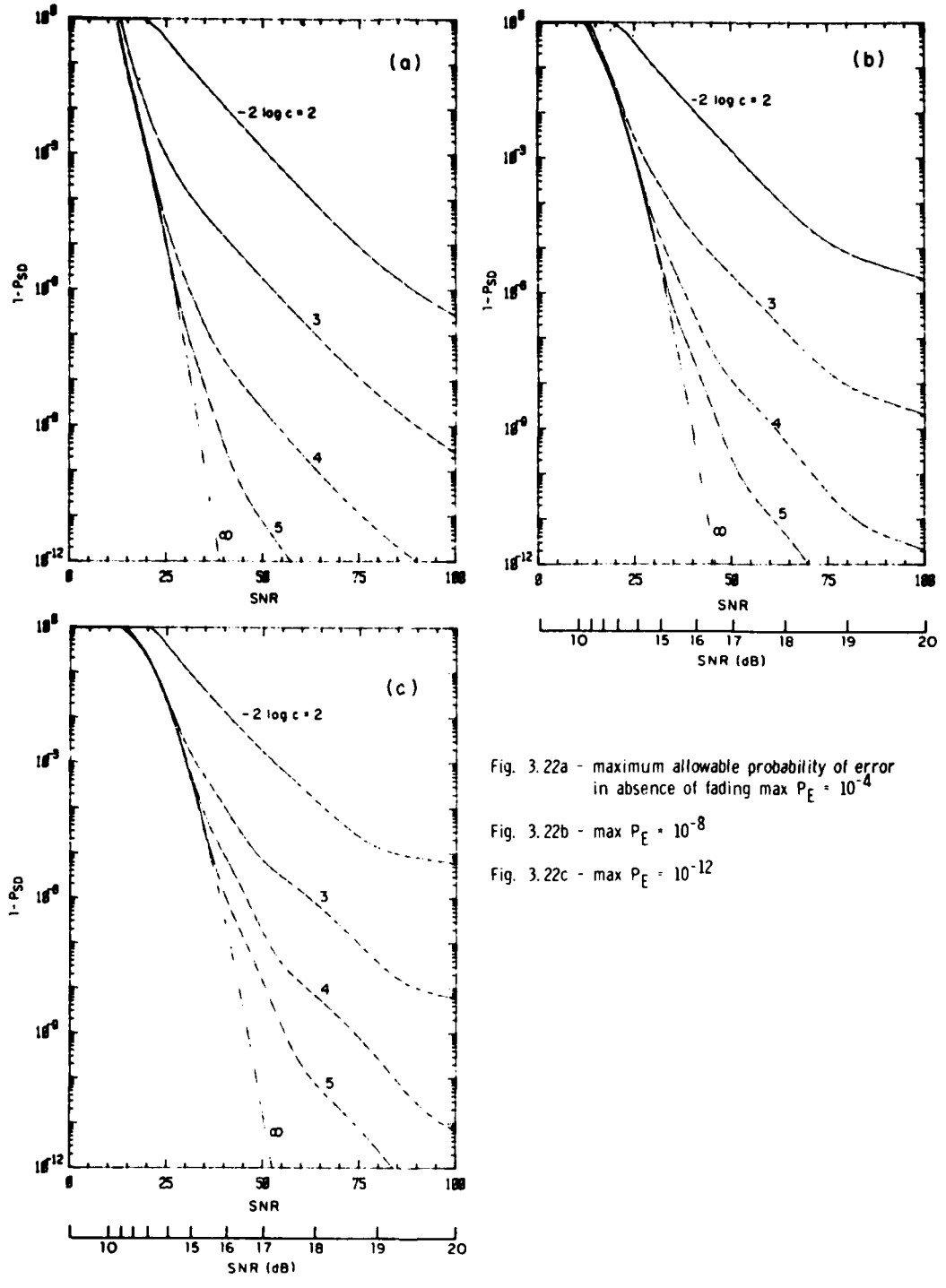

Fig. 3.22a - maximum allowable probability of error in absence of fading max $P_E = 10^{-4}$

Fig. 3.22b - max $P_E = 10^{-8}$

Fig. 3.22c - max $P_E = 10^{-12}$

Fig. 3.22 Performance of synchronization algorithms in presence of fading. Probability of detection vs SNR/pulse for five synchronization pulses and different levels of fading contrast c.

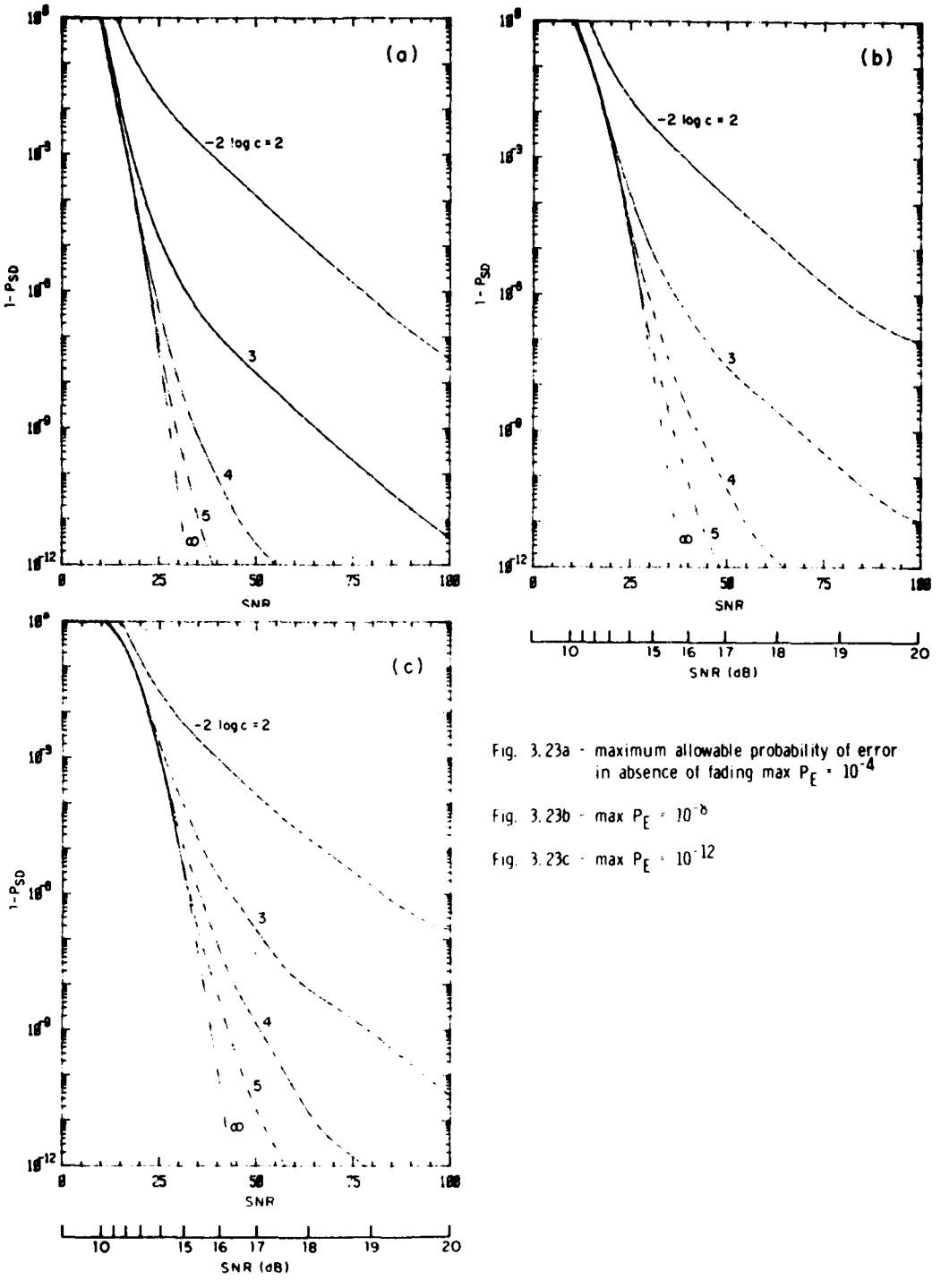

Fig. 3.23a - maximum allowable probability of error in absence of fading max $P_E = 10^{-4}$

Fig. 3.23b - max $P_E = 10^{-8}$

Fig. 3.23c - max $P_E = 10^{-12}$

Fig. 3.23 Performance of synchronization algorithms in presence of fading. Probability of detection vs SNR/pulse for six synchronization pulses and different levels of fading contrast c.

for two to six synchronization pulses. Each set of the three graphs shows the performance of algorithm C in the presence of fading with thresholds selected for the maximum allowable probabilities of error, in the absence of fading, equal to 10^{-4}, 10^{-8} and 10^{-12}.

We have selected the probabilities P_o of losing the pulse at values 10^{-2}, 10^{-3}, 10^{-4}, 10^{-5}, and zero. For such values of P_o, the contrast is approximately equal to P_o. The degradation caused by the fading is apparent. One interesting feature, especially clear (for the displayed range of SNR values) with two and three synchronization pulses, is that probability of detection becomes constant at sufficiently large SNR values. In fact, the appropriate expressions in Section 3.2.5 give the following asymptotic behavior:

$$1 - P_{SD} \xrightarrow[SNR \to \infty]{} P_o^{n_s} + n_s P_o^{n_s - 1}(1 - P_o),$$

$$P_{SE} \xrightarrow[SNR \to \infty]{} n_s P_o^{n_s - 1}(1 - P_o) + P_o^{n_s} P_{SE}(0), \tag{3.31}$$

where $P_{SE}(0)$ is the error probability (not exceeding max P_E) for SNR equal zero.

The above behavior of $(1-P_{SD})$ in the limit of large SNR values is desirable for the SLC applications. The synchronization pattern will not be detected if all, or all but one, synchronization pulses are "lost". (The second factor in the expression for $(1-P_{SD})$ and the first factor in expression for P_{SE} will be proportional to (n_s-1) rather than n_s if the "union" bound is not used in the calculations.)

The fact that the probability of detection is bounded no matter how large an SNR we have is referred to as a

"fading-limited" performance. The only way to improve the probability of detection is to add additional synchronization pulses.

The behavior of P_{SE} for our algorithm is also fading-limited. Let us point out that even if the probability of detection meets the performance requirements, the maximum probability of error is not smaller than $n_s P_o^{n_s-1} (1 - P_o)$. This means for instance that to achieve max P_{SE} of the order of 10^{-12} when the probability of "losing" a pulse is 10^{-12}, requires seven or eight synchronization pulses.

The behavior of P_{SE} described here is not what could be expected from all detection algorithms. For instance, one can modify algorithm C so that for any number of synchronization pulses ($n_s \geq 2$) the probability of error will not exceed the desired level.

An example of a set of such algorithms is the following. Once the position of the synchronization pattern has been found by means of algorithm C, additional constraints are imposed. We require that the output in any j signal slots exceeds a certain threshold value. Different algorithms are obtained depending on the selected value of j, ($2 \leq j \leq n_s$). With appropriate choice of threshold values, the maximum probability of error will not exceed the desired level. With this type of algorithm the probability of detection for large SNR is bounded by the probability of "losing" ($n_s - j$) pulses. Application of algorithm C to the decoding problem ("soft" decoder with threshold) leads to similar results. Again, the probability of error is not smaller than the probability of "losing" more than n_p pulses. Modification of decoding algorithms could be similar to that described above.

If the "hard" decoder is tested for a fluctuating signal, the decoding probability is again fading-limited. Improvement, however, can be achieved not only by increasing the number of parity checks, but also by changing the decoding mode, e.g., by increasing the threshold values and the number of erasure corrections. There are important differences as compared to the "soft" decoder with threshold, in the behavior in the error probability: it is affected only slightly by the signal fluctuations. In fact, the modification of algorithm C mentioned above, where certain local tests are added, brings the character of a "soft" decoder with threshold closer to that of a "hard" decoder.

Fig. 3.24 shows the largest attainable probability of decoding (fading-limited performance) for different numbers of information pulses and parity checks. Note, however, that in order to reach these probabilities one may need unreasonably high thresholds and SNR/pulse values.

Let us point out that the contrast value alone is not sufficient to describe the performance of signal processing in the presence of fading nor does it allow one to assess the modifications necessary to combat its effects. In our model of signal fading (Sec. 2.4) it is useful to parametrize N_{s1}, N_{s2}, and P_o as follows:

$$N_{s1} = \bar{N}_s \ (1 - C\, e^{-x})$$

$$N_{s2} = \bar{N}_s \ (1 + C\, e^{x}) \qquad (3.32)$$

$$P_o = 1/2 \ (1 + \tanh x) \quad \text{and} \quad e^{x} \geq C$$

Therefore, for given values of $\bar{N}_s$ and C, different types of fading are described by varying the value of x. The simple model discussed so far corresponds to the choice of $e^{x}=C$. If the value of $e^{x}=C$ is 1/3, this would correspond to P_o equal 10^{-1}.

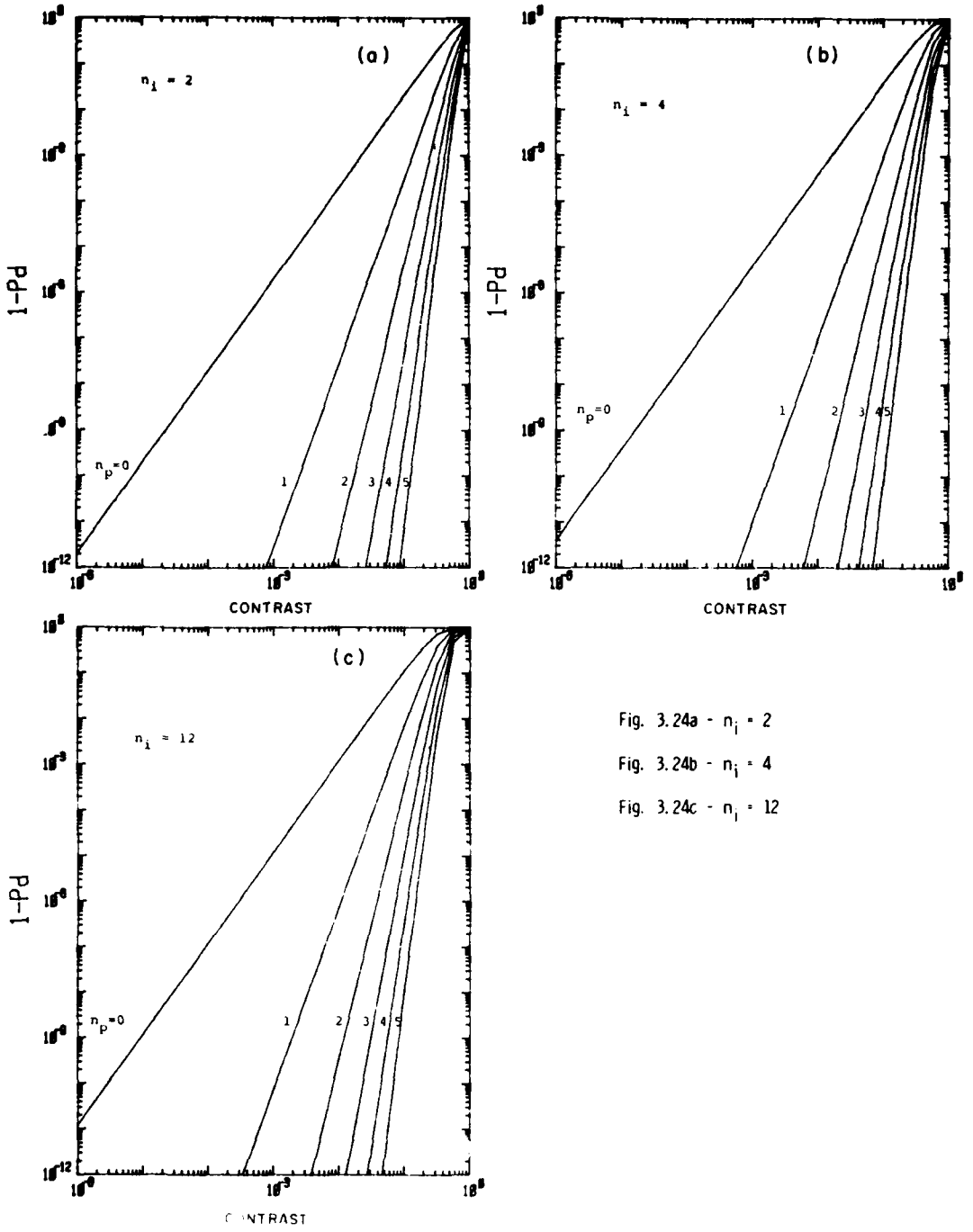

Fig. 3.24a - n_i = 2

Fig. 3.24b - n_i = 4

Fig. 3.24c - n_i = 12

Fig. 3.24 Fading-limited performance of "hard" decoder. Probability of decoding vs fading contrast for different numbers of information pulses n_i and different numbers of parity checks n_p. Decoding mode corrects up to n_p erasures.

In order to obtain a probability of decoding of the order of .9999, five or more parity checks are required. On the other hand, if $e^x = 1$, which corresponds to symmetric oscillations of signal around a mean value, we can overcome the fading-induced degradation by increasing the SNR value by no more than 20%. A realistic fading model may contain elements of these two fluctuating behaviors. The probability of sending a very weak pulse would correspond to the probability of "losing" a pulse, and the way to overcome the degradation caused by this effect is (if necessary) to increase redundancy. The degradation, due to dispersion of the signal around the mean value can be handled (if necessary) by either increasing SNR or increasing redundance, or both.

Signal processing in the SLC system should in our opinion possess the following additional "robustness" property: for any choice of $\bar{N}_s$, C and x, the maximum probability of error should not exceed a selected value. In order to develop this type of signal processing it is necessary to specify several types of fading for which the probability of decoding cannot degrade beyond an acceptable level.

4. DISCUSSION OF RESULTS

4.1 PERFORMANCE FOR NON-FADING SIGNALS

One of the problems in selecting the message format in the PPM encoding scheme is the proper distribution of pulses between synchronization pulses and parity checks.

In general, the probability of correct decoding a message for a given SNR/pulse will be limited either by the probability of correct synchronization or by the probability of correct decoding for an information segment. Figures 4.1 - 4.3 help to resolve the problem of how to distribute redundancy between the synchronization and information segments for different performance requirements.

In Figs. 4.1 (a - c) we have plotted the minimum value of SNR necessary to achieve the probability of correct synchronization .99, .999, and .9999 vs. the number of synchronization pulses. These graphs also include plots for information blocks consisting of two and twelve information pulses, and different numbers of parity checks for "soft" and "hard" decoding.

We used algorithm A and its modification for synchronization, for the "soft" decoder and for computation of frame errors. For the "hard" decoder, we plotted only values for $n_p = 0$, $n_p = 2$ in the single error correcting mode and $n_p = 4$ in the double error correcting mode. This is because for the considered decoding modes, probabilities of decoding with one, three or five parity checks cannot exceed those with zero, two and four parity checks, respectively.

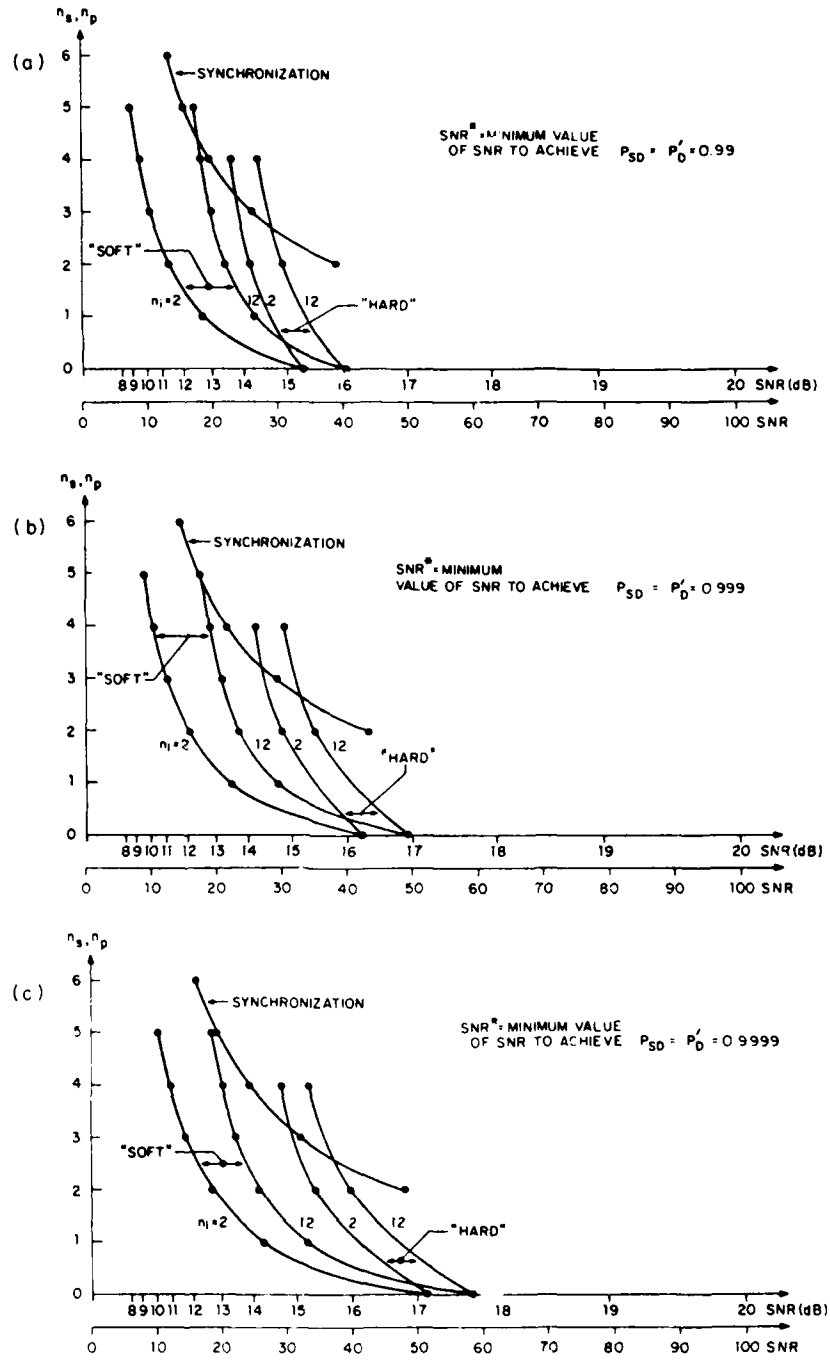

Fig. 4.1 Redundancy vs minimum SNR/pulse to achieve different levels of probability of detection for synchronization and "soft" and "hard" decoding. The redundancy vs min SNR is traded for $n_l = 2$ and 12. Algorithm A.

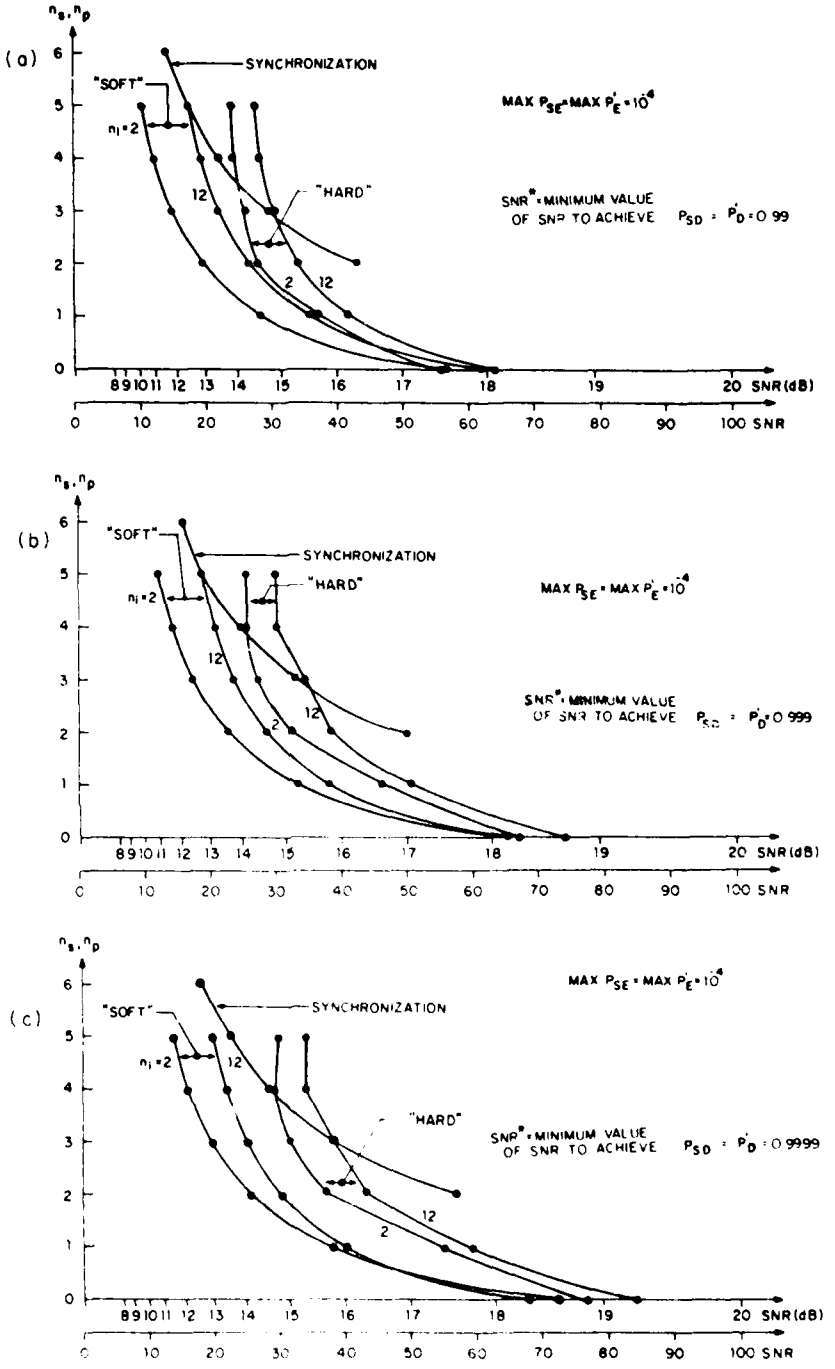

Fig. 4.2 Redundancy vs minimum SNR/pulse to achieve different levels of probability of detection for synchronization and "soft" and "hard" decoding. The redundancy vs min SNR is traded for $n_i = 2$ and 12. Algorithm C, maximum allowable probability of error 10^{-4}

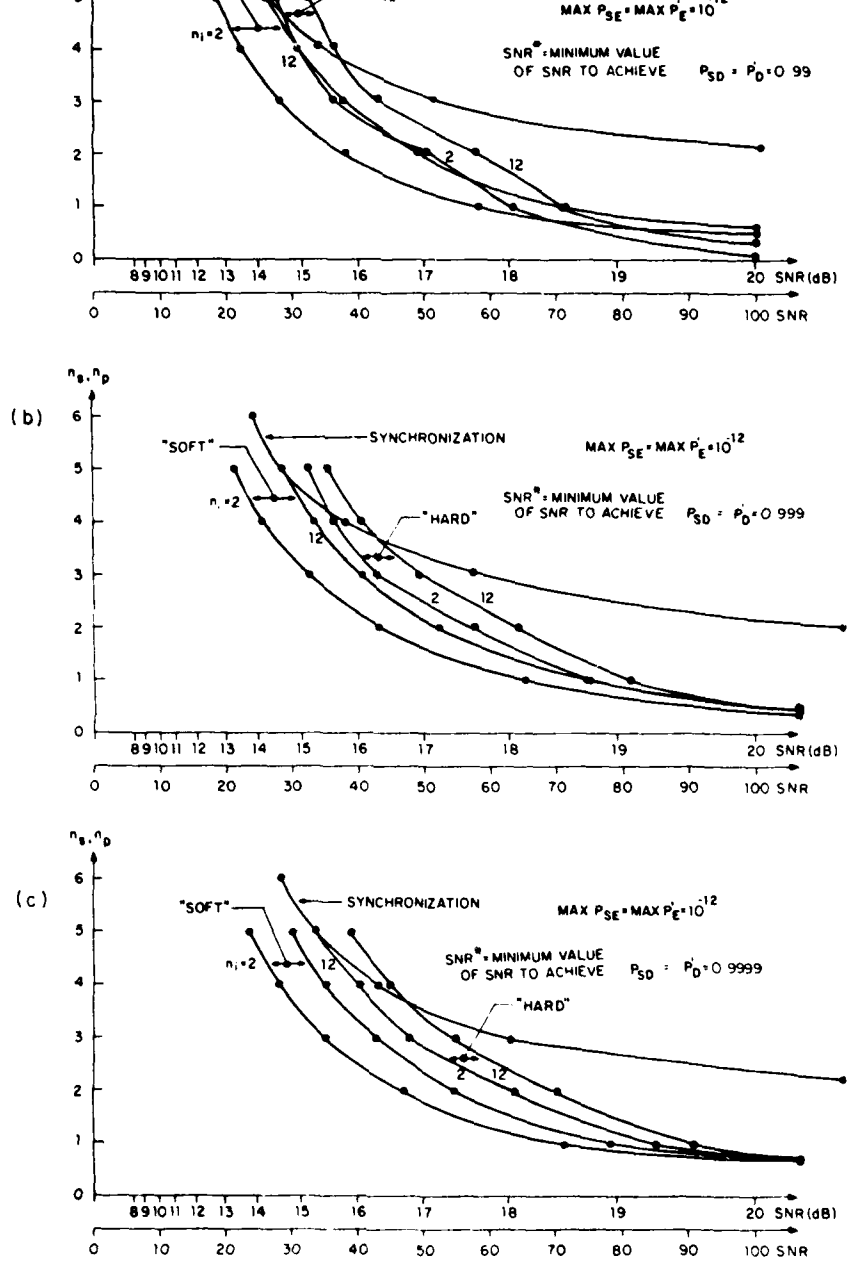

Fig. 4.3 Redundancy vs minimum SNR/pulse to achieve different levels of probability of detection for synchronization and "soft" and "hard" decoding. The redundancy vs min SNR is traded for n_1 = 2 and 12. Algorithm C, maximum allowable probability of error 10^{-12}.

Consider first Fig. 4.1a. If the number of pulses in an information block is twelve, and the "hard" decoder is used, then for two parity checks a synchronization segment with two or three pulses should be used. With two synchronization pulses the overall probability of decoding is limited by the synchronization and probability of decoding of 0.99 can be achieved at approximately 16 dB. With three synchronization pulses one is limited by the performance of the "hard" decoder and a probability of decoding of 0.99 can be achieved at about 15 dB. There is no gain from increasing the number of synchronization pulses to four. If the "soft" decoder is used with the same number of information pulses and parity checks, a synchronization segment with three or four pulses is appropriate. Use of five synchronization pulses would not provide a substantial gain.

Figure 4.1c leads to the observation that in order to achieve a probability of decoding of 0.9999 with SNR/pulse of 14.5 dB, the redundancy required is four synchronization pulses and one parity check for a block of two information pulses ("soft" decoder). In this case, the use of the "hard" decoder would require more than five parity checks. Figure 4.1 (a - c) allow one to quantify 1) the advantage of a "soft" decoder and 2) the improvement in SNR with the probability of decoding. The "soft" decoder and the algorithm used to estimate the position of the synchronization segment are optimal. They have, however, the property that when SNR/pulse approaches zero, the probability of error approaches unity. Figures 4.2 - 4.3 show the same relationship as Fig. 4.1 but with an additional constraint: maximum probability of error cannot exceed 10^{-4} and 10^{-12}, respectively for both the synchronization segment and the decoder.

As one can see, the minimum value of SNR/pulse required to obtain the desired level of the probability of decoding increases with higher performance requirements. This increase is of the

order of 1 or 2 dB for zero parity checks and even smaller for two synchronization pulses (Fig. 4.2). As the redundancy is increased, the increase of SNR/pulse becomes small or negligible. In Fig. 4.3, (max P'_E = max P_{SE} = 10^{-12}) the increases of SNR/pulse are much more significant.

For low redundancy blocks and synchronization segments one may need to increase SNR/pulse by more than 3 dB. Again, the increase becomes smaller for higher redundancies. It is worth noting that the margin of gain in SNR/pulse due to the use of a "soft" rather than a "hard" decoder is much smaller in this case.

It is evident that increased redundancy allows the use of lower SNR/pulse values for a given level of probability of correct decoding. The tradeoffs between redundancy and SNR/pulse is of particular interest when the scanning time is an important figure of merit.

The expression for minimum scanning time may be written as

$$T^*_{sc} = a \cdot \sqrt{(SNR)^*} \cdot n \,. \qquad (4.1)$$

The units for minimum scanning time have been so selected that the numerical value of the proportionality coefficient, a, equals unity. $(SNR)^*$ denotes the minimum SNR/pulse value required to obtain a probability of correct decoding equal to a preselected value, and n denotes the total number of pulses in a message.

Tables 4.1 - 4.8 show the values of minimum relative scanning time (T^*_s) and minimum SNR/pulse required to reach a probability of correct decoding 0.9999. Each table

TABLE 4.1 "SOFT" DECODER TRADEOFF BETWEEN REDUNDANCY, SNR (dB) AND RELATIVE SCANNING TIME FOR

$n_i = 4$, $P_D = 0.9999$, and $10^{-8} \leq \max P_E \leq 2 \cdot 10^{-8}$

n_s \ n_p	0	1	2	3	4	5
2	1.03 (20.4)	1.08 (19.4)	1.23 (19.4)	1.39 (19.4)	1.54 (19.4)	1.69 (19.4)
3	1.20 (20.4)	1.00 (17.6)	1.02 (16.7)	1.13 (16.7)	1.25 (16.7)	1.36 (16.7)
4	1.38 (20.4)	1.12 (17.6)	1.03 (15.9)	1.08 (15.4)	1.17 (15.4)	1.27 (15.4)
5	1.55 (20.4)	1.25 (17.6)	1.14 (15.9)	1.09 (14.8)	1.14 (14.5)	1.22 (14.5)
6	1.72 (20.4)	1.37 (17.6)	1.24 (15.9)	1.17 (14.8)	1.14 (13.9)	1.20 (13.7)

TABLE 4.2 "HARD" DECODER TRADEOFF BETWEEN REDUNDANCY, SNR (dB) AND RELATIVE SCANNING TIME FOR

$n_i = 4$, $P_D = 0.9999$, and $10^{-8} \leq \max P_E \leq 2 \cdot 10^{-8}$

n_s \ n_p	0	1	2	3	4	5
2	1.00 (20.4)	1.04 (19.4)	1.19 (19.4)	1.34 (19.4)	1.49 (19.4)	1.63 (19.4)
3	1.17 (20.4)	1.07 (18.5)	1.05 (17.3)	1.10 (16.7)	1.21 (16.7)	1.32 (16.7)
4	1.33 (20.4)	1.21 (18.5)	1.16 (17.2)	1.12 (16.1)	1.15 (15.5)	1.23 (15.5)
5	1.50 (20.4)	1.34 (18.5)	1.28 (17.2)	1.22 (16.1)	1.22 (15.4)	1.24 (14.9)
6	1.67 (20.4)	1.47 (18.5)	1.40 (17.2)	1.32 (16.1)	1.31 (15.4)	1.33 (14.9)

TABLE 4.3 "SOFT" DECODER TRADEOFF BETWEEN REDUNDANCY, SNR (dB) AND RELATIVE SCANNING TIME FOR

$n_i = 4$, $P_D = 0.9999$, and $10^{-12} \leq \max P_E \leq 2 \cdot 10^{-12}$

n_s \ n_p	0	1	2	3	4	5
2	1.04 (21.6)	1.12 (20.9)	1.28 (20.9)	1.44 (20.9)	1.60 (20.9)	1.76 (20.9)
3	1.22 (21.6)	1.00 (18.8)	1.03 (18.0)	1.14 (18.0)	1.26 (18.0)	1.37 (18.0)
4	1.39 (21.6)	1.12 (18.8)	1.03 (17.1)	1.03 (16.3)	1.13 (16.3)	1.22 (16.3)
5	1.57 (21.6)	1.25 (18.8)	1.13 (17.1)	1.07 (15.8)	1.08 (15.2)	1.16 (15.2)
6	1.74 (21.6)	1.37 (18.8)	1.23 (17.1)	1.16 (15.8)	1.12 (14.9)	1.14 (14.4)

TABLE 4.4 "HARD" DECODER TRADEOFF BETWEEN REDUNDANCY, SNR (dB) AND RELATIVE SCANNING TIME FOR

$n_i = 4$, $P_D = 0.9999$, and $10^{-12} \leq \max P_E \leq 2 \cdot 10^{-12}$

n_s \ n_p	0	1	2	3	4	5
2	1.00 (21.4)	1.10 (20.9)	1.26 (20.9)	1.42 (20.9)	1.57 (20.9)	1.73 (20.9)
3	1.17 (21.4)	1.06 (19.4)	1.04 (18.3)	1.13 (18.0)	1.24 (18.0)	1.35 (18.0)
4	1.33 (21.4)	1.19 (19.4)	1.16 (18.2)	1.10 (16.9)	1.12 (16.3)	1.20 (16.3)
5	1.50 (21.4)	1.32 (19.4)	1.27 (18.2)	1.20 (16.9)	1.18 (16.1)	1.18 (15.5)
6	1.67 (21.4)	1.46 (19.4)	1.39 (18.2)	1.30 (16.9)	1.28 (16.1)	1.26 (15.4)

TABLE 4.5 "SOFT" DECODER TRADEOFF BETWEEN REDUNDANCY, SNR (dB) AND RELATIVE SCANNING TIME FOR

$n_i = 2 \times 12 = 24$, $P_D = 0.9999$, $2 \times 10^{-8} \leq \max P_E \leq 3 \cdot 10^{-8}$

n_s \ n_p	0	1	2	3	4	5
2	1.36 (20.3)	1.32 (19.4)	1.41 (19.4)	1.50 (19.4)	1.60 (19.4)	1.69 (19.4)
3	1.41 (20.3)	1.13 (17.8)	1.07 (16.7)	1.14 (16.7)	1.21 (16.7)	1.28 (16.7)
4	1.46 (20.3)	1.17 (17.8)	1.05 (16.3)	1.02 (15.5)	1.07 (15.4)	1.13 (15.4)
5	1.51 (20.3)	1.21 (17.8)	1.09 (16.3)	1.03 (15.3)	1.00 (14.6)	1.04 (14.5)
6	1.57 (20.3)	1.24 (17.8)	1.12 (16.3)	1.05 (15.3)	1.02 (14.5)	1.00 (13.9)

TABLE 4.6 "HARD" DECODER TRADEOFF BETWEEN REDUNDANCY, SNR (dB) AND RELATIVE SCANNING TIME FOR

$n_i = 2 \times 12 = 24$, $P_D = 0.9999$, $2 \times 10^{-8} \leq \max P_E \leq 3 \cdot 10^{-8}$

n_s \ n_p	0	1	2	3	4	5
2	1.24 (20.7)	1.15 (19.4)	1.23 (19.4)	1.31 (19.4)	1.39 (19.4)	1.47 (19.4)
3	1.29 (20.7)	1.12 (18.9)	1.05 (17.7)	1.00 (16.8)	1.06 (16.7)	1.12 (16.7)
4	1.33 (20.7)	1.15 (18.9)	1.08 (17.7)	1.01 (16.6)	1.00 (16.0)	1.00 (15.6)
5	1.38 (20.7)	1.19 (18.9)	1.11 (17.7)	1.04 (16.6)	1.03 (16.0)	1.02 (15.4)
6	1.43 (20.7)	1.23 (18.9)	1.15 (17.7)	1.07 (16.6)	1.06 (16.0)	1.05 (15.4)

TABLE 4.7 "SOFT" DECODER TRADEOFF BETWEEN REDUNDANCY, SNR (dB) AND RELATIVE SCANNING TIME FOR

$n_i = 2 \times 12 = 24$, $P_D = 0.9999$, $2 \times 10^{-12} \leq \max P_E \leq 3 \cdot 10^{-12}$

n_s \ n_p	0	1	2	3	4	5
2	1.42 (21.6)	1.41 (20.9)	1.51 (20.9)	1.61 (20.9)	1.71 (20.9)	1.81 (20.9)
3	1.48 (21.6)	1.17 (19.0)	1.12 (18.0)	1.19 (18.0)	1.26 (18.0)	1.33 (18.0)
4	1.53 (21.6)	1.21 (19.0)	1.08 (17.4)	1.02 (16.4)	1.07 (16.3)	1.12 (16.3)
5	1.59 (21.6)	1.25 (19.0)	1.11 (17.4)	1.04 (16.3)	1.00 (15.5)	1.02 (15.2)
6	1.64 (21.6)	1.29 (19.0)	1.15 (17.4)	1.07 (16.3)	1.03 (15.5)	1.00 (14.8)

TABLE 4.8 "HARD" DECODER TRADEOFF BETWEEN REDUNDANCY, SNR (dB) AND RELATIVE SCANNING TIME FOR

$n_i = 2 \times 12 = 24$, $P_D = 0.9999$, $2 \times 10^{-12} \leq \max P_E \leq 3 \cdot 10^{-12}$

n_s \ n_p	0	1	2	3	4	5
2	1.29 (21.7)	1.27 (20.9)	1.36 (20.9)	1.45 (20.9)	1.54 (20.9)	1.63 (20.9)
3	1.34 (21.7)	1.15 (19.7)	1.08 (18.6)	1.07 (18.0)	1.13 (18.0)	1.20 (18.0)
4	1.39 (21.7)	1.19 (19.7)	1.12 (18.6)	1.04 (17.5)	1.00 (16.6)	1.02 (16.3)
5	1.44 (21.7)	1.23 (19.7)	1.15 (18.6)	1.07 (17.5)	1.02 (16.6)	1.01 (16.0)
6	1.49 (21.7)	1.27 (19.7)	1.19 (18.6)	1.10 (17.5)	1.05 (16.6)	1.04 (16.0)

consists of two parts; in the first we have results for a "soft" decoder (algorithm C), and in the second the results are for a "hard" decoder.

Tables are constructed for two values of the maximum allowable probability of error (max $P_E \sim 10^{-8}$ and max $P_E \sim 10^{-12}$) and for three values of the number of information pulses $n_i = 2$, $n_i = 4$, and $n_i = 12$ (two blocks). The minimum relative scanning time in each panel of the table is normalized, i.e., each minimum scanning time has been divided by the smallest scanning time in the set.

This type of table makes it possible to select the most advantageous format depending on the importance of each of the parameters: scanning time or SNR/pulse. For instance in Tables 4.1 and 4.2 we would select the following sequence of formats:

"Soft" Decoder	"Hard" Decoder
$\{(n_s, n_p), T_s^*$ (SNR)* in dB$\}$	$\{(n_s, n_p), T_s^*$ (SNR)* in dB$\}$
{(3, 1), 1.00, (17.6)}	{(2, 0), 1.00, (20.4)}
{(3, 2), 1.02, (16.7)}	{(2, 1), 1.04, (19.4)}
{(4, 2), 1.03, (15.9)}	{(3, 1), 1.07, (18.5)}
{(4, 3), 1.08, (15.4)}	{(3, 2), 1.05, (17.3)}
{(5, 3), 1.09, (14.8)}	{(3, 3), 1.10, (16.7)}
{(6, 4), 1.14, (13.9)}	{(4, 3), 1.12, (16.1)}
{(6, 5), 1.20, (13.7)}	{(5, 4), 1.22, (15.4)}
	{(5, 5), 1.24, (14.9)}

The smallest minimum scanning time is about 4% lower for the "soft" than for the "hard" decoder. Thus, in comparing the T_s^* values listed above, those for the "hard" decoder should be increased by 4%.

In both cases the optimum scanning time is obtained for low redundancy. In addition, often a change of message format may lead to relatively small changes in scanning time but to a more pronounced change in required SNR/pulse value.

The lowest achievable SNR/pulse value in the set describing the "soft" decoder corresponds to 13.7 dB, and for the "hard" decoder is about 1.2 dB higher. In addition, the scanning time for the "hard" decoder will be almost 10% higher for this increased SNR value.

Similar analyses can be performed using results from Tables 4.3 and 4.4 for which the maximum allowable proability of decoding error was set at about 2×10^{-12} per message. In this table the smallest minimum scanning time for the "soft" decoder is about 2% lower than for the "hard" decoder. The selection of advantageous formats is even simpler for messages containing two information blocks with twelve information pulses. For instance, in Tables 4.5 and 4.6 we would select the following formats:

"Soft" Decoder	"Hard" Decoder
$\{(n_s, n_p), T_s^*, (SNR)^* \text{ in dB}\}$	$\{(n_s, n_p), T_s^*, (SNR)^* \text{ in dB}\}$
$\{(6, 5), 1.00, (13.9)\}$	$\{(4, 4), 1.00, (16)\}$
	$\{(4, 5), 1.00, (15.6)\}$
	$\{(5, 5), 1.00, (15.4)\}$

The smallest minimum scanning time is about 14% lower for the "soft" than for the "hard" decoder.

In both cases the optimum scanning time is obtained for rather high redundancy. Again small changes of message formats

may lead to relatively small changes in scanning time but to a larger change in required SNR/pulse value. The lowest achievable SNR/pulse value in the set describing the "soft" decoder corresponds to 13.9 dB, and for the "hard" decorder is about 1.5 dB higher. In addition, the scanning time for the "hard" decoder will be higher by about 14% for this increased SNR value.

In applying results from Tables 4.7 and 4.8 (max $P_E \leq 3 \cdot 10^{-12}$) it should be remembered that the minimum scanning time for the "soft" decoder is about 11% lower than for the "hard" decoder.

In general, the "soft" decoder which is optimal in the absence of thresholds remains better than the "hard" decoder with increased performance requirements. The only exception is the case in which messages with zero parity checks are used (this case is discussed below).

The gain in SNR/pulse values resulting from use of the "soft" decoder is in the range of 1 to 3 dB. The advantage from use of the "soft" decoder, however, decreases with higher performance requirements (max P_E, P_D).

On the other hand, the "hard" decoder has some advantages of its own; it is easier to implement in real time and it is "robust" in the sense that the probability of error can be kept below desired levels (without major modifications) even in the presence of fading.

As indicated before, the preferable approach to minimize scanning time for short messages ($n_i = 2$ or 4) is to use messages with relatively high SNR/pulse and low redundancy. For long messages ($n_i = 24$), the preferable approach to minimize scanning time is to operate at relatively low values of SNR/pulse and with relatively high redundancy.

Table 4.9 through 4.14 show the dependence of minimum scanning time on different performance requirements. For each value of

TABLE 4.9 "SOFT" DECODER
DEPENDANCE OF MINIMUM RELATIVE SCANNING TIME
ON THE PERFORMANCE REQUIREMENTS

$n_i = 2,\ 1 \leq \gamma \leq 2$

$\max P_E$ \ P_D	.99	.999	.9999
$\gamma\ 10^{-4}$	1.00 (17.5 (2, 0)	1.07 (18.1) (2, 0)	1.13 (18.6) (2, 0)
$\gamma\ 10^{-8}$	1.25 (19.5) (2, 0)	1.33 (20.0) (2, 0)	1.39 (20.4) (2, 0)
$\gamma\ 10^{-12}$	1.46 (20.8) (2, 0)	1.53 (21.2) (2, 0)	1.59 (21.6) (2, 0)

TABLE 4.10 "HARD" DECODER
DEPENDANCE OF MINIMUM RELATIVE SCANNING TIME
ON THE PERFORMANCE REQUIREMENTS

$n_i = 2,\ 1 \leq \gamma \leq 2$

$\max P_E$ \ P_D	.99	.999	.9999
$\gamma\ 10^{-4}$	1.00 (17.4) (2, 0)	1.10 (18.2) (2, 0)	1.18 (18.6) (2, 0)
$\gamma\ 10^{-8}$	1.21 (19.1) (2, 0)	1.30 (19.7) (2, 0)	1.38 (20.2) (2, 0)
$\gamma\ 10^{-12}$	1.40 (20.3) (2, 0)	1.48 (20.8) (2, 0)	1.56 (21.3) (2, 0)

T_s
(SNR)
(n_s, n_p)

TABLE 4.11 "SOFT" DECODER
DEPENDANCE OF MINIMUM RELATIVE SCANNING TIME
ON THE PERFORMANCE REQUIREMENTS

$n_i = 4,\ 1 \leq \gamma \leq 2$

max P_E \ P_D	.99	.999	.9999
$\gamma\ 10^{-4}$	1.00 (15.0) (3, 1)	1.06 (15.5) (3, 1)	1.11 (16.0) (3, 1)
$\gamma\ 10^{-8}$	1.23 (16.8) (3, 1)	1.29 (17.3) (3, 1)	1.34 (17.6) (3, 1)
$\gamma\ 10^{-12}$	1.43 (18.1) (3, 1)	1.49 (18.5) (3, 1)	1.53 (18.8) (3, 1)

TABLE 4.12 "HARD" DECODER
DEPENDANCE OF MINIMUM RELATIVE SCANNING TIME
ON THE PERFORMANCE REQUIREMENTS

$n_i = 4,\ 1 \leq \gamma \leq 2$

max P_E \ P_D	.99	.999	.9999
$\gamma\ 10^{-4}$	1.00 (17.7) (2, 0)	1.08 (18.4) (2, 0)	1.16 (19.0) (2, 0)
$\gamma\ 10^{-8}$	1.20 (19.3) (2, 0)	1.29 (19.9) (2, 0)	1.36 (20.4) (2, 0)
$\gamma\ 10^{-12}$	1.37 (20.4) (2, 0)	1.45 (21.0) (2, 0)	1.53 (21.4) (2, 0)

T_s
(SNR)
(n_s, n_p)

TABLE 4.13 "SOFT" DECODER
DEPENDANCE OF MINIMUM RELATIVE SCANNING TIME
ON THE PERFORMANCE REQUIREMENTS

$n_i = 2 \times 12 = 24$
$2 \leq \gamma \leq 3, 2 \leq n_s \leq 6, 0 \leq n_p \leq 5$

P_D / max P_E	.99	.999	.9999
$\gamma\ 10^{-4}$	1.00 (12.9) (5, 4)	1.04 (13.3) (5, 4)	1.08 (13.6) (5, 4)
$\gamma\ 10^{-8}$	1.13 (14.0) (5, 4)	1.17 (14.3) (5, 4)	1.21 (14.6) (5, 4)
$\gamma\ 10^{-12}$	1.26 (14.3) (5, 5)	1.31 (14.6) (6, 5)	1.34 (14.8) (6, 5)

TABLE 4.14 "HARD" DECODER
DEPENDANCE OF MINIMUM RELATIVE SCANNING TIME
ON THE PERFORMANCE REQUIREMENTS

$n_i = 2 \times 12 = 24$
$2 \leq \gamma \leq 3, 2 \leq n_s \leq 6, 0 \leq n_p \leq 5$

P_D / max P_E	.99	.999	.9999
$\gamma\ 10^{-4}$	1.00 (15.5) (3, 2)	1.06 (16.0) (3, 2)	1.12 (16.5) (3, 2)
$\gamma\ 10^{-8}$	1.10 (15.8) (3, 3)	1.17 (15.6) (4, 4)	1.23 (16.0) (4, 4)
$\gamma\ 10^{-12}$	1.19 (15.7) (4, 4)	1.26 (16.2) (4, 4)	1.32 (16.7) (4. 4)

T_s
(SNR)
(n_s, n_p)

maximum allowable probability of error (max P_E) and for each value of the probability of decoding (P_D), the following three values are listed: normalized minimum scanning time (T*), required SNR/pulse in dB, and the message format (n_s, n_p) leading to the minimum scanning time for the particular performance requirement. The term "normalized" refers to the fact that in each table the value of the minimum scanning time for the lowest performance requirement has been scaled to unity.

Tables 4.9 and 4.10 are for two information pulses. They show that the scanning time increases by more than 50% as one moves towards the highest performance requirements. This increase is accompanied by an increase of SNR/pulse of about 4 dB. This is the only case in which the "hard" decoder requires generally shorter scanning time than the "soft" decoder.

For such messages minimum scanning time is obtained when the number of parity checks is zero. Since "hard" and "soft" decoders coincide in such a case in the absence of thresholding, the difference between the two tables is due to the different way of thresholding.

The results are similar for Tables 4.11 and 4.12 where four information pulses are considered.

In contrast, in Tables 4.13 and 4.14 for information blocks each containing twelve information pulses, the increase in scanning time ranges from 32 to 34% and the increase in SNR/pulse ranges from 1.2 to 1.9 dB.

The values of SNR/pulse shown in Tables 4.9 through 4.14 could be partially misleading. As mentioned in the previous discussion of the more detailed set of Tables 4.1 through 4.8, a small change in scanning time may result in larger changes in the required SNR/pulse.

4.2 PERFORMANCE DEGRADATION DUE TO SIGNAL FADING

The performance of signal processing schemes designed to meet the requirements for deterministic signals will be altered when fading is present. Our goal here is to evaluate this fading-induced performance degradation. We considered signal processing in which the detection algorithm for synchronization (Algorithm C) is followed by a "hard" decoder with thresholds.

An idealized fading model in which a pulse is "lost" with probability P_o was used to bound the performance degradation. Several aspects of fading-induced effects were discussed earlier in Section 3.3.5. Tables 4.15 through 4.23 describe fading-induced performance degradation of several algorithms designed to keep maximum allowable probability of error below preselected values in the absence of fading. These tables are for different numbers of information pulses. In each table we specify the message format defined by the number of parity checks, n_p and synchronization pulses, n_s. For each of these formats we have listed the value of relative minimum scanning time followed by the value of minimum SNR/pulse required to obtain the probability of decoding, $P_D = .9999$. The fading is characterized by $-2 \log C$, where C is the fading contrast; for the contrast values under consideration this parameter is simply related to the probability of "losing" a pulse, P_o. Indeed, since $C \simeq P_o^{\frac{1}{2}}$ and $P_o = 10^{-t}$, then $-2 \log C \simeq t$. The relative scanning time was defined as in Tables 4.1 through 4.8. All the positions marked by asterisks indicate that either the "hard" decoder performs with the probability of decoding lower than 0.9999 for any SNR/pulse, or that the maximum probability of synchronization error exceeds a preselected level (indicated in individual Table legends). As noted in Section 3.3.5, for the specified contrast values the "hard" decoder is "robust" in the sense that maximum error probability is not affected by fading.

TABLE 4.15

FADING INDUCED PERFORMANCE DEGRADATION OF "HARD" DECODING TOGETHER WITH SYNCHRONIZATION

$n_i = 2$, $P_D = 0.9999$, $10^{-4} \leq \max P_E \leq 2 \times 10^{-4}$

n_s	-LOG C \ n_p	0	1	2	3	4	5
2	2	**** (****)	**** (****)	**** (****)	**** (****)	**** (****)	**** (****)
	3	**** (****)	**** (****)	**** (****)	**** (****)	**** (****)	**** (****)
	4	**** (****)	**** (****)	**** (****)	**** (****)	**** (****)	**** (****)
	5	1.01 (19.0)	1.11 (17.8)	1.29 (17.6)	1.51 (17.6)	1.73 (17.6)	1.94 (17.6)
	∞	1.00 (18.9)	1.09 (17.6)	1.29 (17.5)	1.50 (17.5)	1.71 (17.5)	1.93 (17.5)
3	2	**** (****)	**** (****)	**** (****)	**** (****)	**** (****)	**** (****)
	3	**** (****)	**** (****)	1.54 (17.7)	1.75 (17.7)	1.97 (17.7)	2.19 (17.7)
	4	**** (****)	**** (****)	1.40 (16.9)	1.60 (16.9)	1.80 (16.9)	2.00 (16.9)
	5	1.26 (18.9)	1.28 (17.5)	1.30 (16.3)	1.48 (16.2)	1.66 (16.2)	1.84 (16.2)
	∞	1.25 (18.9)	1.26 (17.4)	1.25 (15.9)	1.40 (15.8)	1.58 (15.8)	1.75 (15.8)
4	2	**** (****)	**** (****)	**** (****)	2.15 (18.5)	2.36 (18.4)	2.59 (18.4)
	3	**** (****)	**** (****)	1.60 (16.9)	1.80 (16.9)	2.00 (16.9)	2.20 (16.9)
	4	**** (****)	**** (****)	1.41 (15.8)	1.50 (15.4)	1.64 (15.2)	1.80 (15.2)
	5	1.51 (18.9)	1.49 (17.5)	1.40 (15.7)	1.46 (15.1)	1.55 (14.7)	1.71 (14.8)
	∞	1.50 (18.9)	1.47 (17.4)	1.40 (15.7)	1.46 (15.1)	1.54 (14.7)	1.71 (14.7)
5	2	**** (****)	**** (****)	**** (****)	2.28 (18.1)	2.48 (18.0)	2.71 (18.0)
	3	**** (****)	**** (****)	1.60 (15.9)	1.67 (15.4)	1.78 (15.1)	1.95 (15.1)
	4	**** (****)	**** (****)	1.57 (15.8)	1.63 (15.1)	1.68 (14.6)	1.85 (14.6)
	5	1.76 (18.9)	1.71 (17.5)	1.57 (15.7)	1.62 (15.1)	1.68 (14.6)	1.84 (14.6)
	∞	1.75 (18.9)	1.68 (17.4)	1.57 (15.7)	1.62 (15.1)	1.68 (14.6)	1.84 (14.6)
6	2	**** (****)	**** (****)	**** (****)	2.28 (17.2)	2.45 (17.1)	2.65 (17.1)
	3	**** (****)	**** (****)	1.77 (15.9)	1.79 (15.2)	1.84 (14.6)	2.00 (14.7)
	4	**** (****)	**** (****)	1.75 (15.8)	1.79 (15.1)	1.83 (14.6)	2.00 (14.6)
	5	2.01 (18.9)	1.92 (17.5)	1.75 (15.7)	1.79 (15.1)	1.83 (14.6)	2.00 (14.6)
	∞	2.00 (18.9)	1.89 (17.4)	1.75 (15.7)	1.79 (15.1)	1.83 (14.6)	2.00 (14.6)

MINIMUM T_s = 35.1

TABLE 4.16
FADING INDUCED PERFORMANCE DEGRADATION OF "HARD" DECODING TOGETHER WITH SYNCHRONIZATION

$n_I = 2$, $P_D = 0.9999$, $10^{-8} \leq \max P_E \leq 2 \times 10^{-8}$

n_s	-2 LOG c \ n_p	0	1	2	3	4	5
2	2	**** (****)	**** (****)	**** (****)	**** (****)	**** (****)	**** (****)
	3	**** (****)	**** (****)	**** (****)	**** (****)	**** (****)	**** (****)
	4	**** (****)	**** (****)	**** (****)	**** (****)	**** (****)	**** (****)
	5	**** (****)	**** (****)	**** (****)	**** (****)	**** (****)	**** (****)
	∞	1.00 (20.3)	1.13 (19.4)	1.36 (19.4)	1.58 (19.4)	1.81 (19.4)	2.04 (19.4)
3	2	**** (****)	**** (****)	**** (****)	**** (****)	**** (****)	**** (****)
	3	**** (****)	**** (****)	**** (****)	**** (****)	**** (****)	**** (****)
	4	**** (****)	**** (****)	**** (****)	**** (****)	**** (****)	**** (****)
	5	1.26 (20.3)	1.22 (18.5)	1.21 (17.1)	1.34 (16.8)	1.51 (16.8)	1.68 (16.8)
	∞	1.25 (20.3)	1.21 (18.4)	1.21 (17.0)	1.34 (16.8)	1.50 (16.8)	1.67 (16.8)
4	2	**** (****)	**** (****)	**** (****)	**** (****)	**** (****)	**** (****)
	3	**** (****)	**** (****)	1.42 (17.3)	1.56 (17.1)	1.72 (17.0)	1.89 (17.0)
	4	**** (****)	**** (****)	1.37 (17.0)	1.39 (16.1)	1.49 (15.8)	1.64 (15.7)
	5	1.51 (20.3)	1.42 (18.5)	1.37 (17.0)	1.37 (16.0)	1.45 (15.5)	1.59 (15.5)
	∞	1.50 (20.3)	1.41 (18.4)	1.37 (17.0)	1.37 (16.0)	1.45 (15.5)	1.59 (15.5)
5	2	**** (****)	**** (****)	**** (****)	**** (****)	**** (****)	**** (****)
	3	**** (****)	**** (****)	1.57 (17.1)	1.56 (16.2)	1.59 (15.5)	1.71 (15.4)
	4	**** (****)	**** (****)	1.54 (17.0)	1.52 (16.0)	1.54 (15.2)	1.61 (14.8)
	5	1.76 (20.3)	1.63 (18.5)	1.54 (17.0)	1.52 (15.9)	1.54 (15.2)	1.60 (14.8)
	∞	1.75 (20.3)	1.61 (18.4)	1.54 (17.0)	1.52 (15.9)	1.54 (15.2)	1.60 (14.8)
6	2	**** (****)	**** (****)	**** (****)	**** (****)	2.12 (17.2)	2.26 (17.1)
	3	**** (****)	**** (****)	1.74 (17.1)	1.70 (16.1)	1.68 (15.2)	1.73 (14.8)
	4	**** (****)	**** (****)	1.72 (17.0)	1.68 (16.0)	1.68 (15.2)	1.72 (14.8)
	5	2.01 (20.3)	1.83 (18.5)	1.71 (17.0)	1.67 (15.9)	1.68 (15.2)	1.72 (14.8)
	∞	2.00 (20.3)	1.81 (18.4)	1.71 (17.0)	1.67 (15.9)	1.67 (15.2)	1.72 (14.8)

MINIMUM T_s = 41.2

TABLE 4.17

FADING INDUCED PERFORMANCE DEGRADATION OF "HARD" DECODING TOGETHER WITH SYNCHRONIZATION

$n_i = 2$, $P_D = 0.9999$, $10^{-12} \leq \max P_E \leq 2 \times 10^{-12}$

n_s	-2 LOG C \ n_p	0	1	2	3	4	5
2	2	**** (****)	**** (****)	**** (****)	**** (****)	**** (****)	**** (****)
	3	**** (****)	**** (****)	**** (****)	**** (****)	**** (****)	**** (****)
	4	**** (****)	**** (****)	**** (****)	**** (****)	**** (****)	**** (****)
	5	**** (****)	**** (****)	**** (***)	**** (****)	**** (****)	**** (****)
	∞	1.00 (21.3)	1.20 (20.9)	1.43 (20.9)	1.67 (20.9)	1.91 (20.9)	2.15 (20.9)
3	2	**** (****)	**** (****)	**** (****)	**** (****)	**** (****)	**** (****)
	3	**** (****)	**** (****)	**** (****)	**** (****)	**** (****)	**** (****)
	4	**** (****)	**** (****)	**** (****)	**** (****)	**** (****)	**** (****)
	5	**** (****)	**** (****)	**** (****)	**** (****)	**** (****)	**** (****)
	∞	1.25 (21.3)	1.19 (19.3)	1.22 (18.2)	1.37 (18.0)	1.54 (18.0)	1.71 (18.0)
4	2	**** (****)	**** (****)	**** (****)	**** (****)	**** (****)	**** (****)
	3	**** (****)	**** (****)	**** (****)	**** (****)	**** (****)	**** (****)
	4	**** (****)	**** (****)	**** (****)	**** (****)	**** (****)	**** (****)
	5	1.51 (21.3)	1.40 (19.4)	1.38 (18.1)	1.35 (16.8)	1.42 (16.4)	1.55 (16.3)
	∞	1.50 (21.3)	1.39 (19.3)	1.38 (18.1)	1.34 (16.8)	1.42 (16.4)	1.55 (16.3)
5	2	**** (****)	**** (****)	**** (****)	**** (****)	**** (****)	**** (****)
	3	**** (****)	**** (****)	**** (****)	**** (****)	**** (****)	**** (****)
	4	**** (****)	**** (****)	1.55 (18.1)	1.49 (16.8)	1.52 (16.2)	1.54 (15.5)
	5	1.76 (21.3)	1.61 (19.4)	1.55 (18.1)	1.49 (16.8)	1.52 (16.1)	1.52 (15.4)
	∞	1.75 (21.3)	1.59 (19.3)	1.55 (18.1)	1.49 (16.8)	1.52 (16.1)	1.52 (15.4)
6	2	**** (****)	**** (****)	**** (****)	**** (****)	**** (****)	**** (****)
	3	**** (****)	**** (****)	1.75 (18.2)	1.67 (17.0)	1.70 (16.3)	1.65 (15.4)
	4	**** (****)	**** (****)	1.73 (18.1)	1.64 (16.8)	1.66 (16.2)	1.64 (15.3)
	5	2.01 (21.3)	1.81 (19.4)	1.72 (18.1)	1.64 (16.8)	1.66 (16.1)	1.63 (15.3)
	∞	2.00 (21.3)	1.79 (19.3)	1.72 (18.1)	1.64 (16.8)	1.66 (16.1)	1.63 (15.3)

MINIMUM T_s = -46.4

TABLE 4.18

FADING INDUCED PERFORMANCE DEGRADATION OF "HARD" DECODING TOGETHER WITH SYNCHRONIZATION

$n_i = 4$, $P_D = 0.9999$, $10^{-4} \leq \max P_E \leq 2 \times 10^{-4}$

n_s	-2 LOG c \ n_p	0	1	2	3	4	5
2	2	**** (****)	**** (****)	**** (****)	**** (****)	**** (****)	**** (****)
	3	**** (****)	**** (****)	**** (****)	**** (****)	**** (****)	**** (****)
	4	**** (****)	**** (****)	**** (****)	**** (****)	**** (****)	**** (****)
	5	1.05 (19.2)	1.03 (17.9)	1.13 (17.6)	1.27 (17.6)	1.41 (17.6)	1.56 (17.6)
	∞	1.00 (19.0)	1.00 (17.7)	1.12 (17.5)	1.26 (17.5)	1.41 (17.5)	1.55 (17.5)
3	2	**** (****)	**** (****)	**** (****)	**** (****)	**** (****)	**** (****)
	3	**** (****)	**** (****)	1.30 (17.8)	1.45 (17.8)	1.58 (17.7)	1.72 (17.7)
	4	**** (****)	**** (****)	1.18 (16.9)	1.31 (16.9)	1.44 (16.9)	1.58 (16.9)
	5	1.18 (19.1)	1.14 (17.7)	1.09 (16.3)	1.21 (16.3)	1.33 (16.2)	1.45 (16.2)
	∞	1.17 (19.0)	1.12 (17.5)	1.06 (16.0)	1.16 (15.9)	1.26 (15.8)	1.38 (15.8)
4	2	**** (****)	**** (****)	**** (****)	**** (****)	1.85 (18.4)	2.02 (18.4)
	3	**** (****)	**** (****)	1.32 (17.0)	1.45 (17.0)	1.57 (16.9)	1.70 (16.9)
	4	**** (****)	**** (****)	1.17 (15.9)	1.27 (15.8)	1.29 (15.2)	1.40 (15.2)
	5	1.35 (19.1)	1.28 (17.7)	1.16 (15.9)	1.26 (15.7)	1.24 (14.9)	1.35 (14.9)
	∞	1.34 (19.0)	1.26 (17.5)	1.16 (15.9)	1.26 (15.7)	1.24 (14.9)	1.35 (14.9)
5	2	**** (****)	**** (****)	**** (****)	**** (****)	1.92 (18.0)	2.08 (18.0)
	3	**** (****)	**** (****)	1.31 (16.1)	1.42 (16.0)	1.39 (15.2)	1.50 (15.2)
	4	**** (****)	**** (****)	1.28 (15.9)	1.37 (15.7)	1.34 (14.8)	1.45 (14.9)
	5	1.52 (19.1)	1.43 (17.7)	1.28 (15.9)	1.37 (15.7)	1.34 (14.8)	1.45 (14.9)
	∞	1.50 (19.0)	1.40 (17.5)	1.28 (15.9)	1.37 (15.7)	1.34 (14.8)	1.45 (14.9)
6	2	**** (****)	**** (****)	**** (****)	**** (****)	1.87 (17.1)	2.02 (17.2)
	3	**** (****)	**** (****)	1.42 (16.1)	1.53 (16.0)	1.44 (14.8)	1.56 (14.9)
	4	**** (****)	**** (****)	1.39 (15.9)	1.49 (15.7)	1.44 (14.8)	1.55 (14.9)
	5	1.69 (19.1)	1.57 (17.7)	1.39 (15.9)	1.48 (15.7)	1.44 (14.8)	1.55 (14.9)
	∞	1.67 (19.0)	1.54 (17.5)	1.39 (15.9)	1.48 (15.7)	1.44 (14.8)	1.55 (14.9)

MINIMUM $T_s = 53.6$

TABLE 4.19

FADING INDUCED PERFORMANCE DEGRADATION OF "HARD" DECODING TOGETHER WITH SYNCHRONIZATION

$n_i = 4$, $P_D = 0.9999$, $10^{-8} \leq \max P_E \leq 2 \times 10^{-8}$

n_s	-2 LOG C \ n_p	0	1	2	3	4	5
2	2	**** (****)	**** (****)	**** (****)	**** (****)	**** (****)	**** (****)
	3	**** (****)	**** (****)	**** (****)	**** (****)	**** (****)	**** (****)
	4	**** (****)	**** (****)	**** (****)	**** (****)	**** (****)	**** (****)
	5	**** (****)	**** (****)	**** (****)	**** (****)	**** (****)	**** (****)
	∞	1.00 (20.4)	1.04 (19.4)	1.19 (19.4)	1.34 (19.4)	1.49 (19.4)	1.63 (19.4)
3	2	**** (****)	**** (****)	**** (****)	**** (****)	**** (****)	**** (****)
	3	**** (****)	**** (****)	**** (****)	**** (****)	**** (****)	**** (****)
	4	**** (****)	**** (****)	**** (****)	**** (****)	**** (****)	**** (****)
	5	1.18 (20.5)	1.09 (18.7)	1.05 (17.3)	1.10 (16.8)	1.21 (16.8)	1.32 (16.8)
	∞	1.17 (20.4)	1.07 (18.5)	1.05 (17.3)	1.10 (16.8)	1.21 (16.8)	1.32 (16.8)
4	2	**** (****)	**** (****)	**** (****)	**** (****)	**** (****)	**** (****)
	3	**** (****)	**** (****)	1.20 (17.6)	1.26 (17.1)	1.35 (17.0)	1.47 (17.0)
	4	**** (****)	**** (****)	1.17 (17.3)	1.13 (16.2)	1.18 (15.8)	1.27 (15.7)
	5	1.35 (20.5)	1.21 (18.7)	1.16 (17.3)	1.12 (16.1)	1.15 (15.6)	1.23 (15.5)
	∞	1.33 (20.4)	1.21 (18.5)	1.16 (17.3)	1.12 (16.1)	1.15 (15.6)	1.23 (15.5)
5	2	**** (****)	**** (****)	**** (****)	**** (****)	**** (****)	**** (****)
	3	**** (****)	**** (****)	1.31 (17.5)	1.26 (16.4)	1.25 (15.6)	1.31 (15.4)
	4	**** (****)	**** (****)	1.28 (17.3)	1.22 (16.1)	1.22 (15.4)	1.25 (15.0)
	5	1.52 (20.5)	1.36 (18.7)	1.28 (17.3)	1.22 (16.1)	1.22 (15.4)	1.25 (14.9)
	∞	1.50 (20.4)	1.34 (18.5)	1.28 (17.3)	1.22 (16.1)	1.22 (15.4)	1.24 (14.9)
6	2	**** (****)	**** (****)	**** (****)	**** (****)	1.67 (17.5)	1.72 (17.1)
	3	**** (****)	**** (****)	1.43 (17.5)	1.36 (16.3)	1.32 (15.4)	1.34 (15.0)
	4	**** (****)	**** (****)	1.40 (17.3)	1.32 (16.1)	1.31 (15.4)	1.33 (14.9)
	5	1.69 (20.5)	1.50 (18.7)	1.40 (17.3)	1.32 (16.1)	1.31 (15.4)	1.33 (14.9)
	∞	1.67 (20.4)	1.47 (18.5)	1.40 (17.3)	1.32 (16.1)	1.31 (15.4)	1.33 (14.9)

MINIMUM T_s = 62.6

TABLE 4.20

FADING INDUCED PERFORMANCE DEGRADATION OF "HARD" DECODING TOGETHER WITH SYNCHRONIZATION

$n_i = 4$, $P_D = 0.9999$, $10^{-12} \leq \max P_E \leq 2 \times 10^{-12}$

n_s	-2 LOG c \ n_p	0	1	2	3	4	5
2	2	**** (****)	**** (****)	**** (****)	**** (****)	**** (****)	**** (****)
	3	**** (****)	**** (****)	**** (****)	**** (****)	**** (****)	**** (****)
	4	**** (****)	**** (****)	**** (****)	**** (****)	**** (****)	**** (****)
	5	**** (****)	**** (****)	**** (****)	**** (****)	**** (****)	**** (****)
	∞	1.00 (21.4)	1.10 (20.9)	1.26 (20.9)	1.42 (20.9)	1.57 (20.9)	1.73 (20.9)
3	2	**** (****)	**** (****)	**** (****)	**** (****)	**** (****)	**** (****)
	3	**** (****)	**** (****)	**** (****)	**** (****)	**** (****)	**** (****)
	4	**** (****)	**** (****)	**** (****)	**** (****)	**** (****)	**** (****)
	5	**** (****)	**** (****)	**** (****)	**** (****)	**** (****)	**** (****)
	∞	1.17 (21.4)	1.06 (19.4)	1.04 (18.3)	1.13 (18.0)	1.24 (18.0)	1.35 (18.0)
4	2	**** (****)	**** (****)	**** (****)	**** (****)	**** (****)	**** (****)
	3	**** (****)	**** (****)	**** (****)	**** (****)	**** (****)	**** (****)
	4	**** (****)	**** (****)	**** (****)	**** (****)	**** (****)	**** (****)
	5	1.35 (21.5)	1.21 (19.6)	1.16 (18.2)	1.10 (17.0)	1.12 (16.4)	1.21 (16.3)
	∞	1.35 (21.4)	1.19 (19.4)	1.16 (18.2)	1.10 (17.0)	1.12 (16.4)	1.20 (16.3)
5	2	**** (****)	**** (****)	**** (****)	**** (****)	**** (****)	**** (****)
	3	**** (****)	**** (****)	**** (****)	**** (****)	**** (****)	**** (****)
	4	**** (****)	**** (****)	1.27 (18.2)	1.20 (17.0)	1.19 (16.2)	1.19 (15.6)
	5	1.51 (21.5)	1.35 (19.6)	1.27 (18.2)	1.20 (17.0)	1.19 (16.2)	1.18 (15.5)
	∞	1.50 (21.4)	1.32 (19.4)	1.27 (18.2)	1.20 (17.0)	1.18 (16.2)	1.18 (15.5)
6	2	**** (****)	**** (****)	**** (****)	**** (****)	**** (****)	**** (****)
	3	**** (****)	**** (****)	1.41 (18.4)	1.33 (17.2)	1.32 (16.4)	1.27 (15.5)
	4	**** (****)	**** (****)	1.39 (18.2)	1.30 (17.0)	1.28 (16.2)	1.26 (15.5)
	5	1.68 (21.5)	1.48 (19.6)	1.39 (18.2)	1.30 (17.0)	1.28 (16.2)	1.26 (15.5)
	∞	1.67 (21.4)	1.46 (19.4)	1.39 (18.2)	1.30 (17.0)	1.28 (16.2)	1.26 (15.5)

MINIMUM T_s = 70.5

TABLE 4.21

FADING INDUCED PERFORMANCE DEGRADATION OF "HARD" DECODING TOGETHER WITH SYNCHRONIZATION

$n_i = 2 \times 12 = 24$, $P_D = 0.9999$, $10^{-4} \leq \max P_E \leq 2 \times 10^{-4}$

n_s	n_p / -2 LOG C	0	1	2	3	4	5
2	2	**** (****)	**** (****)	**** (****)	**** (****)	**** (****)	**** (****)
	3	**** (****)	**** (****)	**** (****)	**** (****)	**** (****)	**** (****)
	4	**** (****)	**** (****)	**** (****)	**** (****)	**** (****)	**** (****)
	5	**** (****)	**** (****)	1.10 (17.6)	1.17 (17.6)	1.24 (17.6)	1.32 (17.6)
	∞	1.17 (19.4)	1.07 (18.0)	1.09 (17.5)	1.16 (17.5)	1.23 (17.5)	1.31 (17.5)
3	2	**** (****)	**** (****)	**** (****)	**** (****)	**** (****)	**** (****)
	3	**** (****)	**** (****)	**** (****)	1.22 (17.7)	1.30 (17.7)	1.37 (17.7)
	4	**** (****)	**** (****)	1.06 (17.0)	1.12 (16.9)	1.19 (16.9)	1.26 (16.9)
	5	**** (****)	**** (****)	1.01 (16.6)	1.04 (16.3)	1.09 (16.2)	1.16 (16.2)
	∞	1.21 (19.4)	1.10 (17.9)	1.00 (16.5)	1.01 (16.0)	1.04 (15.8)	1.10 (15.8)
4	2	**** (****)	**** (****)	**** (****)	**** (****)	1.50 (18.7)	**** (****)
	3	**** (****)	**** (****)	**** (****)	1.15 (16.9)	1.22 (16.9)	1.29 (16.9)
	4	**** (****)	**** (****)	1.04 (16.6)	1.03 (16.6)	1.04 (15.5)	1.09 (15.5)
	5	**** (****)	**** (****)	1.03 (16.5)	1.03 (16.0)	1.02 (15.4)	1.08 (15.4)
	∞	1.26 (19.4)	1.14 (17.9)	1.03 (16.5)	1.03 (16.0)	1.02 (15.4)	1.08 (15.4)
5	2	**** (****)	**** (****)	**** (****)	**** (****)	1.47 (18.3)	**** (****)
	3	**** (****)	**** (****)	**** (****)	1.08 (16.1)	1.07 (15.5)	1.13 (15.6)
	4	**** (****)	**** (****)	1.07 (16.6)	1.06 (16.0)	1.05 (15.4)	1.11 (15.4)
	5	**** (****)	**** (****)	1.06 (16.5)	1.06 (16.0)	1.05 (15.4)	1.11 (15.4)
	∞	1.30 (19.4)	1.18 (17.9)	1.06 (16.5)	1.06 (16.0)	1.05 (15.4)	1.11 (15.4)
6	2	**** (****)	**** (****)	**** (****)	**** (****)	1.39 (17.6)	**** (****)
	3	**** (****)	**** (****)	**** (****)	1.10 (16.0)	1.08 (15.4)	1.1[illegible] (15.5)
	4	**** (****)	**** (****)	1.10 (16.6)	1.09 (16.0)	1.08 (15.4)	1.13 (15.4)
	5	**** (****)	**** (****)	1.10 (16.5)	1.09 (16.0)	1.08 (15.4)	1.13 (15.4)
	∞	1.35 (19.4)	1.21 (17.9)	1.10 (16.5)	1.09 (16.0)	1.08 (15.4)	1.13 (15.4)

MINIMUM T_s = 202.3

TABLE 4.22

FADING INDUCED PERFORMANCE DEGRADATION OF "HARD" DECODING TOGETHER WITH SYNCHRONIZATION

$n_i = 2 \times 12 = 24$, $P_D = 0.9999$, $10^{-8} \leq \max P_E \leq 2 \times 10^{-8}$

n_s	n_p / -2 LOG C	0	1	2	3	4	5
2	2	**** (****)	**** (****)	**** (****)	**** (****)	**** (****)	**** (****)
	3	**** (****)	**** (****)	**** (****)	**** (****)	**** (****)	**** (****)
	4	**** (****)	**** (****)	**** (****)	**** (****)	**** (****)	**** (****)
	5	**** (****)	**** (****)	**** (****)	**** (****)	**** (****)	**** (****)
	∞	1.24 (20.7)	1.15 (19.4)	1.23 (19.4)	1.31 (19.4)	1.39 (19.4)	1.47 (19.4)
3	2	**** (****)	**** (****)	**** (****)	**** (****)	**** (****)	**** (****)
	3	**** (****)	**** (****)	**** (****)	**** (****)	**** (****)	**** (****)
	4	**** (****)	**** (****)	**** (****)	**** (****)	**** (****)	**** (****)
	5	**** (****)	**** (****)	1.05 (17.8)	1.01 (16.9)	1.06 (16.8)	1.12 (16.8)
	∞	1.29 (20.7)	1.12 (18.9)	1.05 (17.7)	1.00 (16.8)	1.06 (16.8)	1.12 (16.8)
4	2	**** (****)	**** (****)	**** (****)	**** (****)	**** (****)	**** (****)
	3	**** (****)	**** (****)	**** (****)	**** (****)	1.12 (17.0)	1.18 (17.0)
	4	**** (****)	**** (****)	1.09 (17.8)	1.02 (16.7)	1.01 (16.1)	1.03 (15.8)
	5	**** (****)	**** (****)	1.08 (17.7)	1.01 (16.6)	1.00 (16.0)	1.00 (15.6)
	∞	1.33 (20.7)	1.15 (18.9)	1.08 (17.7)	1.01 (16.6)	1.00 (16.0)	1.00 (15.6)
5	2	**** (****)	**** (****)	**** (****)	**** (****)	**** (****)	**** (****)
	3	**** (****)	**** (****)	**** (****)	**** (****)	1.05 (16.2)	1.05 (15.7)
	4	**** (****)	**** (****)	1.12 (17.8)	1.05 (16.7)	1.03 (16.0)	1.02 (15.5)
	5	**** (****)	**** (****)	1.12 (17.7)	1.04 (16.6)	1.03 (16.0)	1.02 (15.5)
	∞	1.38 (20.7)	1.19 (18.9)	1.11 (17.7)	1.04 (16.6)	1.03 (16.0)	1.02 (15.5)
6	2	**** (****)	**** (****)	**** (****)	**** (****)	**** (****)	**** (****)
	3	**** (****)	**** (****)	**** (****)	**** (****)	1.07 (16.2)	1.06 (15.6)
	4	**** (****)	**** (****)	1.16 (17.8)	1.08 (16.7)	1.06 (16.0)	1.05 (15.5)
	5	**** (****)	**** (****)	1.15 (17.7)	1.07 (16.6)	1.06 (16.0)	1.05 (15.5)
	∞	1.43 (20.7)	1.23 (18.9)	1.15 (17.7)	1.07 (16.6)	1.06 (16.0)	1.05 (15.5)

MINIMUM $T_s = 227.8$

TABLE 4.23

FADING INDUCED PERFORMANCE DEGRADATION OF "HARD" DECODING TOGETHER WITH SYNCHRONIZATION

$n_i = 2 \times 12 = 24$, $P_D = 0.9999$, $10^{-12} \leq \max P_E < 2 \times 10^{-12}$

n_S	-2 LOG C	n_P = 0	1	2	3	4	5
2	2	**** (****)	**** (****)	**** (****)	**** (****)	**** (****)	**** (****)
	3	**** (****)	**** (****)	**** (****)	**** (****)	**** (****)	**** (****)
	4	**** (****)	**** (****)	**** (****)	**** (****)	**** (****)	**** (****)
	5	**** (****)	**** (****)	**** (****)	**** (****)	**** (****)	**** (****)
	*	1.29 (21.7)	1.27 (20.9)	1.36 (20.9)	1.45 (20.9)	1.54 (20.9)	1.63 (20.9)
3	2	**** (****)	**** (****)	**** (****)	**** (****)	**** (****)	**** (****)
	3	**** (****)	**** (****)	**** (****)	**** (****)	**** (****)	**** (****)
	4	**** (****)	**** (****)	**** (****)	**** (****)	**** (****)	**** (****)
	5	**** (****)	**** (****)	**** (****)	**** (****)	**** (****)	**** (****)
	*	1.34 (21.7)	1.15 (19.7)	1.08 (18.6)	1.07 (18.0)	1.13 (18.0)	1.20 (18.0)
4	2	**** (****)	**** (****)	**** (****)	**** (****)	**** (****)	**** (****)
	3	**** (****)	**** (****)	**** (****)	**** (****)	**** (****)	**** (****)
	4	**** (****)	**** (****)	**** (****)	**** (****)	**** (****)	**** (****)
	5	**** (****)	**** (****)	**** (****)	1.04 (17.5)	1.00 (16.7)	1.02 (16.4)
	*	1.39 (21.7)	1.19 (19.7)	1.12 (18.6)	1.04 (17.5)	1.00 (16.7)	1.02 (16.3)
5	2	**** (****)	**** (****)	**** (****)	**** (****)	**** (****)	**** (****)
	3	**** (****)	**** (****)	**** (****)	**** (****)	**** (****)	**** (****)
	4	**** (****)	**** (****)	**** (****)	1.08 (17.5)	1.03 (16.7)	1.01 (16.1)
	5	**** (****)	**** (****)	**** (****)	1.07 (17.5)	1.03 (16.6)	1.01 (16.1)
	*	1.44 (21.7)	1.23 (19.7)	1.15 (18.6)	1.07 (17.5)	1.02 (16.6)	1.01 (16.1)
6	2	**** (****)	**** (****)	**** (****)	**** (****)	**** (****)	**** (****)
	3	**** (****)	**** (****)	**** (****)	**** (****)	**** (****)	1.05 (16.2)
	4	**** (****)	**** (****)	**** (****)	1.11 (17.5)	1.06 (16.7)	1.04 (16.1)
	5	**** (****)	**** (****)	**** (****)	1.10 (17.5)	1.05 (16.6)	1.04 (16.1)
	*	1.49 (21.7)	1.27 (19.7)	1.19 (18.6)	1.10 (17.5)	1.05 (16.6)	1.04 (16.1)

MINIMUM T_S = 244.9

An examination of Table 4.15 indicates that if the probability of "losing" a pulse is $P_o = 10^{-5}$, the effects of fading are negligible or relatively small. With an increase of P_o, however, there are more cases for which the performance requirements cannot be met. As one example, the performance requirements cannot be met for any SNR/pulse if the synchronization pattern consists of two pulses or if the information block has less than two parity checks and the probability of "losing" a pulse exceeds 10^{-4}.

Results shown in Table 4.16 indicate that at least six synchronization pulses are required to meet performance requirements when the probability of "losing" the pulse is $P_o = 10^{-2}$.

Table 4.17 shows that the most stringent performance requirements are not met for any message formats considered when $P_o = 10^{-2}$. Tables 4.18 through 4.23 illustrate similar trends.

For long messages, Tables 4.21, 4.22 and 4.23 show that, with higher redundancies, fading-induced degradation is usually small if performance requirements are met. Let us recall that for long messages, the preferable approach of minimizing the scanning time was to operate at relatively high redundancies.

In contrast, low redundancies are preferable for short messages in which fading-induced degradation is most pronounced. Thus, if the message formats were selected to minimize scanning time, we may expect that the fading-induced degradation would be more significant for short than for long messages.

The present analyses of fading-induced degradations were performed for signal processing schemes designed for deterministic signals. As mentioned previously (Section 3.3.5), modifications of the signal processing may reduce some of the effects of fading. For the "hard" decoder, relatively simple modifications, not requiring any major alteration of the general scheme, would be adequate. Increasing the threshold

values and/or changing the decoding mode (e.g., more erasure corrections) may be helpful. The "soft" decoder (with threshold) and detection algorithm C for the synchronization pattern will require more complex alterations if the probability of error is not to exceed a desired level. (See Section 3.3.5.) These alterations are necessary because one of the main effects of fading on performance of these algorithms is an increased probability of error.

The following "robustness" property for signal processing in the SLC system is recommended: for any fading law the maximum allowable probability of error should not exceed a predetermined value. The actual choice of signal processing schemes satisfying this condition and the choice of message formats should be based on a careful analysis of tradeoffs as done here for deterministic signals. This should be done for several simple fading signal models incorporating realistic parameter values, i.e., values which may be anticipated for realistic fading behaviors.

REFERENCES

1. This request will be made available to qualified military and government agencies on request from RADC (OCSP), Griffiss AFB NY 13441.

2. Peterson, W.W. and Weldon, Jr., W.J., "Error-Correcting Codes, Second Edition", The MIT Press, Cambridge, Mass., and London, England.

3. Berlekamp, Elwyn R., "Algebraic Coding Theory", McGraw-Hill Book Company, New York, St. Louis, San Francisco.

4. NOSC Letter on SNR.

5. Viterbi, A.J. and Omura, J.K., "Principles of Digital Communication and Coding", McGraw-Hill Book Company.

addresses	number of copies
Donald W. Hanson RADC/OCSP	2
RADC/TSLD GRIFFISS AFB NY 13441	1
RADC/DAP GRIFFISS AFB NY 13441	2
ADMINISTRATOR DEF TECH INF CTR ATTN: DTIC-DDA CAMERON STA BG 5 ALEXANDRIA VA 22314	12
Riverside Research Institute 330 West 42nd Street New York, NY 10036 Attn: Dr. Marek Elbaum	5
AFWL/ART Kirtland AFB, NM 87117 ATTN: Dr. C.B. Hogge	1
DARPA/DEO 1400 Wilson Blvd lington,VA 22209 ATTN: LCDR William Wright	1
DARPA/DEO 1400 Wilson Blvd Arlington, VA 22209 ATTN: Lt Col R. Benedict	1

Naval Electronic Systems Command 2
PME 106-48
NC 1 Rm 3W80
Washington DC 20360
ATTN: CDR Donald R McConathy

Naval Electronic Systems Command 1
PME 106-4A
NC 1
Washington DC 20360
ATTN: Mr Charles Good

Naval Electronic Systems Command 1
PME 110-34
NC 1
Washington DC 20360
ATTN: Mr Wendell Larson

Office of Naval Research Detachment 1
495 Summer Street
Building 114, Section D
Boston, MA 02210
ATTN. Dr M. White

Navy Space Systems Activity 1
P.O. Box 92960
Worldway Postal Center
Los Angeles, CA 90009
ATTN: CAPT Lorin Brown

Navy Space Systems Activity 1
P.O. Box 92960
Worldway Postal Center
Los Angeles, CA 90009
ATTN: Hugh Hanson

Naval Ocean Systems Center 5
271 Catalina Blvd.
San Diego, CA 92152
Attn: Mr. Roy Schindler (8114)

Naval Sea Systems Command 1
NC 1 Rm 11N08
PMS 405-200
Washington DC 20360
ATTN: CDR F. Marcell

RADC (OL-AB) 1
c/o AVCO Everett Research Labs
P.O. Box 261
Puunene, HI 96784
ATTN: Maj. Richard Fisher

Naval Research Laboratory 1
Attn: Dr. John L. Walsh
Code 6530
Washington DC 20375

Adaptive Optics Associates 1
2336 Massachusetts Ave.
Cambridge, MA 02140
ATTN: Dr. Julius Feinleib

Itek Corporation 2
10 Maquire Road
Lexington, MA 02173
Attn: Mr. Al McGovern

Itek Corporation 1
10 Maquire Road
Lexington, MA 02173
Attn: Dr. L. Soloman

Itek Corporation 1
10 Maquire Road
Lexington, MA 02173
Attn: Mr. Ralph Aldrich

TRW, INC. 5
Defense and Space Systems Group
One Space Park, R3/2182
Redondo Beach, CA 90278
Attn: Mr. Harold Koletsky

TRW, Space & Technology Group 2
One Space Park
SNTE/1513
Redondo Beach, CA 90278
Attn: Mr. A. Fiul

Eastman Kodak Company 1
Kodak Apparatus
901 Elmgrove Road
Rochester, NY 14650
ATTN: Mr. A. Kriesen

Hughes Aircraft Co/Aerospace Groups 2
Electro-OPtical and Engineering Division
Attn: Mr. Robert Hill
P.O. Box 902
El Segundo, CA 90245

Hughes Research Laboratory 2
3011 Malibu Canyon Road
Malibu, CA 90265
Attn: Dr. C. Giuliano

Lockheed Missile Space Company, Inc. 2
Palo Alto Research Labs
3251 Hanover St.
Palo Alto, CA 94304
Attn: Dr. T. Karr, O/5254, B/202

Lockheed Missiles and Space Company, Inc. 2
Attn: Mr. B.W. Marsh, Dept. 61-83, Bldg 576
1111 Lockheed Way
P.O. Box 504
Sunnyvale, CA 94088

Rockwell International Corporation 2
Rocketdyne Division
6633 Canoga Ave.
Canoga Park, CA 91304
Attn: Dr. Ken Kissell (FA-36)

Science Applications, Inc. 1
803 W. Broad St.
Suite 600
Falls Church, VA 22046
Attn: Dr. Emmanuel Goldstein

AVCO Everett Research Laboratory 1
P.O. Box 261
Puunene, HI 96784
ATTN: Dr. P. McCormick

Western Research Corp. 1
Attn: Dr. Jack Hammond or Mrs. Jane Methvin
1901 N. Ft. Meyer Dr.; Suite 903
Arlington, Va. 22209

Western Research Corp. 1
Attn: Dr. Robert O. Hunter
8618 Commerce Ave.
San Diego, CA. 92121

NOAA/Environmental Research Lab 1
Attn: Mr. G. Ochs
Wave Propagation Lab R 45x1
325 Broadway
Boulder, CO 80302

Riverside Research Institute 1
1701 N. Fort Meyer Dr.
Suite 714
Arlington, VA 22209
ATTN: SLC Library

The Optical Sciences Company 1
P. O. Box 1329
Placentia, CA 92670
Attn: Dr. David L. Fried

MIT/Lincoln Lab 1
P.O. Box 73
Lexington, MA 02173
ATTN: Dr. Darryl Greenwood, L-382

Scripps Institute of Oceanography 1
University of California, San Diego
P.O. Box 6049
San Diego, CA 92106
Attn: Mr. Ben L. McGlamery

Scripps Institute of Oceanography 1
University of California, San Diego
P.O. Box 6049
San Diego, CA 92106
Attn: Roswell Austin

ORI, Inc. 2
1400 Spring St.
Silver Spring, MD 20904
ATTN: Dr. John R. Tuttle

W.J. Schafer Assoc., Inc. 2
1901 N. Fort Meyer Dr.
Suite 800
Arlington, VA 22209
ATTN: Dr. Thomas Norwood, Dr. Joseph Stregach

Titan Systems 3
8950 LaJolla Village Dr.
Suite 2232
LaJolla, CA 92037
Attn: Dr. Gary Lee

Booz, Allen, and Hamilton 1
4330 East West Hwy
Bethesda, MD 20014
Attn: Dr. Allen Durling

Jet Propulsion Laboratory 1
4800 Oak Grove Drive
Pasadena, CA 91103
Attn: Mr. B. Breshears

Mitre Corporation 1
c/o Naval Ocean Systems Center
San Diego, CA 92152
Attn: Dr. James A. Quarato

MISSION
of
Rome Air Development Center

RADC plans and executes research, development, test and selected acquisition programs in support of Command, Control Communications and Intelligence (C^3I) activities. Technical and engineering support within areas of technical competence is provided to ESD Program Offices (POs) and other ESD elements. The principal technical mission areas are communications, electromagnetic guidance and control, surveillance of ground and aerospace objects, intelligence data collection and handling, information system technology, ionospheric propagation, solid state sciences, microwave physics and electronic reliability, maintainability and compatibility.